

**VENTILATION DISTRIBUTION IN THE LUNG
DURING CYCLIC BREATHING**

BARBARA ELLEN SHYKOFF
Department of Chemical Engineering
McGill University, Montréal

August, 1984.

A thesis submitted to the Faculty of Graduate Studies and Research in partial fulfillment of the requirements for the degree of Doctor of Philosophy.

ABSTRACT

The dynamic distribution of pulmonary ventilation was studied both theoretically and experimentally. The human lungs were simulated as two compartments driven by independent cyclic pleural pressures. The distribution of tidal volume depended primarily on the regional pressures, but dissimilar pressure swings generated sequential flows. A model of the tracer dynamics in the lung during a breath showed that the ventilation per unit volume was proportional to the time derivative of krypton-81m activity normalized by the activity itself. In gamma camera measurements, the average flow distribution was independent of frequency and tidal volume, but the flow per unit volume in left lateral decubitus subjects was greater in the dependent than the non-dependent lung, and sequential flows were evident. However, lung sound amplitudes were in phase over the dependent and non-dependent regions, varying as the square of the airflow at the mouth. The frequency composition of the sounds remained constant. Thus, nonhomogeneous pleural pressure swings appear to control the dynamic distribution of ventilation. This time-varying quantity can be measured using a short-lived isotope but not directly with lung sounds.

RESUME

La distribution dynamique de la ventilation pulmonaire fut étudiée en théorie et par expérience. Un modèle à deux compartiments, mû par des pressions pleurales indépendantes, fut utilisé pour simuler les poumons humains. La distribution du volume-courant dépendait principalement des pressions régionales. Cependant, une inégalité des variations de pression produisait une séquence dans les débits régionaux. Un modèle de la dynamique d'un traceur dans le poumon au cours d'une respiration montra que la ventilation normalisée par unité de volume était proportionnelle à la dérive dans le temps de l'activité du krypton-81m normalisée par cette même activité. La scintigraphie montra que la distribution du débit moyen était indépendante de la fréquence ou du volume-courant. Chez les sujets en décubitus latéral gauche le débit normalisé par unité de volume était supérieur au poumon dépendant par rapport au non-dépendant et une séquence dans les débits était évidente. Néanmoins, les amplitudes des bruits pulmonaires étaient en phase dans les régions dépendant et non-dépendant, variant selon le carré du débit gazeux mesuré à la bouche. Le spectre de fréquence de ces sons demeura constant. Donc, des variations inhomogènes de pression pleurale semblent contrôler la distribution de la ventilation. Cette distribution peut être mesurée par un isotope de courte demi-vie mais pas directement avec les bruits pulmonaires.

ACKNOWLEDGEMENTS

I acknowledge with pleasure the help, support, and encouragement that I have received from many people in the course of my thesis work. I can thank only a few by name.

Dr. H. K. Chang, my thesis supervisor, has contributed as much to my general education as to my technical development. He has provided me with many experiences and opportunities to learn. I thank him. Financial support for four years from MRC grant MA-7046 also is gratefully acknowledged.

At the Hôpital Henri Mondor, Créteil, France, I had the privilege of working with Dr. Michel Meignan, Dr. Louis Oliveira, Dr. Luc Cinotti, and Dr. Alain Harf. At Brookhaven National Laboratories, New York, I was able to work with Dr. Herbert Susskind and again, with Dr. Luc Cinotti. These people put their equipment and their considerable technical expertise at my disposal and helped me in every way they could. To them and to all of their support staff who aided, I express my thanks for the warm welcome and for all they taught me about krypton-81m. I am particularly grateful to Luc for his processing and sending me the data we collected.

During the measurements of lung sounds, I depended heavily on borrowed equipment. Dr. Yongyudh Ploysongsang loaned me his microphones. Dr. Robert Kearney provided filters and amplifiers and once his computer as well. More importantly, he offered his time. I

benefited considerably from his patient advice on data analysis, for which I express my thanks. I thank Dr. Ploysonsang also for his suggestions and for the enthusiasm he showed for my project.

The Biomedical Engineering Unit has been a good home for the last few years. I express my thanks to everyone. The facilities and support, particularly for computing and word processing, have been excellent. In the frenzied last few months, I have enjoyed extra help. Mr. Carmelo Granja ensured that data collection and processing were possible. Dr. Robert Funnell whose command procedures and programs were a great help in manuscript preparation also implemented any typeface known to man, permitting the generation of tidy-looking equations and, inadvertently, of many pages of coded messages during the editing stages.

My thanks go to Alex Weiss for the preparation of some of my figures, to Daniel Chartrand for rewriting my Résumé, and to Jean-Michel Maarek for helping to analyse some of my data. Thanks are due to Anil Menon for helpful discussions, loaned books, and moral support. Particular thanks go to Patrice Weiss for the many important discussions about data analysis, thesis formatting, literature, and politics, for advice about figures, for my Table of Contents, and for tremendous encouragement. I thank the late-night thesis writing crowd for keeping me home from Tibet.

TABLE OF CONTENTS

Abstract	i
Acknowledgements	iii
Table of Contents	v
CHAPTER 1 INTRODUCTION	1
CHAPTER 2 LITERATURE REVIEW	5
2.1 DISTRIBUTION OF VENTILATION	5
2.1.1 Bolus Studies	5
2.1.2 Pleural Pressure Effects	12
2.1.3 Tidal Breathing	14
2.1.4 Single Lung Studies	16
2.2 MATHEMATICAL MODELS	19
2.3 KRYPTON-81m	21
2.3.1 Production and Rationale	23
2.3.2 Steady State Measurements with Krypton-81m	23
2.3.3 Dynamic Studies with Isotopes	27
2.3.4 Washout Models	29
2.4 BREATH SOUNDS	31
2.4.1 Origins and Transmission of Lung Sound	31
2.4.2 Subjective Measurement of Lung Sounds	33
2.4.3 Sound Spectra	34
2.4.4 Sound Intensity	37
CHAPTER 3 THE PLEURAL PRESSURE-DRIVEN MODEL	48
3.1 INTRODUCTION	48
3.2 THE MODEL	48
3.3 RESULTS	52
3.3.1 Tidal Volume Distributions	52
3.3.2 Flow Rate	59
3.3.3 Waveform Effects	62
3.4 DISCUSSION	64
3.4.1 Non-linear Pressure Volume Curve	64
3.4.2 Pleural Pressure Ratios	66

3.4.3 Phase Differences	68
3.4.4 Differences from Constant Flow Inspiration	67
3.4.5 Waveforms	72
3.5 CONCLUSIONS	73
CHAPTER 4 A MODEL OF KRYPTON-81m DYNAMICS IN THE LUNG	74
4.1 INTRODUCTION	74
4.2 THE MODEL DEVELOPMENT	74
4.2.1 The Conducting Airways	75
4.2.2 The Respiratory Zone	76
4.3 THE CONCENTRATION IN THE CONDUCTING ZONE	77
4.3.1 Inspiration	77
4.3.2 Expiration	78
4.4 THE RESPIRATORY ZONE CONCENTRATION	79
4.4.1 The Steady State Solution	79
4.4.2 The Transient Solution	80
4.4.3 Superposition of the Boundary Conditions: Solution for Concentration	81
4.5 REGIONAL ACTIVITY	82
4.5.1 The Conducting Airways	82
4.5.2 Respiratory Zone	83
4.6 THE NORMALIZED DERIVATIVES OF ACTIVITY	84
4.6.1 Inspiration	84
4.6.2 Expiration	85
4.7 DISCUSSION	86
CHAPTER 5 KRYPTON-81m EXPERIMENTS	87
5.1 INTRODUCTION	88
5.2 MATERIALS AND METHODS	89
5.2.1 Experimental Protocol	89
5.2.2 The Gamma Camera	92
5.2.3 The Mixing Chamber	93
5.2.4 Methods of Analysis	97
5.3 RESULTS	101
5.3.1 Steady State	101
5.3.2 Washouts	109
5.3.3 Dynamic Cycle	109
5.3.4 Phase	125

5.4 DISCUSSION	125
5.4.1 Steady State Scans	125
5.4.2 Curves of Flow per Unit Volume	129
5.4.3 The Sequence of Flows	132
5.4.4 Phase	134
5.4.5 Problems of Methodology	134
5.5 CONCLUSIONS	136
CHAPTER 6 LUNG SOUND MEASUREMENTS	138
6.1 INTRODUCTION	138
6.2 MATERIALS AND METHODS	139
6.2.1 Measurement	139
6.2.2 Analysis	146
6.3 RESULTS	154
6.3.1 System Statics: Algebraic Equation	154
6.3.2 System Dynamics: Differential Equation	166
6.3.3 Cross Correlations	171
6.3.4 Spectral Analysis	174
6.4 DISCUSSION	180
6.4.1 Statics: The Algebraic Relation	180
6.4.2 Dynamics	187
6.4.3 The Generation of Breath Sounds	189
6.4.4 Phase Relationship	191
6.4.5 Spectra	193
6.4.6 Suggestions for Further Work	194
6.5 CONCLUSIONS	195
CHAPTER 7 CONCLUDING SUMMARY	198
7.1 SYNOPSIS	198
7.1.1 The Pleural Pressure Model	198
7.1.2 A Model of Krypton-81m Dynamics	200
7.1.3 Krypton Measurements	201
7.1.4 Breath Sound Measurements	203
7.2 SIGNIFICANCE OF THE PRESENT WORK	204
Bibliography	206

CHAPTER 1
INTRODUCTION

The distribution of ventilation within the lung is one of the major determinants of gas exchange. It is affected by factors ranging from the external forces acting on the body to molecular effects that can modify the properties of the small airways and the alveoli. In healthy lungs, the distribution of the inspired air is important; in diseased lungs, it can provide important information for diagnosis and treatment.

Interest in the regional distribution of pulmonary ventilation and in the factors that govern it probably has existed for as long as the function of the lungs has been known. The modern contribution has been more in providing the methods of measurement than in the problem formulation. As with most research, the questions have grown to keep ahead of the answers. A review of some of the recent work and techniques is presented in Chapter 2. Current issues include the differences between the known distributions of air under conditions of little or no flow and those during normal cyclic breathing, the principal factors controlling the distributions under the dynamic conditions, and the efficacy of methods of measurement. These are the questions addressed in this dissertation.

The regional lung volume under conditions of low flow has been shown to follow the distribution of the local lung compliances (Milic-Emili et al, 1966). Lung compliance, itself a function of lung volume, therefore depends indirectly on the hydrostatic gradient in

pleural pressure. The lung fills and empties at very low flows in a uniform manner that preserves the gradient. However, at higher flow rates conditions are different. A flow rate dependence of the distribution of a marked bolus of air is observed for constant rate inspiration (Bake et al, 1974), as would be expected if only the regional compliances and resistances of the lung determined the sequence of filling (Pedley et al, 1972). However, the position of the subject modifies the distribution in a way that cannot be explained by the resistances and compliances unless non-homogeneities of the pleural pressure swings are invoked (Sybrecht et al, 1976). A preliminary mathematical model incorporating this feature was presented by Chang and van Grondelle (1981). The further development of the model, which features independent pleural pressures as the driving force for airflow on each of its two compartments, regional compliances and resistances determined as non-linear functions of volume and volume and flow, respectively, and a common resistance between the compartments and the mouth, is presented in Chapter 3.

Direct measurements of regional gas flow may be made by bronchspirometry. However, the high resistance of the tubes and the discomfort for the subject make the the technique impractical and the results physiologically unrepresentative. The accepted tools for regional measurements in the lung are radioactive gases and aerosols. Historically, xenon-133 has been used more than any other respiratory tracer but other isotopes are more suitable for dynamic studies. Krypton-81m, with its 190 keV gamma ray and its 13 s half-life yields a good image and disappears quickly. It cannot be used to measure lung volume in man because it does not equilibrate in the lungs before it decays, but it provides an image of the steady state ventilation (Fazio

and Jones, 1975).

The sequence of the distribution of a single breath is as interesting as the average over multiple cycles. Dynamic effects of isotope transport must be considered in the measurements. A model of the time-varying activity of krypton-81m during a breath is presented in Chapter 4.

Experiments using krypton-81m to measure normal cyclic breathing are discussed in Chapter 5 for subjects in the left lateral decubitus position. The results are compared with the model predictions for both the distribution of tidal breathing (Chapter 3) and the sequence of a breath (Chapter 4). The regional flow per unit volume is obtained from average breaths reconstructed from many respiratory cycles during the lung scans.

Although radioactive isotope methods are non-invasive, they carry some risk. More importantly, they require large expensive installations in hospital or research centres. Because the equipment is unavailable to most clinicians and researchers, other techniques for measurement of the regional distribution of ventilation during cyclic breathing are sought. One which has been proposed is the recording of breath sounds. A study of the relationship of the sounds detected over the chest to the flow of air at the mouth is presented in Chapter 6. The sounds are shown to vary with the square of the flow rate at the mouth, but in a way that suggests that it is the velocity at some location in the bronchi rather than the local ventilation which determines the sound.

In brief, Chapter 2 is a selective review of the literature on the distribution of ventilation, on krypton-81m measurements, and on lung sounds. Chapter 3 is the description of a simulation of a two compartment lung driven by pleural pressure swings. Chapter 4 contains the derivation of an expression for the activity of krypton-81m in the lung during a breath. In Chapter 5, measurements of the distribution of ventilation made using krypton-81m are reported. Chapter 6 is an analysis of the sounds of normal breathing and their relation to the flow of air into and out of the lungs. Chapter 7 consists of a summary of the principal findings.

CHAPTER 2

LITERATURE REVIEW

2.1 DISTRIBUTION OF VENTILATION

2.1.1 BOLUS STUDIES

2.1.1.1 *Quasi-static Distribution*

The majority of the studies of the distribution of pulmonary ventilation have been performed since the advent of radioactive gas techniques. Knipping et al. (1955, 1957) pioneered in this area, initiating the use of xenon-133 as a non-invasive investigative tool. Subjects or patients inhaled the gas from a spirometer and the radioactivity was recorded over the chest with scintillation counters. The qualitative distribution of air was observed directly (i.e., normal or obstructed lung) but no attempt was made to interpret the data quantitatively.

The static or quasi-static distribution of gas within normal lungs was established quantitatively by Milic-Emili et al. (1966) and Kaneko et al. (1966) for seated and decubitus subjects, respectively. The results and those of later studies were thoroughly reviewed by Milic-Emili (1977). Volunteers inhaled xenon-133 mixed with air in increments from a starting volume to total lung capacity. At each step they held their breath while the xenon counts were recorded. The counts obtained after the lungs were equilibrated with xenon-133 were used to correct for the different thicknesses of lung tissue beneath the counters and the regional volumes were found as a percent of the total regional lung capacity.

A constant gradient of expansion was seen down the lung from the more expanded non-dependent to the less expanded dependent zones both in upright (Milic-Emili et al., 1966) and in supine, prone and lateral decubitus (Kaneko et al., 1966) positions. The change of percent inflation with distance down the lung was less steep at RV than at higher lung volumes in all positions. Regional lung volume in the non-dependent regions increased rapidly and curvilinearly with increasing total lung volume for low lung volumes and more slowly and linearly for higher volumes. In the dependent zones it increased very slowly and curvilinearly for low lung volume and more rapidly and linearly at higher volumes. In seated subjects the linear portion of the relationship between regional expansion and total lung volume change began below 40% TLC (Milic-Emili et al., 1966). It did also in supine and prone subjects, but in the lateral decubitus positions the relation became linear only at higher lung volumes (Kaneko et al., 1966).

The influence of the starting volume on the distribution of slow inspirations was studied by Dollfus et al. (1967). Boli were injected into the inspirate at lung volumes between residual volume and 95% vital capacity in standing subjects. The boli inhaled at residual volume favoured the upper zones. As the volume at which the tracer was added was increased, the gradient of the distribution was seen to reverse gradually until at 25% vital capacity, the basal regions were favoured. From that lung volume up, the xenon concentration decreased linearly from the lung bases to the apices.

The differences in regional lung expansion were explained by the gradient of the static pleural pressure with gravity which had been documented in normal subjects by Daly and Bondurant (1963). At low lung volumes airway closure in the dependent regions delays the onset of filling until the pressure gradient is fairly large but for most of the volume range the pattern of expansion is determined by the regional pressure-volume curve. The filling of the lung zones under conditions of very low flow can be predicted from the regional compliance which is determined by the regional volume.

Rehder et al. (1977) compared distributions of xenon-133 in awake and anaesthetized subjects in the seated, supine and right lateral decubitus positions during step-wise inhalation of xenon-133 in air. In conscious man the vertical gradient of lung volume was similar in all positions at all inspired volumes while the gradient of regional ventilation, computed as the ratio of the existing concentration of xenon-133 to that which would have existed if the ventilation were uniform, was a function of the volume inhaled in all but the seated position. In anaesthetized, paralysed subjects, however, the vertical gradient of regional volume was greater in the lateral decubitus position than in the other two positions while the regional ventilation was uniform in the lateral decubitus position, more uniform than in awake subjects in the supine posture, and similar to that in awake subjects in the seated position at low inspired volumes. The different mechanics of the thorax and abdomen in the different postures and in conscious and paralysed man were postulated as the explanation. Because of the breath holding at the end of each inspiration, the experiments do not model tidal breathing, although the term "tidal volume" was used by the authors.

In more recent work on the distribution of boli in supine subjects, Engel and Prefaut (1981) measured the cranio-caudal distribution of xenon-133 inspired at different lung volumes by 8 volunteers. At FRC there was preferential ventilation of the cranial lung zones, at 40% VC the distribution was uniform, and at 60% VC it was preferential to the caudal regions even though the gravitational effects acting directly on the lung tissue would be the same for all three zones. In subjects where a helium washout showed airway closure at volumes greater than FRC, almost twice as much xenon-133 entered the apical zones as entered the basal regions when boli were inspired from FRC. As the starting lung volume was increased, the distribution became more uniform. In subjects whose closing capacity was less than FRC, the ratio of apical to basal xenon counts for inspirations of boli from FRC was unity. The authors postulated that with airway closure in the dependent, paradiaphragmatic lung caused by the hydrostatic pressure of the abdomen, the cranial lung zones were favoured.

At low flow rates, the hydrostatic gradient of pleural pressure controls the distribution of air along the axis parallel to the gravitational field. For decubitus subjects, it influences the distribution of air in the axis perpendicular to gravity as well.

2.1.1.2 Higher Flow Rates

Robertson et al. (1969) studied the effects of fast and slow inspirations from different lung volumes on the distribution of gas in the lungs. Slow inspiration from residual volume (RV) caused preferential distribution of the xenon-133 boli to the apical regions with almost no tracer going to the basal zones. Very high flow rates (greater than 3 L s^{-1} ($3 \times 10^{-3} \text{ m}^3 \text{ s}^{-1}$)) caused the distribution of a

bolus inspired at RV to be somewhat more even, but even at the maximum flow rates generated, the apical regions had twice the xenon concentration of the basal ones. Inspiration from volumes above functional residual capacity (FRC), that is, above about 40% of the total lung capacity (TLC) produced different distributions, with the bases favoured relative to the apices. At higher flow rates the apical concentration of xenon-133 increased and the basal concentration decreased, but the majority of the bolus went to the lower lung.

At low lung volumes the airways in the lung bases remained closed until after the distribution of the bolus in the upper lung. The large transpulmonary pressures required to generate the fast inspirations opened the airways at somewhat lower total lung volumes than were needed with the slow flows, but once the total lung volume was above 40% total lung capacity, all the airways were open. For low rates of inspiration the distribution of air then followed the regional compliances. For higher flow rates the resistance appeared to be important.

The lung was modelled as the parallel combination of two branches, a dependent and a non-dependent zone, each consisting of a resistive element in series with a compliant one (Otis et al., 1956). When the pleural pressure swings over the lung were assumed uniform and the distributions at high flow rates were attributed to differences in regional time constants, the computed resistances were found to be uniform throughout the lung. This contrasted with the expected volume dependence of the resistance which would have caused the upper to be about half the lower resistance. The authors concluded that either the pressure difference across the central airways was large enough to render the effects of the vertical pressure gradient negligible or the

regional pleural pressure changes were non-uniform during forced inspiration.

Bake et al. (1974) performed similar experiments in seated subjects breathing from FRC. The results confirmed the findings of Robertson et al. (1969) that at very low flow rates a bolus (the second 100 ml of the inspired air) was distributed in the ratio of the regional compliances but that at higher rates of inspiration the distribution became more even. The ratio of upper to lower xenon-133 concentrations changed rapidly from 0.65 at very low flows to 0.88 at 1.5 L s^{-1} ($1.5 \times 10^{-3} \text{ m}^3 \text{ s}^{-1}$) and slowly to 0.93 at 4.5 L s^{-1} ($4.5 \times 10^{-3} \text{ m}^3 \text{ s}^{-1}$).

The data were interpreted with the aid of the model of Pedley et al. (1972) in which the series-parallel arrangement of Otis et al. (1956) was used, but with the compliances and resistances varying as functions of volume and flow rate. The differences in regional time constants (the products of resistance and compliance) caused by the volume dependence of compliance were used to explain the distribution. With additional data obtained from experiments with sulphur hexafluoride, the resistances were determined to be equal throughout the lung but to vary as the square root of flow rate and gas density. The uniformity of the resistance despite the differences in regional volume was postulated to result from the large pressure drop between the mouth and the apical regions caused by the redirection of flow in the upper airways, from the dynamic distention of the lower airways, or from differences in the regional dynamic pressures. As larger pressure swings were recorded from the lower of two esophageal balloons during forced inspiration, the last mechanism was considered likely.

Grant et al. (1974) pursued the investigation of bolus distribution during constant rate inspiration in the upright posture. Bolus of xenon-133 were injected through a tracheal catheter to mark the earliest part of inspiration, at the mouth to mark the second 100 ml of the inspiration, and after an added deadspace to mark the later part of inspiration. For slow flow rates (0.1 L s^{-1}) ($10^{-4} \text{ m}^3 \text{ s}^{-1}$), the bolus injected into the trachea were distributed more basally than those inhaled from the mouth, which themselves were more basally distributed than those injected late in inspiration. With faster flow rates, (0.4 L s^{-1}) ($4 \times 10^{-4} \text{ m}^3 \text{ s}^{-1}$), the distribution became more uniform. Earlier parts of the breath were distributed more apically than were the later portions. At high rates of flow, (1.0 L s^{-1}) ($10^{-3} \text{ m}^3 \text{ s}^{-1}$), the early portion of the breath went to the lung apices and the later portion to the bases. The data of Grant et al. (1974) were explained using the concept of regional compliances and resistances and their dependence on lung volume without considering the nonhomogeneity of the pressure swings.

Further experiments on the effects of inspiratory flow rate on bolus distribution were conducted by Sybrecht et al. (1976) who studied the effect of the pleural pressure differences. In seated subjects their data confirmed those of Grant et al. (1974). However, in supine subjects the apico-basal difference in distribution was increased over that in the vertical position. As the differences among regional compliances are reduced in supine subjects, it was impossible to compute a reasonable set of resistances and compliances to account for the distribution unless a small (less than $1 \text{ cm H}_2\text{O}$ (98 Pa)) nonhomogeneous change in the pleural pressure swings was introduced. When the difference in the regional dynamic pressure was included, the

data could be predicted accurately using a simple model. The authors concluded that the time constant theory alone could not explain the distribution of a bolus, that the resistances had little effect on the distribution of ventilation because it was much more sensitive to small changes in the differences in applied pleural pressure than to changes in the local time constants. The distribution of ventilation under dynamic conditions cannot be understood without considering nonhomogeneous pleural pressure swings.

2.1.2 PLEURAL PRESSURE EFFECTS

There is clear evidence that the magnitude of the pleural pressure can influence the distribution of ventilation. Roussos et al. (1976) measured helium washouts at low flow rates after very slow inspiration in supine and lateral decubitus subjects. When diaphragmatic tone was high (transdiaphragmatic pressure relatively constant) throughout expiration, the sequential nature of lung emptying was considerably reduced over that when the diaphragm was relaxed (changing transdiaphragmatic pressure). The authors concluded that the greater ventilation of the dependent lung in horizontal man was due both to its position on the steeper part of the pressure volume curve and to the greater swings of the pleural pressure over the dependent lung.

In seated, supine and lateral decubitus volunteers, Roussos et al. (1977a) found further that boli of xenon-133 inspired slowly could be distributed preferentially to the dependent regions by predominant use of the abdominal muscles during inspiration or more uniformly or even preferentially to the nondependent regions by strong contractions of the intercostal and accessory muscles while the

diaphragm remained relaxed. The gradient of alveolar expansion in lateral decubitus subjects also was shown to be influenced by the diaphragmatic tone (Roussos et al., 1977b). With increasing tone during expiration the difference between the dependent and nondependent zones decreased.

Fixley et al. (1978) demonstrated the same phenomenon in seated subjects for faster inspirations (up to 1.5 L s^{-1} ($1.5 \times 10^{-3} \text{ m}^3 \text{ s}^{-1}$)). Although the flow rate influenced the distribution of the tracer, the pattern of muscle use affected it more. Diaphragmatic contractions caused more of the bolus to enter the basal regions while intercostal and accessory muscle use produced a more even distribution at all flow rates. The data of Bake et al. (1974) for natural breathing fell neatly between the two.

The studies of Roussos et al. (1976, 1977a) and Fixley et al. (1978) showed that the pattern of muscle use during breathing could influence the distribution of ventilation, but they did not prove that unequal pleural pressure swings occurred during normal breathing. That had been demonstrated by Daly and Bondurant (1963) who introduced a small (less than 2 ml ($2 \times 10^{-6} \text{ m}^3$)) air bubble into the pleural space of seated subjects and measured the pressure with a needle probe. A larger change in the intrapleural pressure during tidal breathing was seen in the lower chest than in the upper. Oddly enough, this information was not used in the hypotheses about bolus distribution.

Hida et al. (1981) investigated the relationship between breathing frequency and the magnitude of the esophageal pressure swings at three vertical locations. Although the resistive component (the difference between the pressures measured at maximum inspiratory and

expiratory flow, divided by the total flow) did not change with frequency, the elastic component (the difference between pressures measured at subsequent zero flow points, divided by tidal volume) increased by 107%, 119%, and 157% in the upper, middle and lower balloons respectively when the frequency was increased from zero to 60 breaths min^{-1} . Changes in muscular activity over the regions was not considered. The change in the regional pressure difference with flow rate was in the opposite direction from that predicted by the constant flow results. Even at low flow, the pressure changes were greater in the most apical of the esophageal balloons, in contrast to the findings of Daly and Bondurant (1963) for direct pleural pressure measurements.

2.1.3 TIDAL BREATHING

The differences and similarities between constant flow rate inspiration and tidal breathing are interesting. Bouhuys et al. (1961) and Cutillo et al. (1972) found that, unlike constant flow bolus distributions, nitrogen washouts in normal subjects were not affected by changes in flow rate caused by changes in frequency, although in patients with obstructive disease they were (Cutillo et al., 1972). However, Chevrolet et al. (1979) found that xenon-133 washouts were influenced similarly to the bolus distributions by the selective use of one or the other set of respiratory muscles during voluntary tidal breathing in the lateral position. Also, with the diaphragm completely relaxed during intermittent positive pressure ventilation (IPPB) the washouts showed a more uniform pattern of ventilation than that from natural breathing at the same frequency (Chevrolet et al., 1978). IPPB produced a distribution similar to that during breathing with the intercostal muscles.

Secker-Walker et al. (1973) measured tidal breathing with xenon-133 washin and washout experiments. Seated subjects breathed normally from a reservoir system while a gamma camera recorded the activity. Regional ventilation, defined as the fractional exchange of air, was calculated from the peak of xenon activity divided by the area under the washout (or washin) curve after correction for the concentration of xenon-133 dissolved in the tissue. Both washout and washin measurements showed a gentle gradient of ventilation increasing from the apices to the bases although the values calculated from the washout were slightly greater than those from the washin. The overall fractional exchange for both lungs was 0.145 per breath, or 0.03 s^{-1} , as calculated from the washout. In patients with obstructive disease, the gradient was reversed and the overall mean fractional exchange was reduced to 0.01 s^{-1} (Secker-Walker et al., 1975).

Sampson and Smaldone (1984) measured xenon-133 washouts in seated subjects who were instructed to use different respiratory muscle groups during tidal breathing. The washout from the dependent region was always faster than that from the nondependent region, but with predominantly intercostal breathing the difference was less than it was with only diaphragmatic contraction. The ratios of the regional decay constants were linearly related to the ratios of the simultaneous regional esophageal pressure swings. Regional pleural pressures appear to control the regional washout, that is, the regional ventilation, during tidal breathing in seated man.

The evidence of the effect of breathing frequency on ventilation distribution is mixed. Kronenberg et al. (1976) found that the highest rate of xenon-133 clearance was near the lung bases in seated subjects breathing normally but was closer to the middle of the

lung field at 50 breaths min^{-1} . However Jones et al. (1977) detected only non-significant changes in the xenon-133 clearance rates for frequencies between 10 breaths min^{-1} and 50 breaths min^{-1} in either normal or bronchitic subjects. Rehder et al. (1981) similarly found the distribution of xenon-133 clearance rates to be independent of flow during tidal breathing with constant inspiratory rates in normal, lateral decubitus subjects. Forkert et al. (1978) found that the overall (mouth) washout rates of xenon-133 were constant for frequencies from 12 to 57 breaths min^{-1} in seated subjects, but that regional washouts changed markedly. There were intraregional differences suggesting variations by as much as a factor of ten among parallel RC time constants while the average washout was not affected. Washout measurements at the mouth could not show true regional behaviour, which may be highly inhomogeneous, but over the entire lung field the ventilation as measured by washout techniques was frequency independent.

2.1.4 SINGLE LUNG STUDIES

2.1.4.1 *Conscious Subjects*

The function of the individual lungs during tidal breathing has been studied with double-lumen endotracheal tubes. Lillington et al. (1959) measured nitrogen clearance in awake subjects in the left and right lateral and supine decubitus positions. In the supine subjects, the clearance from the right and left lung was the same, despite the slightly larger volume of the right lung. In the lateral decubitus positions, the FRC of the dependent lung remained unchanged or decreased slightly from that in the supine position, while that of the non-dependent lung increased. The tidal volume of the dependent lung was slightly greater than that of the non-dependent lung. The

clearance of the non-dependent lung was slower than it had been in the supine position (right lung 0.0095 s^{-1} vs 0.017 s^{-1} ; left lung 0.0062 s^{-1} vs 0.016 s^{-1}) while that in the dependent lung was slightly faster (right 0.018 s^{-1} ; left 0.024 s^{-1}). Overall, the clearance rate was slower in the lateral postures.

Not only the ventilation differs between the lungs in the lateral decubitus positions. The timing of filling and emptying is also dependent on the position. Frazier et al. (1976) performed single breath oxygen tests in awake subjects in the right lateral decubitus and the supine positions. In four of five subjects, the closing volume remained unchanged with position, but flow limitation was seen sequentially, first in the dependent, then in the non-dependent lung, and emptying was similarly asynchronous in the lateral decubitus position. In the supine position, however, emptying was synchronous.

2.1.4.2 Anaesthetized Subjects

Rehder et al. (1972) performed similar experiments in anaesthetized, paralysed subjects in the supine and lateral decubitus positions. In the supine anaesthetized subjects, as in the conscious subjects of Lillington et al. (1959), nitrogen clearance did not differ between the lungs. In the lateral positions, functional residual capacity increased because of the increase in size of the nondependent lung. In the left lateral position, the tidal volume of the nondependent lung was significantly greater than that of the dependent lung but its nitrogen clearance was significantly slower (0.014 s^{-1} vs 0.018 s^{-1}). In the right lateral position, the difference between the lungs was nonsignificant.

The disparity between spontaneously breathing and artificially ventilated paralysed subjects is striking. In paralysed subjects in the lateral decubitus positions the ventilation is uniformly distributed between the lungs, while in spontaneously breathing subjects the difference can be as great as a factor of four between the lungs. Probably the more uniform distribution of driving pressures between the lungs, during mechanical ventilation causes the difference.

Hedenstierna et al. (1981) measured airway closure in anaesthetized subjects in the supine and lateral decubitus positions using both nitrogen and argon washout techniques. In supine subjects the closing volumes of both lungs were similar and exceeded functional residual capacity. In the lateral positions, the residual volume of the nondependent lung decreased and the total functional residual capacity increased because that of the nondependent lung increased more than that of the dependent lung decreased. Closing volume, measured as the volume expired during phase IV of the washouts, did not change from the supine value for the dependent lung. In the nondependent lung it was difficult to measure but seemed to decrease slightly relative to the supine value. The dependent lung showed an earlier onset of phase IV during expiration. No closure was evident in the dependent lung until about 0.5 L ($5 \times 10^{-3} \text{ m}^3$) had been expelled after the end of expiration in the dependent lung.

Bindslev et al. (1981) studied the partition of volumes in the same anaesthetized subjects in the supine and lateral decubitus postures. In the left lateral decubitus position they found that the tidal volume was distributed preferentially (61%) to the nondependent lung and that this was increased by the use of positive end expiratory

pressure. The compliance of the nondependent lung ($0.073 \text{ L cm}^{-1} \text{ H}_2\text{O}$, $7.4 \times 10^{-7} \text{ m}^3 \text{ Pa}^{-1}$) was increased from its value in the supine position ($0.063 \text{ L cm}^{-1} \text{ H}_2\text{O}$, $6.4 \times 10^{-7} \text{ m}^3 \text{ Pa}^{-1}$), but the resistance was not changed significantly (3.37 to $3.14 \text{ cm H}_2\text{O/L/s}$, or 3.3×10^5 to $3.07 \times 10^5 \text{ kg m}^4 \text{ s}^{-1}$). The compliance of the dependent lung was decreased ($0.044 \text{ L/cm H}_2\text{O}$ from $0.057 \text{ L/cm H}_2\text{O}$; 4.5×10^{-7} from $5.8 \times 10^{-7} \text{ m}^3 \text{ Pa}^{-1}$ and its resistance entirely unchanged ($3.37 \text{ L/cm H}_2\text{O/s}$, $3.3 \times 10^5 \text{ kg m}^4 \text{ s}^{-1}$). The ventilation distribution ratio for nondependent lung to dependent lung was 1.54, a value closer to the ratio of the time constants (1.53) than to the ratio of the compliances. When the values for the hemithorax rather than the lung were used, the same result was obtained. For paralysed subjects, the distribution of regional ventilation seems to be determined primarily by the time constants of the regions, as the transpulmonary pressures are functions of the ventilator pressure or flow and the regional compliances and resistances of the lungs.

The studies that have been reviewed indicate the importance of the pleural pressure distribution, both the hydrostatic gradient and the dynamic component, in determining the regional ventilation. They also demonstrate that large differences may exist between the dependent and nondependent lung regions during normal breathing.

2.2 MATHEMATICAL MODELS

Mathematical models have been used to explain the distribution of ventilation quantitatively. Otis et al. (1956) considered a two compartment model of the lung with the parallel combination of two branches, each consisting of a resistance in series

with a compliance. If the individual resistances or compliances were unequal or if the driving pleural pressures on the two regions were different an uneven distribution of inspired air was predicted. The authors concentrated on the uneven time constant (resistance-compliance product) explanation.

Using a two-compartment lung model similar to that of Otis et al. (1956) but with the compliances and resistances computed as non-linear functions of instantaneous volume and flow rate, Pedley et al. (1972) modelled the distribution of ventilation during constant inspiratory flow. Pleural pressure differences in the model were static, corresponding only to the hydrostatic pressure difference between the compartments; the uneven distribution of the flow was determined by the regional time constant differences. The model of Pedley et al. (1972) accurately predicted the experimental data of Bake et al. (1974) for regional resistances that were similar throughout the lung, but it could not account for the later findings of Sybrecht et al. (1976). These authors introduced a time-varying pleural pressure into a simplified version of the model, allowing them to generate values similar to their data. The model of Sybrecht et al. (1976) used resistances and compliances that were linear functions of flow rate and volume.

Pedley et al. (1972) and Sybrecht et al. (1976) modelled distribution of ventilation only during constant flow inspiration. Jansson and Jonson (1972) presented a model for continuous breathing with different flow patterns, but based on uniform pleural pressure variations. Chang and van Grondelle (1981) modelled tidal breathing generated by a sinusoidal pleural pressure that was different in magnitude over the two compartments. In this model the distribution of

a tidal volume was seen to be a function of the difference in regional pleural pressures. The work was extended by Shykoff, van Grondelle and Chang (1982) to include different forms of pleural pressure variation and possible phase lags between compartments.

Lutchen et al. (1982) proposed a model in which the difference in composition of the alveolar and deadspace gas was included. In their two compartment model, compliances and resistances were non-linear functions of volume and flow rate but the pleural pressure driving force was the same on both compartments and there was no hydrostatic difference between them. The effect of changes in the static pleural pressure and resultant functional residual capacity and of the frequency on nitrogen washout was modelled. For a lung with equal resistances and compliances in both compartments there was no effect but for a highly non-uniform lung the interactive effect of operating point and frequency could be seen.

2.3 KRYPTON-81m

2.3.1 PRODUCTION AND RATIONALE

Although xenon-133 was and is used widely in lung function studies, it is not the perfect tracer for lung studies. In 1970, two papers appeared in which the production and use of krypton-81m was described. The ventilation studies were done using boli of air marked with krypton-81m (Clark et al., 1970; Yano et al., 1970). Records were made during a single breath. The advantages of krypton-81m over xenon-133 that were given were the higher energy of the gamma ray (190 Kev instead of 90 Kev) and the resultant rapidly acquired images, the low radiation dose to the subject, and the possibility of repeat

studies because of the short half-life of the isotope.

Krypton-81m is produced from rubidium-81 which may be generated in a cyclotron by the bombardment of sodium bromide crystals with alpha particles. The rubidium is separated from the remaining sodium bromide on an acidic cation exchange resin where the isotope is retained. Rubidium-81 (half-life 4.7 hours) decays by electron capture to krypton-81m (half-life 13 s), which then undergoes isomeric transition to stable krypton-81, emitting a 190 Kev gamma ray in the process. The radioactive krypton-81m may be eluted from the parent rubidium by passing air or water through the resin column.

Fazio and Jones (1975) realized the potential of krypton-81m for studying tidal breathing. Because of the short half-life of the isotope, no equilibration of the lungs is possible during quiet breathing in adult man and the decay of the krypton-81m in the lungs was considered to be approximately as fast as its arrival. The number of moles of krypton-81m in the lungs (and hence the number of counts) is proportional to

$$Q/((Q/V)+\lambda),$$

where Q is the rate of ventilation, V is the volume, and $\lambda = 3.2 \text{ min}^{-1}$ is the decay constant of krypton-81m. For quiet breathing when the ratio Q/V is much less than λ , the number of counts becomes proportional to the regional ventilation.

In a review paper, Hughes (1979) discussed the use of krypton-81m. In addition to the advantages mentioned above, he considered two problems: that quantitative measurements of ventilation are difficult without the use of a second isotope to measure the regional lung volume, and that a facemask delivers a time-varying

concentration of the tracer to the subject unless a well-mixed reservoir is provided upstream of the mask. Amis and Jones (1980) discussed, in addition, the underestimation of the ventilation that may result from long transit times to the lung periphery, especially in obstructed lungs. They also reviewed the advantages of the isotope: low tissue solubility, a clean spectrum at 190 Kev, the short half-life, low radiation dose and possibility of repeat measurements, the lack of waste-disposal problems, and the ease of qualitative interpretation of the images.

2.3.2 STEADY STATE MEASUREMENTS WITH KRYPTON-81m

2.3.2.1 *Physiological Studies*

Measurements of the steady-state activity over the chest have been made during tidal breathing of krypton-81m. The isotope was eluted by a constant flow of air through a generator and delivered through a face mask to the subject. The relative number of counts in a region could be interpreted directly as regional ventilation. Fazio and Jones (1975) remarked that technicium-99m perfusion scans could be performed in the same session for immediate comparison with the ventilation images because the similar energy of the photons from the two substances permitted the use of the same detector and the rapid elimination of the krypton gas allowed the perfusion study to be done immediately after the ventilation scan.

The investigative potential of krypton-81m was exploited almost immediately to measure ventilation perfusion ratios. Harf et al. (1976, 1978) used the gas in both tidal breathing ventilation scans and perfusion scans at a single session in seated subjects. The ratios of the ventilation to perfusion were found pixel by pixel. Amis et

al. (1977) extended the work to subjects in other postures. In seated subjects a gradient in the ventilation perfusion ratio was seen from a mean value of 1.8 in the apices to about 0.8 in the bases (Harf et al., 1976, 1978). In other postures the ratios decreased from the superior to inferior part of the lung in lungs that were at a high resting volume (non-dependent lung in the lateral decubitus positions and both lungs in the prone suspended posture) and increased in smaller lungs (dependent lung in the lateral decubitus position and both lungs in the supine position) (Amis et al., 1977). By using krypton-85 also, Amis et al. (1978) obtained volume images, allowing them to quantitate their measurements of ventilation and perfusion ratios. Elderly subjects had ventilation perfusion ratios very similar to those of younger subjects (Harf and Hughes, 1978).

During bicycle exercise seated subjects showed ventilation perfusion ratios more uniform than those at rest (Harf et al., 1978). In the study, the regional counts of both ventilation and perfusion were normalized using the respective total counts. This stabilised the relationship between the normalised counts and the normalised ventilation even for the increased breathing rates at exercise. The proportionality held so long as the regional ventilation per unit volume was similar to the overall value, even if it was non-negligible relative to the decay constant of krypton-81m. To eliminate the factors in the ventilation perfusion ratio of tissue absorbance and of the varying amounts of lung tissue over different parts of the gamma camera, Harf and Meighan (1980) used the same tracer to measure both. This advantage was not stated explicitly in the previous studies in which the technique had been used.

Scans of the lungs of infants and small children must be corrected for the high rates of specific ventilation that occur. Ciofetta et al. (1980) presented a method that incorporated the steady-state counts, in this case more nearly a measure of lung volume, with a regional washout of krypton-81m. The washouts gave the value of the denominator in the expression of Fazio et al. (1975). The technical difficulties inherent in obtaining a repeatable washout measurement with an isotope that decays as fast as krypton-81m does were not discussed. By combining the techniques the authors were able to make quantitative measurements of both ventilation and specific ventilation in infant lungs. The need for such a combined method was further illustrated by Arnot et al (1981); a comparison of nitrogen-13 washouts and krypton-81m steady-state scans in anaesthetized dogs showed that the krypton count rates began to underestimate the regional ventilation when specific ventilation rates reached 1.5 min^{-1} .

2.3.2.2 *Clinical Applications*

The advantages of krypton-81m as a tracer extend to clinical work. Goris et al. (1977) used it for lung imaging in patients because of the low radiation dose and the speed of acquisition. Four views of 250,000 counts each were obtained with only 80 mrad delivered to the lungs. Patient cooperation was not a problem since only tidal breathing from a mask was needed. Georgi et al (1979) also used from two to four views. By using high krypton-81m concentrations in the inspire, they obtained weak images as inspiration began in addition to those at steady state.

Li et al. (1979) suggested that the properties of krypton-81m and the ease of administration made it particularly suitable for pediatric use. Papanicolaou and Treves (1980) agreed because of the low dose delivered and the possibility of sequential studies. They cautioned, however, as did Ciofetta et al (1980), that in small lungs the quantity measured directly is volume, not flow. Not all authors doing pediatric work have taken note of this warning; Heaf et al. (1983) misinterpreted their data when they failed to consider the small lung volumes.

Bartsch and Linsmaux (1980) reviewed the diagnostic patterns seen with krypton-81m scans where pulmonary emboli cause the mismatch of ventilation and perfusion, carcinoma creates a large area where both ventilation and perfusion are abnormal, and emphysema appears as patchy defects in both ventilation and perfusion. Schor et al. (1978) compared the diagnostic use of krypton-81m and xenon-133 in obstructive and embolic disease. They concluded that while krypton-81m was superior in embolic disease, xenon-133 was to be preferred for the diagnosis of obstructive conditions. Susskind et al. (1981a) compared xenon-127 to krypton-81m and similarly found the xenon-127 with its long half life superior for the detection of obstructive disease. The krypton-81m may not have time to penetrate deeply into the severely obstructed lung before it decays.

Because krypton-81m scans may be performed without the patient having to follow particular breathing patterns, examinations may be made during and immediately after asthmatic crises (Fazio et al., 1979). Kawakami et al (1981) showed that tidal breathing of krypton-81m was adequate to detect defects of ventilation in asthmatics before and after exercise but that a bolus inhaled at residual volume

during a vital capacity inspiration was a more sensitive test.

For the detection of embolic lung disease, krypton-81m is well suited. As was discussed above, it may be used to advantage as both the ventilation and perfusion tracer (Harf and Meignan, 1980). It also has been used by Susskind et al. (1980) as a ventilation tracer when technicium-99m on microaggregates was the perfusion tracer and xenon-127 measured volume. Meignan et al. (1982) compared krypton-81m and technicium-99m microaggragate perfusion scans and found them to be equally good at detecting perfusion defects. The areas located were comparable to those seen with angiography.

Some diseases cause localized changes in ventilation. Acevedo et al. (1980) used the differences among nearest-neighbour pixels of krypton-81m ventilation and perfusion scans which had been divided pixel by pixel by xenon-127 volume scans to measure these abnormalities. Susskind et al. (1981b, 1982a, 1982b) continued the work and applied the comparison technique of local ventilation per unit volume to clinical situations, in particular to the diagnosis of pneumoconiosis. For analysis of such small zones, the number of counts recorded must be high.

2.3.3 DYNAMIC STUDIES WITH ISOTOPES

Respiratory motion reduces the resolution of steady state lung images, particularly in the regions near the diaphragm (Alderson and Line, 1980). Also, the variations of the distribution of ventilation with time are obscured by the summation of all parts of the breathing cycle. A series of "motion free" images, a dynamic series that spans the cycle, would both reduce the blurring and provide the temporal information.

The series that is easiest to obtain consists of one or two images per breath. DeLand and Mauderli (1972) used a potentiometer on a tape around the chest to trigger the gamma camera and collected data at a preselected lung volume. Although motion artifacts were reduced considerably, much information was lost and the acquisition was complicated by the extra apparatus.

Alderson et al. (1979) acquired images in mechanically ventilated dogs. The pump signal was used to trigger the camera. In one series of experiments, images were obtained only at peak inspiration and end expiration. In another, fourteen images were obtained per cycle. The mechanical ventilator eliminated the problems of variability among cycles, but also changed the pattern of ventilation.

Touya et al. (1979) obtained four basic images per breath in xenon-133 rebreathing studies. The details of the reconstruction are not given in the abstract, but it seems to have been based entirely on the activity record. Lung volume parameters such as total lung capacity, tidal volume, vital capacity and residual volume were computed in normal subjects and in patients with obstructive lung disease.

Line et al. (1980) used a pneumotachometer at the mouth to measure flow during a scintigraphic acquisition with xenon-127. The flow signal was sampled along with a "list mode" acquisition of the radioactivity, that is, an acquisition in which time coordinates are recorded in addition to the spatial grid. The flow signal was used to match the activity corresponding to the same flows and volumes from successive breaths in the recorded data. Dynamic series were generated

by adding the activities breath by breath.

Deconinck et al. (1982) reconstructed an average cycle and analysed the images by Fourier transforms of the spatial coordinates. The amplitude and phase images for the first two harmonics were examined. Few details are given in the abstract.

Although a pneumotachometer can provide a reliable signal for use in the reconstruction of an average breath, it requires an analog to digital converter channel synchronised with the gamma camera data. Kaplan et al. (1982) showed that the cycle could be reconstructed from the list mode scintigraphic data themselves. The total activity for each 200 msec interval was computed from the smoothed data. The durations of inspiration and expiration were found for each breath and the data were reframed to a constant length of 16 frames per breath. The individual breaths then were summed to produce the dynamic series of an average cycle. Although Kaplan et al. (1982) generated a dynamic series from a krypton-81m scan, they did not attempt to interpret the activity in terms of flow or volume.

2.3.4 WASHOUT MODELS

Because the half-life of krypton-81m is so short, washout measurements must account for decay. Bajzer and Nosil (1977) presented a simple model for the washout of a gas with a short half-life. The lung was depicted as a well-mixed compartment with a constant flow of gas through it from an inlet at a fixed concentration to the atmosphere which does not contain the tracer gas. The specific ventilation of the compartment was calculated from the concentration of the decaying tracer. Despite the simplicity of this model, it produced values comparable to experimental data for a whole-lung washout. Therefore,

Spaventi et al. (1978) used the model to interpret washout measurements for large regions. The mean values of specific ventilation were found to be $0.022 \pm 0.002 \text{ s}^{-1}$ for both lungs together, a value 27% less than that found by Secker-Walker et al (1975) by xenon washout techniques.

Bajzer and Nosil (1980) later improved the model by including an arbitrary number of parallel well-mixed units and periodic breathing and lung volume. The specific ventilation was calculated using the model and washout data for seven subjects. The average for both lungs together was $0.033 \pm 0.003 \text{ s}^{-1}$, closer to the values of $0.031 \pm 0.003 \text{ s}^{-1}$ (Secker-Walker et al, 1973) and $0.030 \pm 0.003 \text{ s}^{-1}$ (Secker-Walker et al., 1975). The average ratio of tidal volume to functional residual capacity was computed to be 0.097 ± 0.005 .

Ciofetta et al. (1980) fit the washout curves that followed both ventilation and perfusion. Because the elimination of krypton-81m by dilution and its decay can be considered to be monoexponential functions, the logarithm of the number of counts was taken to be $Q/V + \lambda$ during the washout phase. It was computed when the number of counts had dropped by one half. For ventilation studies the volume in question was the ventilated alveolar volume while for perfusion it was that into which the gas diffused from the blood. Differences in the clearance rates reflected ventilation perfusion mismatch.

Krypton-81m has proven to be a versatile isotope for functional studies of the lung. Although many uses have been found for it, its potential has not been fully explored, particularly in the generation of dynamic series.

2.4 BREATH SOUNDS

2.4.1 ORIGINS AND TRANSMISSION OF LUNG SOUND

Interest has been shown in vesicular lung sounds since the invention of the stethoscope by Laennec in 1819, but the amount of scientific work done on the subject is small. Murphy (1981) provides an excellent overview of the earlier work.

The interpretation of lung sounds is difficult because the site and mechanism of their production remains unclear and the nature of their propagation is ill-defined. Several studies have been performed to deal with these issues.

Bullar (1884) examined several theories of the production of respiratory sounds. Using isolated sheep or calf lungs in an airtight chamber with a bellows on the bottom, he showed that vesicular sounds were produced by the movement of air within the lungs even when the trachea and glottis were bypassed. However, volume changes of the lungs caused by changing the pressure in the box with the upper airways occluded to prevent flow generated no sounds. He concluded that the sounds came from the flow of air within the lungs rather than from flow at the trachea or from the tissue expansion.

Not everyone was convinced that the sounds were produced in the lungs. Hannon and Lyman (1929) thought that the tracheal flow could be the source of the higher frequency sounds heard through the chest wall. The sound heard from the human chest was very similar to that heard simultaneously across an inflated sheep lung placed against the person's larynx, except that there were more low frequencies heard

over the chest. Banaszak et al. (1973) proposed that lung sounds were generated by turbulent flow at the larynx and at the carinas of the larger bronchi and that the lung acts as a selective band-pass filter. Gavriely et al. (1981) postulated that the sounds heard over the chest were filtered tracheal sounds.

Hardin and Patterson (1979) ascribed the production of respiratory sound to vortex shifting in the fifth to thirteenth generations of branching in the human tracheo-bronchial tree. Both the sound intensity and the frequency then would depend on the flow velocity through the bronchi and on their diameters. Their theory was compared briefly to data for forced expiration, but only in terms of the frequencies of sound that might be generated, not the amplitude. It was used to model inspiration, but without modification from the pattern of four vortices, acceptable for expiration but unrealistic for inspiration.

Kraman (1983a) pointed out that much of the sound detected over the chest may have non-respiratory origins. Muscle sound in particular could contaminate the lower frequencies, as contracting skeletal muscle is reputed to generate sound with a peak frequency at about 25 Hz and a sound pressure of 60 - 70 dB (Oster and Jaffe, 1980).

The transmission properties of excised horse lung were measured by Rice (1983), but the transfer functions were not reported. The speed of sound in the parenchyma was found to be less than that in air or in soft tissue, ranging from 25 to 70 m s^{-1} , depending on the degree of lung inflation. Sound travelled directly through the parenchyma, not through the airways where it would have had the free-field speed in the air (300 m s^{-1}) with little attenuation.

Kraman (1983b) confirmed that sound travels at a similar speed in human lungs in vivo. White noise (125-500 Hz) was applied at the mouth and detected at eight points on the chest wall. The maxima of the cross correlations and estimates of the distance gave sound speeds of 23 to 33 m s⁻¹. The frequency characteristics of the transmission were poorly defined by the data.

2.4.2 SUBJECTIVE MEASUREMENT OF LUNG SOUNDS

2.4.2.1 *Indices*

The simplest method of quantifying lung sounds is to scale subjectively what is heard through a stethoscope. Nairn and Turner-Warwick (1969) graded sound intensity from 0 (absent) to 3 (normal) and compared the score with xenon-133 distribution indices in emphysema patients. Although the two observers disagreed in 52% of the measurements they were within one grade of each other in 90% of them. The means of the isotope distribution indices increased with the sound intensity score but the means plus or minus one standard deviation overlapped for all grades.

Bodhana et al. (1978) also graded sounds from patients breathing at their maximum inspiratory flow rates. They found good correlations between the sum of the grades obtained in all zones and various indices of airflow obstruction. In normal subjects, the sound index was found to be related to inspiratory flow rates.

2.4.2.2 *Expanded Time Base*

If the sounds are recorded, other methods of analysis are available to the investigator. Murphy et al. (1977) examined recorded sound by expanding the time scale. When the time base was stretched,

different waveforms were distinguishable. Adventitious sounds could be differentiated clearly from vesicular sounds.

2.4.3 SOUND SPECTRA

The frequency content of the lung sounds could be a valuable source of information. Banaszak et al. (1973) studied it using a narrow (10 Hz) band-pass filter. They measured the sound intensity (rms voltage from the microphone) between 75 and 500 Hz in data recorded from the right posterior basal lung of subjects, seated in a soundproof room. As flow at the mouth increased, the sound intensity increased at all frequencies, apparently exponentially. No curve fitting was attempted to confirm this form of functional relationship. The intensity at the lower frequencies was always higher than that at the higher ones. Inspiration was louder than expiration, and the sounds were greater at volumes nearer FRC than TLC. The higher frequencies were more attenuated than the lower ones at high lung volume. Using similar techniques in patients with tuberculosis, Majumder and Chowdhury (1981) observed more high frequency components than in normal subjects.

Wooten et al. (1978) placed two microphones over homologous lung segments. The sound signals were amplified, integrated to produce the amplitude, or passed through a real time spectrum analyser. No high pass filtering is mentioned in the text but a filter is shown in the circuit diagram. (Similarly, the rectification of the sound waveform before integrating it is depicted only in the schematic.) The sound intensity was seen to increase curvilinearly with the instantaneous flow rate after a threshold flow was reached. In the presence of an obstruction (mucus plug) the area was silent despite

normal sounds in the surrounding regions. The amplitude of the sound components at a given frequency as a function of time were plotted in three dimensions and showed a steady peak near 200 Hz and time-varying higher frequency components. Abnormal high frequency sounds showed clearly.

Using the same equipment, Schreiber et al. (1981) studied 28 normal subjects ranging in age from 7 to 73 years. The subjects were seated in a soundproof room with paired microphones mounted posteriorly on homologous segments of their chests. The Fourier transforms of 8 - 10 breaths were averaged. In all subjects, the peak frequency was between 116 and 225 Hz, with the overall mean being 162 Hz. The peak frequency increased with age. It was higher over the apex than over the base but was the same for homologous segments.

Urquhart et al. (1981) measured the spectrum of sounds recorded from 5 normal subjects and 15 patients. The subjects were seated and a microphone was hand held against the ninth or tenth posterior intercostal space. No high pass filtering was used. The frequency of the maximum amplitude components ranged from 5 to 50 Hz, in the range of movement artifact and muscle noise. Because of this major problem in methodology it is impossible to interpret the results presented by the authors.

Chowdhury and Majumder (1981) also measured the spectra of breath sounds in normal subjects and in patients. Again, no high pass filtering is mentioned. Frequencies of peak amplitude are reported at 273 Hz in normal subjects and at 59 Hz in patients with tuberculosis.

Gavriely et al. (1981) measured spectra in 10 normal subjects at 5 points on the anterior chest: over the trachea, over the right apex, and over the bases. The sounds were high pass filtered at 75 Hz, digitized at 4 kHz and Fourier transformed. Since the peak power was found at 75 Hz, the cut-off of the filter, any interpretation of the spectra is difficult. In all likelihood, the authors were looking at the edge of the band that they were trying to remove by filtering. Tracheal sounds were reported to be approximately white from 75 to 900 Hz.

Charbonneau et al. (1983) measured only the tracheal sound. Using a hand-held microphone probe, they recorded the sounds above 60 Hz in seated normal subjects and asthmatics breathing at peak flows of 0.5 L s^{-1} and 1 L s^{-1} . The spectrum was not white but demonstrated a peak frequency near 200 Hz and a band-width of less than 200 Hz in normals and of less than 250 Hz in asthmatics. The spectrum was a function of flow rate. On inspiration it shifted to higher frequencies at the higher flow rate in normals but remained approximately constant in asthmatics while on expiration it shifted to lower frequencies in normals and to higher frequencies in asthmatics.

Pasterkamp et al. (1983) recorded breath sounds from healthy newborn infants. The peak frequency of the sounds during inspiration fell near 150 Hz and that for expiration was about 130 Hz. The variation in the sound power among infants was large, but the band-width of the sounds remained similar. All showed lower peak frequencies on expiration, as if the sounds were more like adult tracheal sounds than like adult vesicular sounds.

The reports of the spectral analyses in which the methodology appears to have been well considered give a peak frequency range between about 100 Hz and 250 Hz for adults and slightly less in infants. Tracheal sounds are in a similar band.

2.4.4 SOUND INTENSITY

In a systematic attempt to relate the intensity of lung sounds to regional ventilation, Leblanc et al. (1970) recorded the sounds from the left anterior chest wall at the third intercostal space on the mid-clavicular line and from the left posterior chest wall 3-4 cm below the shoulder blade. Measurements were made from subjects seated upright and in the left and right lateral decubitus positions. The subjects breathed at constant flow rates through their vital capacities for 10-15 breaths. Sound signals were high pass filtered at 100 Hz before being rectified and integrated. In some experiments, the signals were band pass filtered between 200 and 350 Hz, apparently eliminating the expiratory sounds.

In the upright posture, a family of linear relationships was found between the sound intensity (the integrated, rectified, filtered signal) and the inspiratory flow rates measured at the same lung volume. Generally, the greater was the volume the steeper was the slope for the basal region, and the flatter for the apical zone. The difference between 50% and 70% TLC was difficult to distinguish. The sound intensity in the basal region as a function of volume at a constant flow rate increased to a maximum between 30% and 50% TLC, then decreased again. In the apical zone, it decreased steadily in a curvilinear manner. In the lateral decubitus positions the sound

intensity in the dependent lung exhibited a pattern similar to that in the base of the upright lung, and in the non-dependent lung it behaved as in the apex. The sound intensity as a function of total lung volume seemed to depend in some way on the vertical gradient of the distribution of volume and of ventilation.

Ploysongsang et al. (1977) continued to explore the relationship between the intensity of lung sounds and ventilation. They recorded with a pair of microphones, one on the right anterior axillary line 5 cm from the lung apex and the other on the same vertical line either 10, 15, or 20 cm from the apex on the chest wall of seated or supine subjects. The subjects inhaled small volumes from FRC at flow rates ranging from 1 to 2 L s⁻¹ (1×10^{-3} to 2×10^{-3} m³ s⁻¹). The recorded sounds were differentiated, band pass filtered between 150 and 350 Hz, rectified and integrated. In addition, white noise (2 to 700 Hz) with power from 4 to 9 watts was applied at the mouth during low flow rate inspirations to measure the transmission characteristics of the lung and chest wall. After the sound measurements were completed xenon-133 studies were performed.

The instantaneous values of the treated breath sounds and transmitted white noise signals at the three lower positions were compared to those at the most apical point. By considering the ratio of the the sounds detected in one place to the sounds simultaneously recorded in another, the effects of variations with time of total lung volume, of total flow rate, and, for the transmitted sounds, of glottic aperture, were eliminated. Local variations in flow, volume, and transmission properties, in contrast, were not. The average ratio, the "breath sound index", was computed as the slope of the plot of the sound intensity at a position against the sound intensity at the

reference point as both varied with time. The transmission indices were computed in an identical manner. The transmission plot produced a straight line but the breathing sounds caused a narrow loop to form. The inspiratory part was considered to be linear.

The breath sound index decreased from approximately 1.5 at the point 10 cm from the apex to a value only slightly greater than one at the point furthest down the lung in both the upright and the supine positions. The transmission pattern was similar, but decreased to a value somewhat less than one by the 15 cm position. The authors argued that the difference between the ratios of breath sounds and the ratios of transmitted white noise at any location indicated that the breath sounds were generated near each microphone rather than being transmitted from a central point of origin. They then used the transmission ratios to correct for the attenuation of the breath sounds in the chest, despite their argument that the transmission pathways were different.

The breath sound indices were divided by the matching transmission indices to generate the "compensated breath sound indices". The compensated breath sound indices increase with distance down the lung. In the upright position the change was 150% while in the supine posture it was 100%. In discussing these numbers, the difference between the transmission path for the white noise applied at the mouth and that for the locally generated breath sounds was mentioned but could not be corrected. Neither the problem of the difference in power levels between the transmitted and generated sounds, and its effect on the propagation of the sounds nor the possible differential attenuation of the frequency components of the sounds was discussed.

The treated breath sound signals divided by their mean values correlated very poorly ($r=0.54$) with ventilation as measured with xenon-133 in seated subjects and not at all in supine subjects. Compensated breath sounds (treated breath sounds divided by their mean value, the whole divided by the ratio of the treated white noise transmission signals to their mean) correlated slightly better, but still poorly with the xenon-133 ventilation measurements in both upright subjects ($r=0.65$) and supine subjects ($r=0.56$). The correlation with regional volume was similar, with $r=0.61$ and $r=0.75$ in seated and supine subjects, respectively. Although the relationship between compensated breath sounds and regional ventilation accounted for only 42% and 31% of the variance of the data for upright and supine subjects respectively while that between the breath sounds and regional lung volume accounted for 37% and 56%, the authors concluded that the compensated lung sounds were a measure of regional ventilation.

Measurement of the compensated lung sound indices was continued by Ploysongsang et al. (1978). The sounds were measured as a function of lung volume in 5 normal subjects, both seated and supine. Transmission was not a strong function of volume in either position but the compensated breath sound indices increased to a maximum at volumes between 40% and 70% TLC in both positions. The increase was greater in the more basal regions and was both more distinct in the middle zone and at lower volume in the apical region in the upright than in the supine posture.

The mean ventilation per unit volume was computed from the data by making several assumptions. The ratio between the regional lung volumes in the upright and the supine position was assumed to be a constant for all lung regions. The ventilation per unit volume was

assumed to be uniform in the supine posture. Since the compensated breath sound indices were considered to be a measure of regional ventilation, the ratio of the upright to supine compensated indices for a given region was considered to be proportional to the ventilation per unit volume.

In patients with emphysema Ploysongsang et al. (1982) again measured breath sounds and white noise transmission over the range of the vital capacity and compared the data to xenon-133 measurements. The uncompensated breath sounds correlated poorly with ventilation per unit volume ($r=0.47$) and with lung volume ($r=0.48$) but slightly better with ventilation ($r=0.70$) as measured with Xe-133. Compensated breath sounds correlated poorly with ventilation per unit volume ($r=0.38$), with lung volume ($r=0.61$) and with ventilation ($r=0.65$).

When the treated breath sound signals from two locations were plotted against each other, a loop was seen. Ploysongsang et al. (1979) used this to investigate the difference in phase of the ventilation in two lung regions: Esophageal pressures and breath sounds were measured at the same horizontal position in seated subjects. At low lung volumes, loops were generated when the signal from one location was plotted as a function of that from the other, with the apical signal leading the basal one. Phase angles from 0° to 22° were computed by measuring the loops on an oscilloscope screen. At higher lung volumes the pressures and sounds were in phase.

Ploysongsang (1983) used this method to measure the phase differences of breath sounds in 15 smokers and 19 nonsmokers. The differentiated breath sounds from two locations were band pass filtered from 100 to 350 Hz, rectified, integrated, and displayed, one against

the other, on an oscilloscope. The microphones were placed on the anterior midclavicular line at points 5 cm and 20 cm from the clavicle. Two other microphones were placed laterally from the lower position. The subjects inhaled 200 to 300 ml (2×10^{-4} to $3 \times 10^{-4} \text{ m}^3$) from FRC at flow rates from 1 to 5 L s^{-1} (1×10^{-3} to $5 \times 10^{-3} \text{ m}^3 \text{ s}^{-1}$). When the apical signal was used as the Y axis and the basal signal was the X axis, looping was seen during breathing in all subjects, with the apex leading the base. When the signals from the laterally placed microphones were compared, however, only some subjects showed a phase difference. The leading or lagging was greater in smokers than in nonsmokers. Because sequential ventilation of regions that experience the same pleural pressure swing can be caused only by differences in regional time constants, the author suggested that smokers have small airway constrictions that can be measured using lung sound phase angles.

Kraman and his colleagues (Kraman, 1980, 1983c; O'Donnell and Kraman, 1982; Dosani and Kraman, 1983; Kraman and Austrheim, 1983) have investigated the patterns of lung sound intensity in standing subjects. Using two microphones at a time and filtering the signal between 200 Hz and 1 kHz, Kraman (1980) recorded sounds from points separated horizontally by from 1 cm to 6 cm on the back near the lung bases and on the front near the apices of the lungs. Vertical separations also were measured on the back and front. Sounds from the two microphones were balanced for amplitude before both addition and subtraction of the signals. The mean amplitude of the difference of the two signals divided by that of the sum of the two was termed the subtraction intensity index (SII).

The rationale for the use of the SII is that a single sound transmitted without phase distortion to the two locations would produce a SII value of zero no matter what the path differences involved. A lack of cancellation does not imply that the signals have different sources, because there may be a phase change during transmission, but any cancellation that does occur must result from the detection of the same sound twice. The author does not consider a major problem in the amplitude balancing to compensate for the different degrees of attenuation that may exist in the lung: because the recorded sounds are a summation of signals from many source, the attenuation of any particular component will be different from that of any other. Balancing the mean amplitude will not ensure a similar magnitude in two signals for a particular component from a common source unless that component is clearly dominant in both.

For homologous lung segments, the SII of a vocalized tone (central source) was always less than 50%. Vesicular sounds for the same locations, however, had SII greater than 80% in most cases. The SII increased linearly with separation of the microphones from less than 45% and 53% at 2 cm on inspiration and expiration respectively. A loud pleural rub gave an SII of 100% at 2 cm separation.

Because of the different degrees of cancellation of the signals, the authors concluded that the source of sound on expiration is more central than it is on inspiration, but that the vesicular sounds are produced peripherally in both cases. The source of the sounds was more central than the pleura, but it was impossible to define the location.

With a computer to sample the data, Kraman (1983c) made further measurements. Signals from two microphones were band-pass filtered between 200 and 625 Hz for that part of inspiration where the flow was greater than 1.3 L s^{-1} ($1.3 \times 10^{-3} \text{ m}^3 \text{ s}^{-1}$). Sounds were recorded at 24 points around the posterior chest near the lung bases and the anterior chest near the apices. The SII were difficult to interpret, but the sound intensities themselves were significantly different between sides in 7 of 9 subjects at the bases and in 6 of them at the apices. Neither side was consistently louder than the other. As the amplitude of the sound was reproducible in successive measurements, this demonstrated clear heterogeneity of lung sounds in standing normal subjects.

O'Donnell and Kraman (1982) prepared detailed maps of the lung sound intensity over the thorax in normal subjects. Sound signals from two microphones were band passed between 150 and 700 Hz and sampled when the flow at the mouth was greater than 1.3 L s^{-1} ($1.3 \times 10^{-3} \text{ m}^3 \text{ s}^{-1}$). The sound amplitude was averaged over 3 breaths at each point in a 2 cm x 3 cm grid. The amplitude over the anterior chest was greatest over the apices and decreased toward the bases, but on the posterior chest wall, the maximum amplitude occurred over the lung bases. Furthermore, in the lateral direction around the chest, although the average sound amplitude from all the subjects was roughly constant there was much point to point variation in each individual and the left lung sounds were always louder than the right. These results cast doubt on the interpretation of the lung sounds as a measure of regional ventilation.

Kraman and Austrheim (1983) repeated the mapping procedure in 7 subjects, measuring for one breath at each point. The sounds were band pass filtered between 100 and 1100 Hz. Transmission maps using noise, white between 50 and 500 Hz and injected at the mouth were plotted also. All transmitted sounds were normalized by the signal recorded simultaneously over the glottis to correct for the variations in the glottic aperture. The sound maps were in agreement with those produced previously, and the transmission maps over the right anterior chest matched the data of Ploysongsang et al. (1977), but over the left anterior chest where the other investigators had not measured, the transmitted sound amplitude was as little as half that over the homologous segments. Loudness of transmitted white noise was not related to the thickness of the chest wall as measured with a CT scan. The explanation proposed for this phenomenon was that sound injected at the mouth passed directly through the tracheal wall and right mediastinal pleural surface into the right lung but had to pass through the left airways to reach the left lung because the full thickness of the mediastinum insulates the left lung from the trachea. The mechanism of sound transfer from the mouth to the chest wall would seem to be different from that of its transfer within the lung. The authors concluded that it is inadvisable to use transmission from the mouth to characterize sound transfer within the lungs. Because the lung sounds were louder over the left side of the chest and the transmitted white noise was louder over the right side, such an application would have led to the unlikely conclusion that the ventilation in the left lung was more than twice that in the right lung for an erect normal subject.

In a further mapping study, Dosani and Kraman (1983) attempted to correct for the flow rate variation during breathing. Sounds were recorded from a 10 x 10 grid on the posterior chest wall while subjects breathed deeply. The mean amplitude of each 25 ms segment after the flow reached 1.3 L s^{-1} ($1.3 \times 10^{-3} \text{ m}^3 \text{ s}^{-1}$) was divided by the mean airflow for the same segment. All the ratios produced, the sound amplitude indices, were averaged to produce the sound amplitude index for the grid coordinate. The authors found a difference for this index between inspiration and expiration, marked intersubject variation in the intensity of breath sounds, a lack of bilateral symmetry in erect subjects, and a decrease in the sound intensity in the scapular region but none over ribs.

The division of the sound amplitude by the flow to produce the sound amplitude index implies that the relation between sound and flow is linear. In a recent study, Kraman (1984) examined the assumption. Four standing subjects were studied. Sounds from two microphones were recorded as the subject inspired to peak flows between 1.5 and 4 L s^{-1} for 20 breaths. The sounds were high-pass filtered at 200 Hz and recorded for later sampling at 5 kHz. Only those flows of 1.4 L s^{-1} or more were analysed.

The root mean square values of the sounds, the sound amplitudes, were taken in 25 ms increments. Either the maximum or the mean of the sound amplitude segments during a breath was paired with the peak flow rate, instead of matching the sound to the simultaneous flows. The sound amplitudes also were divided by the flows ("flow corrected") before being averaged over a breath, as had been done in the study of Dosani and Kraman (1983). The maximum, mean, and corrected sound amplitudes were plotted against flow on a breath to

breath basis, and linear regressions were performed. The data were scattered but the regression coefficients were acceptable, ranging from 0.69 to 0.88 for the mean and maximum sounds. However, in three of the four cases analysed, the corrected sounds were functions of the flow. The author surprisingly dismissed this point as unimportant and maintained that, since the correlation coefficients obtained with a third order polynomial fit were no better than those for the linear fit, the relation between sound amplitude and flow was linear. The coefficients of the flow terms in the higher order relation were not presented, nor was it considered that the choice of only high flow rates would make the distinction between a quadratic and a linear function more difficult, particularly when the data were scattered. The linearity of the relationship seems doubtful.

The literature of lung sound measurement indicates a number of controversies. The origin of the lung sounds is not established, the methodology for their measurement is not clear, and their precise meaning and quantitative clinical utility remains a mystery. In all the reported measurements, the intersubject variability is extremely high. Although some interpretations have been proposed for the sound indices, they are, for the most part, based on very shaky correlations. Before breath sounds can be used as a quantitative measure, more measurements and careful analysis are required.

CHAPTER 3

THE PLEURAL PRESSURE-DRIVEN MODEL

3.1 INTRODUCTION

Measurements made with xenon-133 showed that inhomogeneities in pleural pressures were highly significant in determining the distribution of boli at higher flow rates (Sybrecht et al., 1976). In washout studies also, the changes in distribution were found to be functions of the changes in the pleural pressure distribution (Sampson and Smaldone, 1984). A two-compartment model of breathing driven by the pleural pressure therefore was developed. The pleural pressure swings on the compartments are independent of each other in both amplitude and phase, and the pressure waveform may be sinusoidal, triangular, or square.

3.2 THE MODEL

The lung was modelled as the parallel combination of two compartments, a resistance in series with a compliance, each with identical intrinsic properties. A common resistance connected the two (Fig. 3.1). The compliances were non-linear functions of volume, the common resistance was a linear function of total flow rate, and the compartmental resistances were non-linear functions of regional volume and flow rate. A static difference in the pleural pressure between compartments represented the hydrostatic gradient between dependent and non-dependent lung regions. The time variations in pleural pressure, the driving force for ventilation, could differ in amplitude, phase and waveform between the compartments.

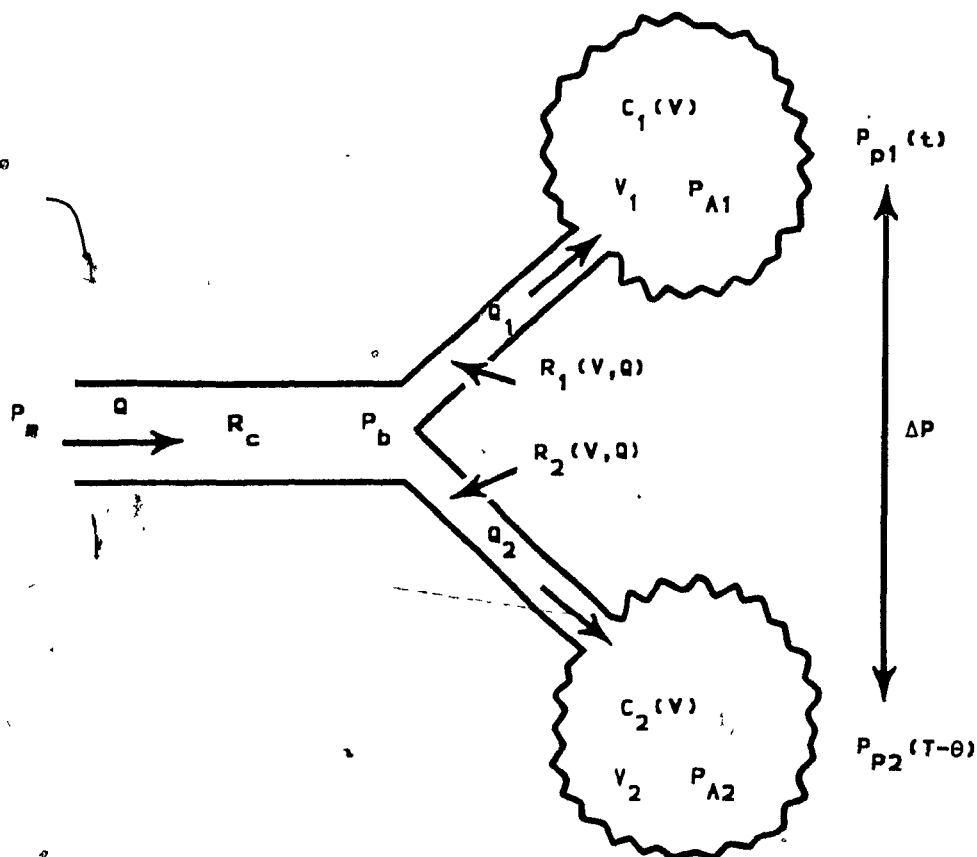


Fig. 3.1 A representation of the two-compartment model. The two compartments are characterized by their compliances C_1 , resistances, R_1 , alveolar pressures P_{A1} , flows, Q_1 and volumes V_1 . The common resistance is R_c causing a pressure drop $P_m - P_b$ when the total flow is Q . The time-varying pleural pressures are P_{p1} and P_{p2} separated by the hydrostatic difference, ΔP . A phase difference θ may exist between the pleural pressure swings.

The governing equations of the model are as follows:

In the common pathway,

$$P_m - P_b = R_c Q_i \quad (3.1)$$

$$Q = Q_1 + Q_2 \quad (3.2)$$

where P_m is the pressure at the mouth, P_b is the pressure at the bifurcation, R_c is the common resistance, Q is the volumetric flow rate, and the subscripts 1 and 2 refer to the compartments.

In the compartments ($i = 1, 2$):

$$P_b - P_{A1} = R_i Q_i \quad (3.3)$$

$$dV_i = C_i d(P_{A1} - P_{p1}) \quad (3.4)$$

where P_{A1} is the alveolar pressure, R_i is the resistance, C_i is the compliance, P_{p1} is the pleural pressure and Q_i is the volume of the compartment.

The compliance and the transpulmonary pressure were computed from the hyperbolic-sigmoid pressure volume curve proposed by Murphy and Engel (1978):

$$P = \frac{c_1}{(V_{max}^* - V^*)} + \frac{c_2}{(V_{min}^* - V^*)} + c_3 \quad (3.5)$$

$$C = \frac{-(V_{max}^* - V^*)^2 (V_{min}^* - V^*)^2}{c_1 (V_{min}^* - V^*)^2 + c_2 (V_{max}^* - V^*)^2} \times \frac{VC}{100} \quad (3.6)$$

where $V^* = 100(V - RV)/VC$, V is volume, VC the vital capacity, RV the residual volume, and c_1 , c_2 , c_3 , V_{max}^* and V_{min}^* are parameters of the curve. Data from Gibson et al. (1976) for healthy young men were used to fit the parameters (Table 3.1).

TABLE 3.1

CONSTANTS OF THE COMPLIANCE AND RESISTANCE RELATIONSHIPS

Compliance

$c_1 = 1500.0 \text{ cm H}_2\text{O}$
 $c_2 = 50.0 \text{ cm H}_2\text{O}$
 $c_3 = -8.5 \text{ cm H}_2\text{O}$

$V_{\text{max}}^* = 135 \%$
 $V_{\text{min}}^* = -2 \%$

Volumes

$\text{TLC} = 7.2 \text{ L}$
 $\text{RV} = 1.4 \text{ L}$

Resistance

	Compartments	Common
k_1	$= 0.3$	$0.3 \text{ cm H}_2\text{O s/L}$
k_2	$=$	$0.4 \text{ cm H}_2\text{O s/L}$
k_3	$= -0.17$	1.0
k_4	$= 0.3$	0.0 1/L

Resistance as a function of flow rate and volume was calculated using a combination of Rohrer's equation and that of Blide et al. (1964):

$$R_i = \frac{k_1 + k_2 Q_i}{k_3 + k_4 V_i} \quad (3.7)$$

for $i=1,2,c$. The k_j , $j=1, 4$ are constants (Table 3.1).

Data from several sources (Blide et al., 1964; Jaeger and Matthys, 1970; Briscoe and DuBois, 1958) were used to calculate the parameters.

The equations for the flow rates were rearranged and combined into two non-linear first-order ordinary differential equations. These were solved using either a second order Runge-Kutta method (Heun's method) (Dahlquist and Bjorck, 1974) (Chang and van Grondelle, 1981; Shykoff, van Grondelle and Chang, 1982) or a predictor-corrector method (FLAP) (Elliot, 1972) within Nexus (Hunter and Kearney, 1984). The compartmental flow rates were integrated to yield the individual tidal volumes, the ratios of which were used to define the distribution of ventilation between the two compartments. The effects of amplitude, frequency, amplitude ratios, phase differences and starting volumes were studied for sinusoidal pressure swings. Amplitude effects were examined also with triangular and square wave pleural pressure variations.

3.3 RESULTS

3.3.1 TIDAL VOLUME DISTRIBUTIONS

3.3.1.1 *Equal Pleural Pressure Swings*

When the amplitudes of the pleural pressure swings on the compartments were the same and the compartmental capacities identical, the distribution of ventilation was nearly independent of the

amplitude. When the static pressure difference was 2 cm H₂O (196 Pa), for a sinusoidally varying pleural pressure of frequency 15 breaths min⁻¹ with a functional residual capacity (FRC) of 54% TLC (total lung capacity), the ratio of non-dependent to dependent tidal volumes was 0.82±0.07 for amplitudes ranging from 0.5 cm H₂O to 5 cm H₂O (49 to 490 Pa). The ratios decreased by approximately 6% when the amplitude increased by a factor of five. The values for a 30 breath per minute sinusoid were almost superimposed on those for the lower frequency (Fig. 3.2a). The tidal volumes at the higher frequency were slightly greater than those at the lower frequency for the same excursion of pleural pressure (Fig. 3.2b). When the static difference in pleural pressure (Fig. 3.2c) was 4 cm H₂O (392 Pa), the tidal volumes were distributed more preferentially to the more dependent compartment and the decrease in the ratios with increasing amplitude of the pleural pressure swings was more marked.

3.3.1.2 Unequal pressure amplitudes

When the ratio of the amplitudes of the pleural pressure swings on the two compartments was different from unity, the tidal volume ratio was altered but remained essentially independent of amplitude (Fig. 3.2a). The effect of the amplitude ratio itself on the distribution was marked (Fig. 3.3), with approximately a 5% increase in the tidal volume ratio for a corresponding 5% increase in the amplitude ratio. The exact changes depended on the frequency and on the magnitude of the pressure swings; changes were greater for higher frequencies and smaller amplitudes.

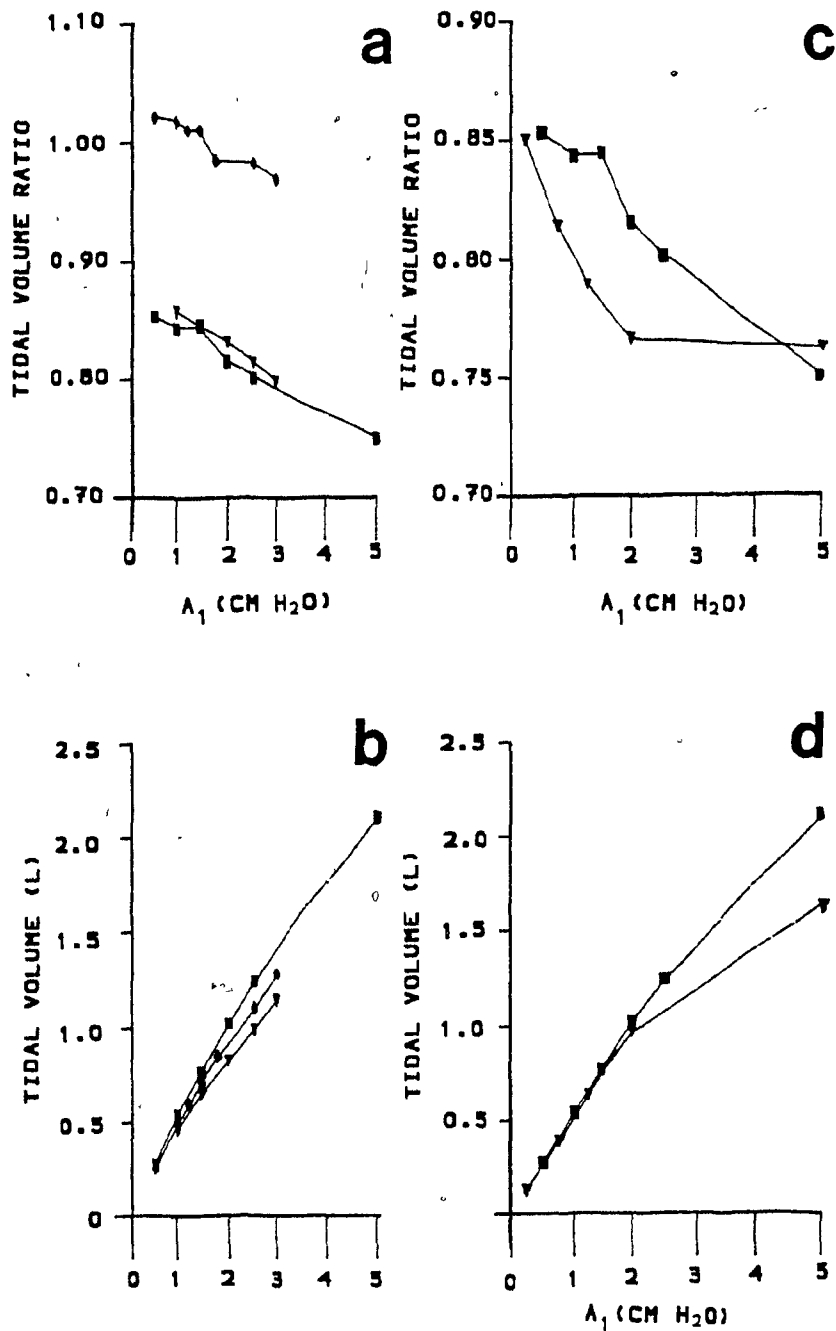


Fig. 3.2 Effect of the amplitude of the pleural pressure swing. The ratio of amplitudes A_1/A_2 is constant. a) Ratios of tidal volumes, non-dependent to dependent compartment. Static pressure difference $\Delta P = 2$ cm H₂O. Squares-- $A_1=A_2$, frequency $f=15$ breaths min^{-1} ; Triangles-- $A_1=A_2$, $f=30$ breaths min^{-1} ; Diamonds-- $A_1=1.2A_2$, $f=15$ breaths min^{-1} . b) Total tidal volumes corresponding to a). c) Ratio of tidal volumes, non-dependent to dependent compartment. Squares-- Same as in a) for reference. Triangles-- $\Delta P=4$ cm H₂O, $A_1=A_2$, $f=15$ breaths min^{-1} ; d) Tidal volumes corresponding to c).

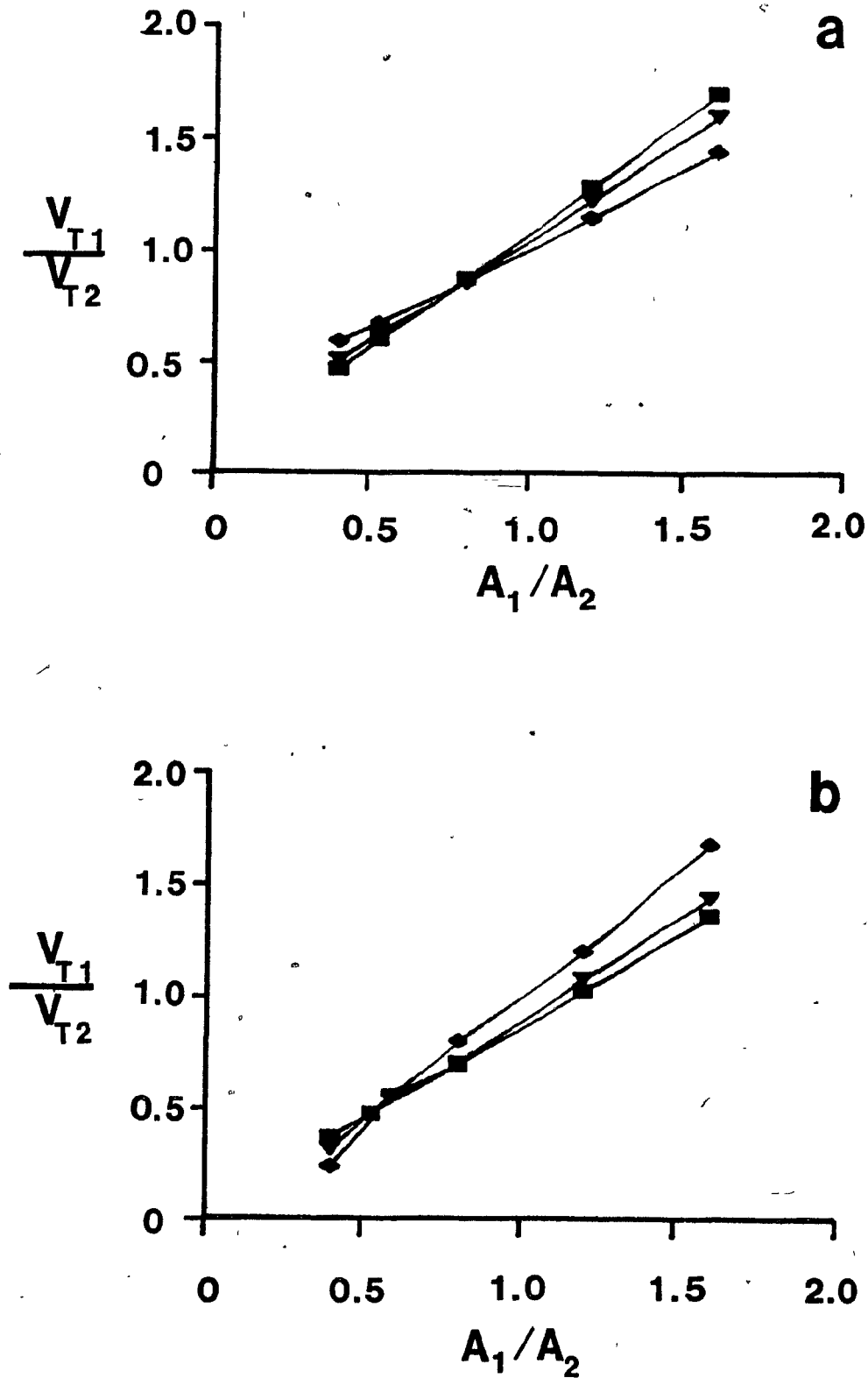


Fig. 3.3 Effects of pleural pressure ratio. Ratios of tidal volumes, non-dependent to dependent compartment as a function of the ratios of pleural pressure amplitudes A_1/A_2 . $\Delta P = 2$ cm H₂O. a) $f=15$ breaths min⁻¹. Squares-- $A_1=1.25$ cm H₂O; Triangles-- $A_1=2.5$ cm H₂O; Diamonds-- $A_1=5$ cm H₂O. b) $A_1=1.25$ cm H₂O. Squares-- $f=15$ breaths min⁻¹; Triangles-- $f=30$ breaths min⁻¹; Diamonds-- $f=45$ breaths min⁻¹.

3.3.1.3 Phase Differences

The phase relationship between the pleural pressures on the dependent and non-dependent compartments also was seen to affect the distribution of tidal volumes (Fig. 3.4a). Over the range of angles from -30° to 30° , the distribution ratio decreased by about 14% when the pressure swings were both 1.5 cm H₂O (147 Pa) and by about 17% when the non-dependent compartment experienced a variation in pressure of 1.5 cm H₂O (147 Pa) and the dependent compartment, of 1.25 cm H₂O (122 Pa). The compartment in which the pressure change lagged received a larger tidal volume than it did when in phase. The overall tidal volume was not affected (Fig. 3.4b).

3.3.1.4 Starting Volume

The results discussed above were obtained for excursions in volume increasing from a constant functional residual capacity (FRC) of 3.9 L ($3 \times 10^{-3} \text{ m}^3$). When the same variations in pleural pressure were applied at different starting volumes, both the tidal volume and its distribution between the compartments were altered (Fig. 3.5). For low starting volumes (less than 45% total lung capacity) the non-dependent compartment received more of the air. At higher starting volumes the distribution favoured the dependent zone, but as the volume increased from FRC, the distribution became more uniform again. The tidal volumes delivered increased slightly from the values at the lowest lung volumes to a maximum near FRC, after which there was a substantial decrease at higher volumes as the increasing stiffness of the lung took effect.

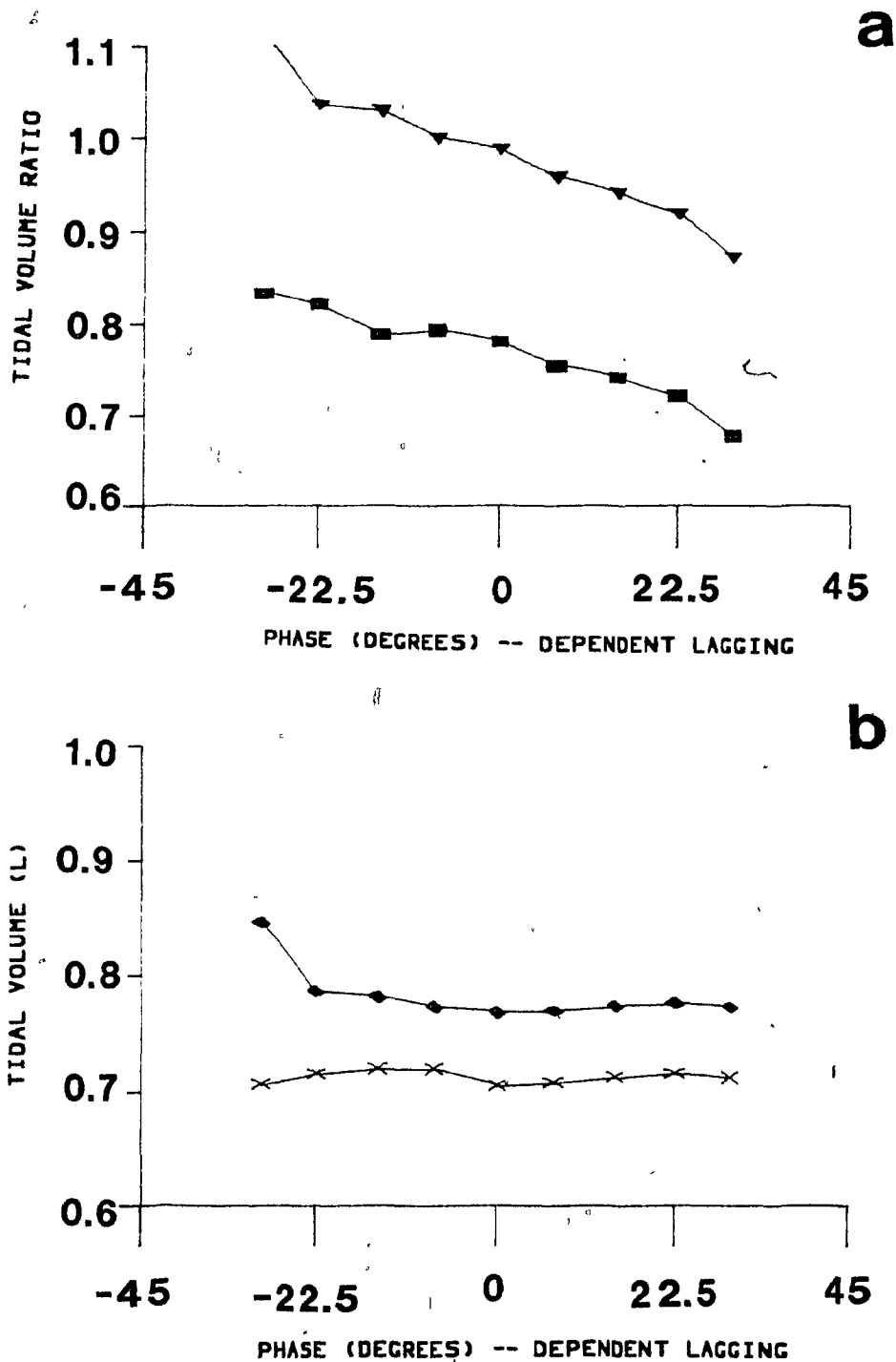


Fig. 3.4 Effects of phase difference in pleural pressure. Frequency $f = 15 \text{ breaths min}^{-1}$, $\Delta P = 2 \text{ cm H}_2\text{O}$. a) Tidal volume ratios, non-dependent over dependent compartment, as a function of phase shift. Squares-- $A_1 = 1.5 \text{ cm H}_2\text{O}$; Triangles-- $A_1 = 1.5 \text{ cm H}_2\text{O}$, $A_2 = 1.25 \text{ cm H}_2\text{O}$. b) Corresponding tidal volumes. Diamonds match squares, crosses match triangles in a).

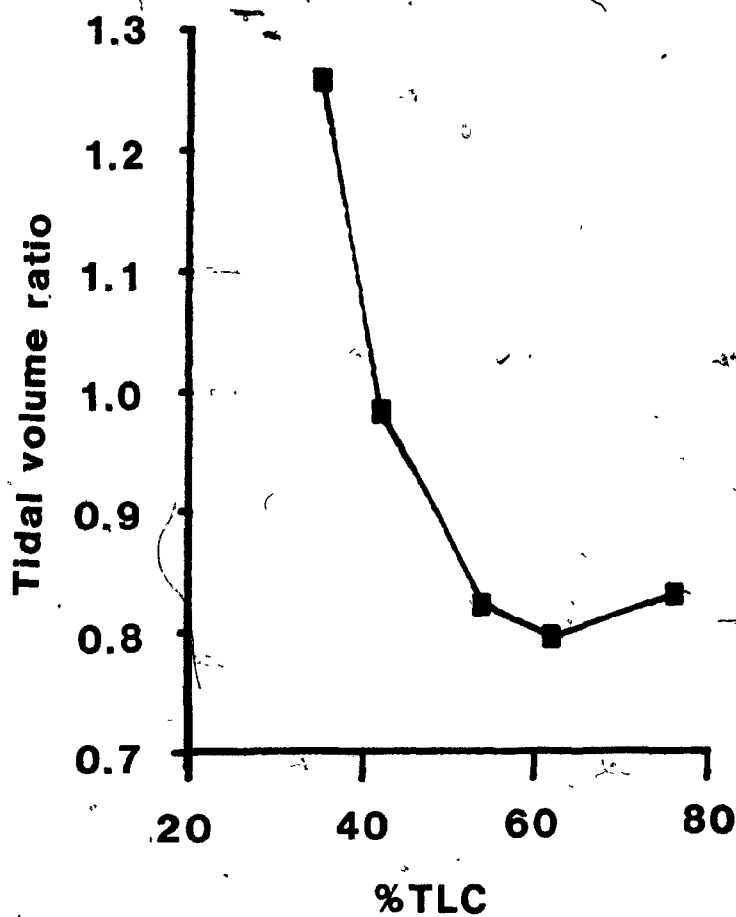


Fig. 3.5 Effect of starting volume. Ratio of tidal volumes, non-dependent over dependent compartment, as a function of the percentage of total lung capacity at FRC. $\Delta P = 2 \text{ cm H}_2\text{O}$, $\Lambda_1 = \Lambda_2 = 1.5 \text{ cm H}_2\text{O}$.

3.3.2 FLOW RATE

Although the applied pleural pressure swings were sinusoidal, the resultant flows were deformed by the nonlinear compliances and resistances. One effect of this was to shift the maximum and minimum flows in the two compartments relative to each other when a hydrostatic gradient existed between them (Fig. 3.6a, d). With a static difference of 2 cm H₂O (196 Pa), when the amplitudes of the pleural pressure swings were 1.5 and 1.25 cm H₂O (147 and 122 Pa) on the nondependent and dependent compartments, respectively, the tidal volume distribution ratio was unity and the total tidal volume was 700 ml ($7 \times 10^{-4} \text{ m}^3$) (Fig. 3.4). The maximum flow rates delivered to the compartments were also similar, but they occurred slightly earlier in the nondependent zone. Under the same conditions but with a phase difference between the pleural pressure swings, the dependent compartment leading by 15°, the tidal volume distribution favoured the nondependent compartment (Fig. 3.4a). Similarly, the maximum flow to the nondependent compartment was greater than that to the dependent one (Fig. 3.6b). Interestingly, the maxima in the two zones occurred almost simultaneously, the pressure lag having compensated for the delay seen in the zero phase difference case. For a phase difference in pleural pressure swings of 15° in the other direction, with the dependent compartment lagging, the tidal volume favoured the dependent compartment slightly (Fig. 3.4a). The slightly greater peak flows also occurred in that compartment (Fig. 3.6c). The phase difference was more evident in the flows in this than in the previous case.

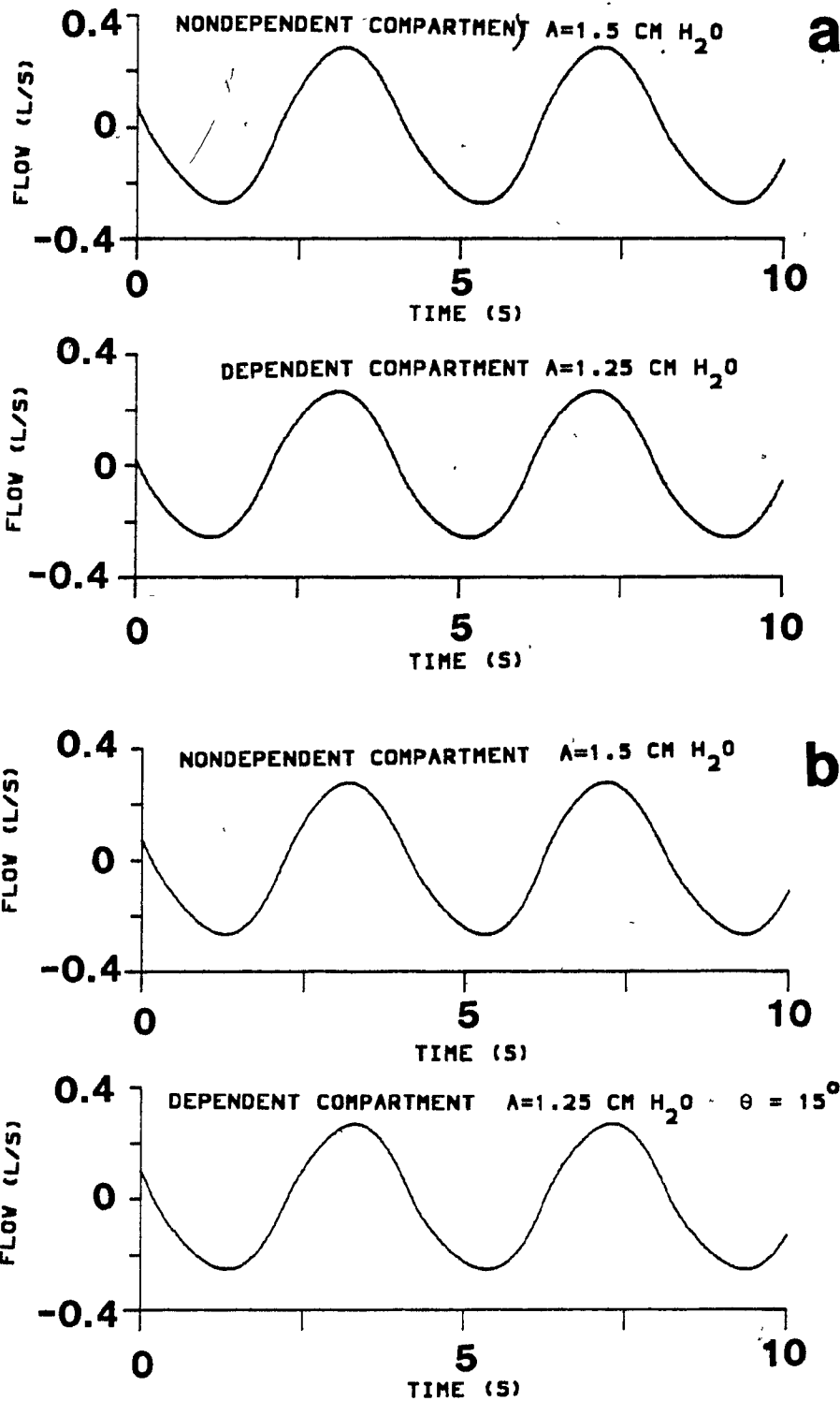


Fig.3.6 Flows generated showing effect of phase differences. a) Pressure swings are in phase. $\Delta P = 2 \text{ cm H}_2\text{O}$. $A_1=1.5 \text{ cm H}_2\text{O}$, $A_2=1.25 \text{ cm H}_2\text{O}$. b) Amplitudes and ΔP as in a). Pressure on dependent compartment leads by 15° .

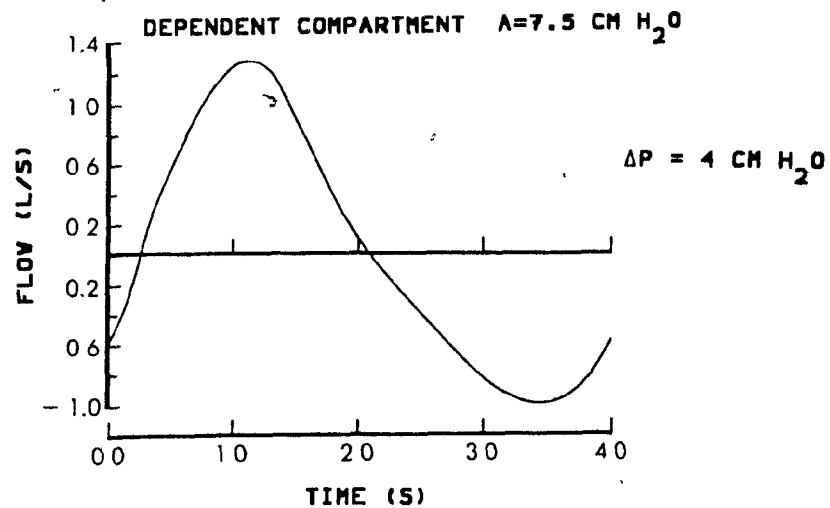
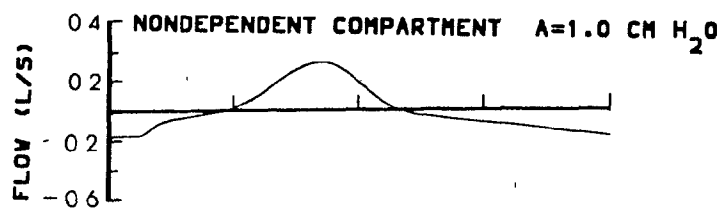
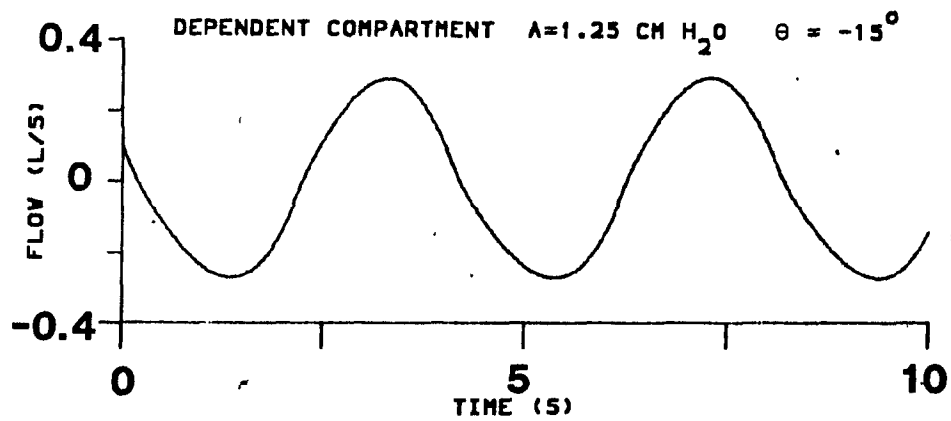
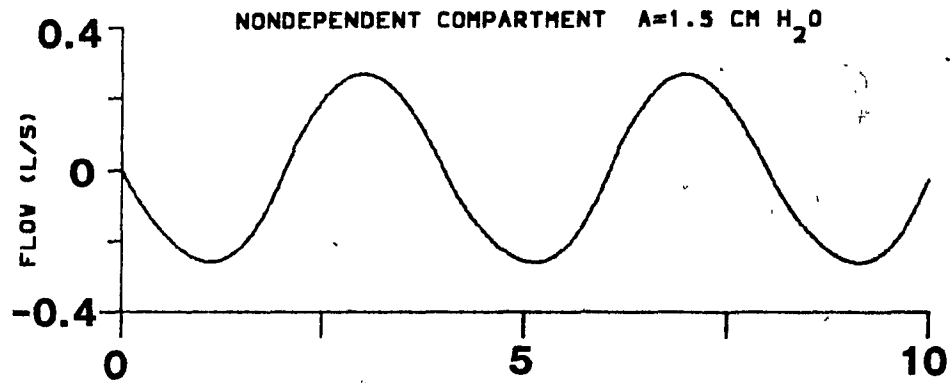


Fig.3.6 --Continued. c) Amplitude and ΔP are as in a). Pressure on non-dependent compartment leads by 15° . d) Pressure swings are in phase. $\Delta P = 4 \text{ cm H}_2\text{O}$. $A_1=1 \text{ cm H}_2\text{O}$. $A_2=7.5 \text{ cm H}_2\text{O}$.

Significant lags between the flows in the two compartments could be generated with extreme differences in the amplitudes of the two pleural pressure swings even when they were in phase. With a large static pressure difference as well, the effects were dramatic (Fig. 3.6d). The maximum flows in this example were almost one quarter of a respiratory period apart. Furthermore, the airflow was not direct from the mouth to one or other compartment. For the first half of the filling cycle of the dependent compartment, the nondependent one was emptying, its expirate transferring to the dependent zone. To a lesser degree, part of the inspirate of the dependent compartment was the early expirate from the nondependent region. Thus, pendelluft could be generated in the absence of intrinsic time constant differences.

3.3.3 WAVEFORM EFFECTS

3.3.3.1 *Tidal Volume*

The effect of amplitude on the distribution of tidal volume was examined for a triangular (sawtooth) pleural pressure variation. With equal pressure swings on the two compartments, the behavior was very similar to that with the sinusoidal variation (Fig. 3.7). The distribution was independent of the amplitude of the applied pressure swings. The tidal volume for a given amplitude was slightly less than in the sinusoidal case, since the lower pressure occurred for a slightly shorter time.

With a square wave pleural pressure swing, equal on both compartments, the tidal volume distribution again varied only slightly with the amplitude of the driving pressure, but in this case, in the opposite direction (Fig. 3.7a). For a five-fold increase in the

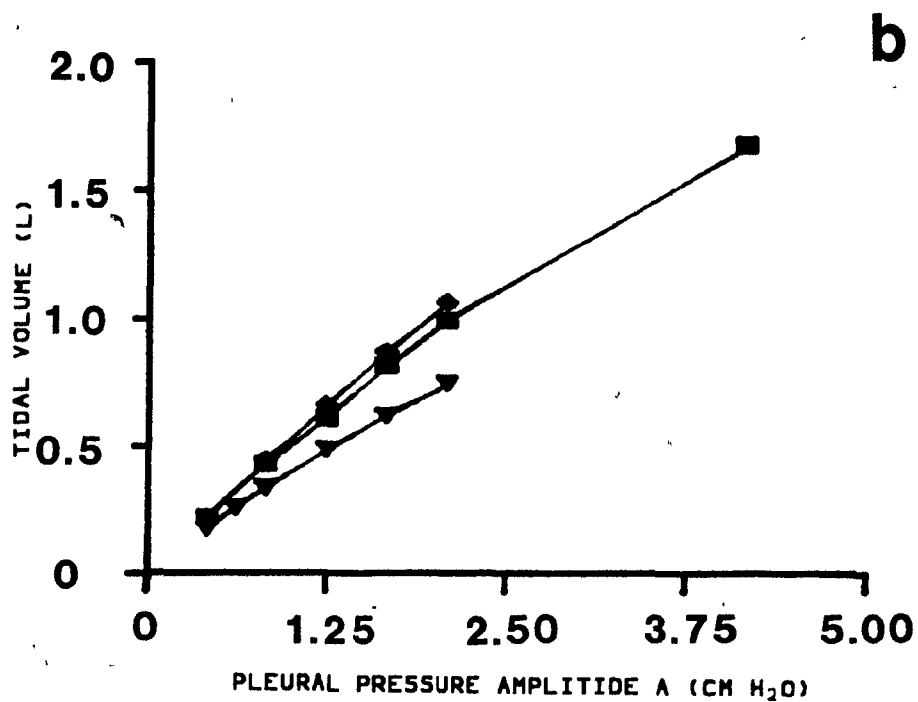
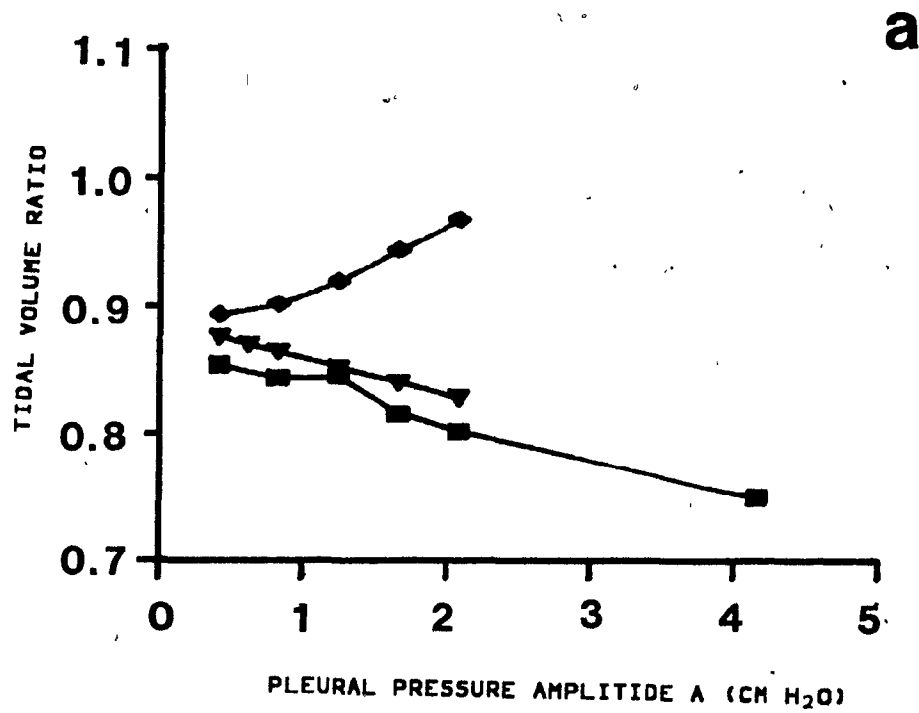


Fig. -3.7 A comparison of pleural pressure waveforms. Frequency $f = 15$ breaths min^{-1} , $\Delta P = 2$ cm H₂O. $A_1 = A_2$. a) Tidal volume ratios, non-dependent over dependent compartment as a function of the ratio of the amplitude of pleural pressure swings. Squares-- sinusoidal pressure swings; Triangles-- triangular (sawtooth) wave pressures; Diamonds-- square wave pressures. b) Corresponding tidal volumes.

amplitude of the pleural pressure swing, the ratio of the tidal volumes in the nondependent to dependent compartment increased by 8%. The total tidal volume delivered was similar to or slightly larger than that with a sinusoidal pressure variation (Fig. 3.7b).

3.3.3.2 Flow Patterns

The patterns of flows generated by the different pleural pressure swings differed considerably (Fig. 3.8). For sinusoidal changes the flows were nearly sinusoidal, for triangular pressure swings, approximately square waves, and for square wave pressure differences, roughly exponentially decaying from an initial impulse. With the same amplitude of pressure swings in all cases, the maximum flow rates from the sinusoidal and triangular waveforms were only about one tenth of those with the square wave pressure, but the flow continued throughout both inspiration and expiration, while it reached zero before the end of both the inspiratory and expiratory phases in the square wave case. Maximum flows occurred near mid-phase in the sinusoidally driven case, in the early part of the phase in the triangular wave case, and at the very onset of each phase in the square wave driven case.

3.4 DISCUSSION

3.4.1 NON-LINEAR PRESSURE VOLUME CURVE

When the amplitudes of the pleural pressure swings on the compartments were the same, regional time constants might have been expected to control the distribution of the tidal volumes. However, the distribution ratios were almost independent of the depth of

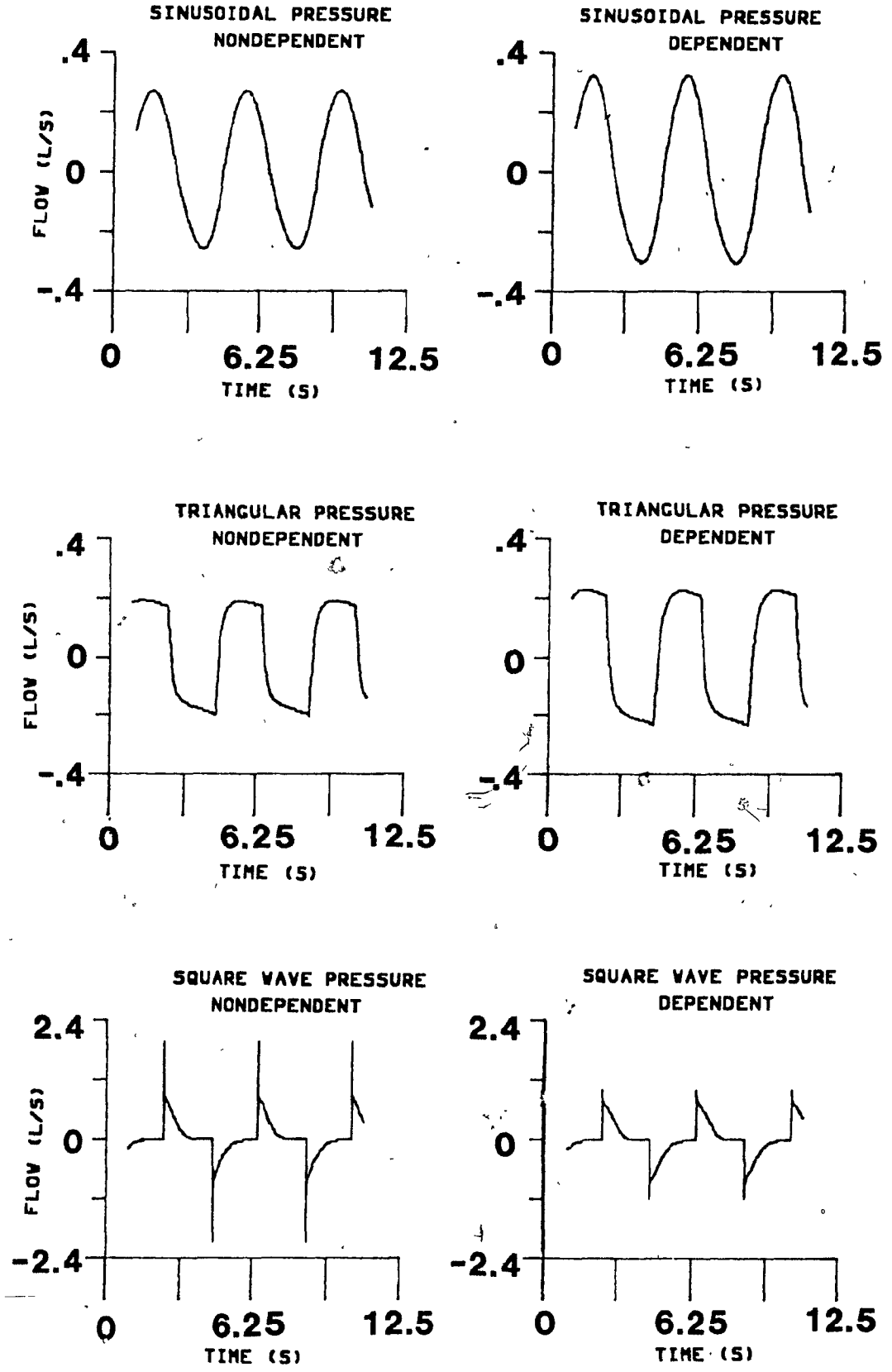


Fig. 3.8 Flows generated by the pressure waveforms. $\lambda_1 = \lambda_2 = 1.25 \text{ cm H}_2\text{O}$. $\Delta P = 2 \text{ cm H}_2\text{O}$.

breathing. The tidal volumes generated by the pleural pressure swings used in the simulations were small relative to the vital capacity of the simulated lung (5.8 L) ($5.8 \times 10^{-3} \text{ m}^3$), and the changes in the lung compliances caused by the volume swings were small enough that the ratios between the compartments remained similar when the pleural pressure swings on both compartments were identical. When the locations of the compartments on the pressure volume curve were further apart (larger static pressure difference), the effect was more pronounced.

The difference from unity of the distribution ratio for sinusoidal and triangular pleural pressure variations reflected the nonlinearity of the pressure volume curve. The initial values of compliance were dissimilar because of the different local starting volumes. As the lung inflated above FRC it became stiffer; this was evident in the model results as the slight decrease in the ratio of nondependent to dependent tidal volume as the amplitude of the pressure swings was increased. The non-dependent compartment was operating onto the stiffer portion of its pressure volume curve while the dependent compartment remained more compliant. Because the flow rates were low (Fig. 3.8a, b), the resistances were less important than the compliances in determining the distribution of ventilation with homogeneous pleural pressure swings.

3.4.2 PLEURAL PRESSURE RATIOS

If the pleural pressure swing over the nondependent compartment was slightly greater than that over the dependent zone, the differences in compliance of the two compartments could be overcome. In the simulation, an upper pressure swing 1.2 times the lower pressure

swing caused an almost uniform distribution between compartments. This distribution ratio varied with the magnitude of the pressure swings in a similar fashion to that with equal excursions of pleural pressure (Fig. 3.2 a).

The ratio of the pressure swings had a strong influence on the ratio of the distributions of tidal volume. A larger pressure driving force generated more flow and therefore more tidal volume in the compartment over which it operated (Fig. 3.2b, d).

The amplitude of the pleural pressure swings modified the effect of the pleural pressure amplitude, as did the frequencies. Larger pressure swings, and thus larger tidal volumes, caused the distribution to become more even, while higher frequencies accentuated the differences (Fig. 3.3). The larger tidal volumes generated by the higher pleural pressure swings changed the regional compliances of the model compartments by moving them along the non-linear pressure-volume curve. The compartment that was more inflated at the start of the inspiration became stiffer when the amplitude was greater, and the other compartment inflated proportionally more. These alterations in the volume distribution would allow both regions to be inflated equally by a vital capacity breath. The changes in the compliance outweighed the changes in flow rate and their interaction with the resistance. The influence of the frequency, however, was to increase the flow without changing the operating point of the lung on the pressure-volume curve. The higher resistances of the less expanded region then caused more air to enter the compartment that was already larger. The changes seen with frequency were caused by the regional resistances and compliances, that is, by the regional time constant.

In this model the amplitudes of the pleural pressure variations on the two compartments may differ. Physiologically such variations occur. D'Angelo et al. (1974) found that the pleural pressure variations at the diaphragms of spontaneously breathing dogs were less than those measured in the intercostal spaces. Daly and Bondurant (1963) found that the pressure changes measured with hypodermic needles inserted in the intrapleural spaces in human subjects were smaller over the upper chest than over the lower regions. Roussos et al. (1976, 1977) showed that the patterns of muscle use during breathing altered the distribution of ventilation, presumably by affecting the pleural pressure distribution by changing the shape of the chest wall. Sampson and Smaldone (1984) demonstrated that the ratio of washouts in different lung regions varies as a linear function of the ratio of the pleural pressure swings. In the model, the ratio of pleural pressure changes was seen to exert a very strong effect on the distribution of a tidal volume between the compartments (Fig. 3.4).

3.4.3 PHASE DIFFERENCES

Phase differences between the pressure swings on the two compartments of the model are possible. Such differences were observed under normal conditions by Ploysongsang et al. (1979) using two esophageal balloons. Sequential emptying of the lungs in lateral decubitus subjects was documented by Frazier et al. (1976). Phase differences in the flow per unit volume also were measured using radioactive krypton-81m in subjects in the lateral decubitus position (Chapter 5). However, as was shown in Fig. 3.6b, a lag in the flow from one compartment does not require that the pleural pressure swings be out of phase.

The compartment of the model in which the pleural pressure lagged experienced an increase in tidal volume relative to the other. By leading the other compartment in pressure variations a region also led in filling. Since the compliance decreases with volume above FRC, this caused the compartment with the leading pressure swing to be stiffer than it would have been if the filling were in phase with or lagging the other compartment. When the dependent compartment was leading, the difference in compliance between the dependent and nondependent zones was reduced, leading to a more uniform distribution of the tidal volume.

3.4.4 DIFFERENCES FROM CONSTANT FLOW INSPIRATION

The distribution of tidal volumes for any chosen waveform in this model was almost independent of the amplitude and frequency of the pleural pressure swings in the range measured, and hence, of the flow rate of air. Pedley et al. (1972) found a strong flow rate dependence of the distribution of instantaneous flows measured at the same lung volume. A number of factors contribute to the difference.

Before attempting to explain the differences between the two models it was necessary to ensure that they they were comparable. Values of the instantaneous flow distribution Q_1/Q_2 were computed using the expressions for resistance and compliance from the tidal breathing model. The results for constant inspiration were similar to those of Pedley et al. (1972) (Fig. 3.9). Thus, the differences between tidal breathing and constant inspiratory flow rates resulted not from the models but from inherent differences between the modes of breathing.

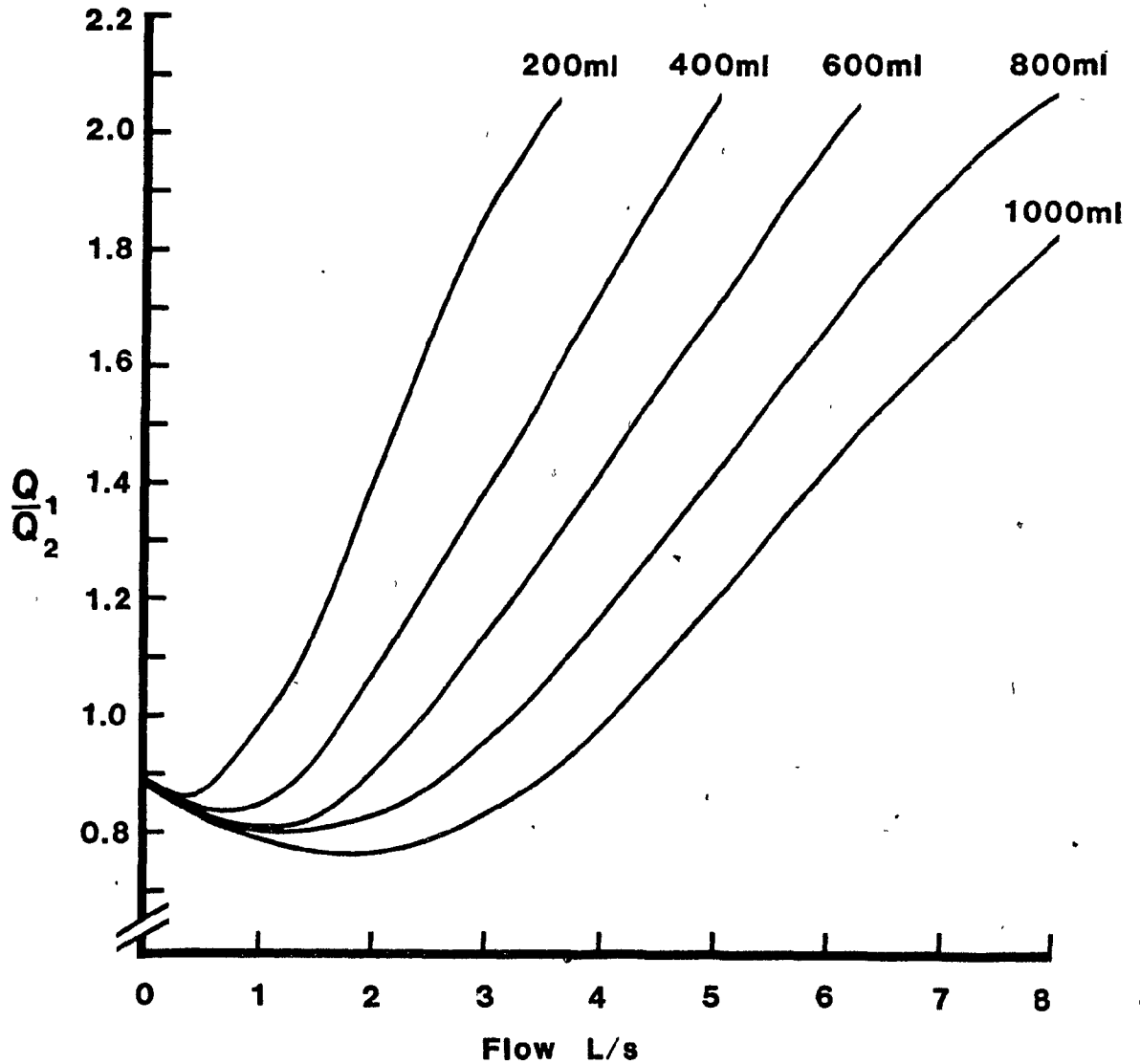


Fig. 3.9 Distribution of instantaneous flows, constant total flow. The ratio of flows, non-dependent over dependent compartment, as a function of total flow for volumes above FRC. (TLC=7.2 L). $\Delta P = 2 \text{ cm H}_2\text{O}$.

The information obtained from a model of tidal breathing is different from that given by a model of bolus inhalation. In examining the ratios of tidal volumes one considers the overall distribution of air throughout the inspiratory cycle. Any transients which may occur are averaged with the rest of the inspiratory flow. In considering the instantaneous flow ratios at a constant lung volume one may be comparing a transient at one flow rate to steady-state flow at another. The duration of transients is governed by time constants which are only weak functions of flow rate while the time for full inspiration is strongly dependent on the flow. Thus, the tidal volume ratios and the instantaneous flow ratios are measures of different phenomena as are bolus studies and tidal volume distribution studies.

Pedley et al. (1972) found a flow rate dependence of the ratio of tidal volumes in the two compartments of their model during breathing at a constant flow rate although it was less marked than that seen for the instantaneous flows. In contrast, with the cyclic breathing model the distribution of a tidal volume was nearly independent of flow rate. The difference can be understood with reference to Fig. 3.9. During inspiration at constant flow, the distribution of a tidal volume was determined by a vertical line on Fig. 3.9; at a given total flow as the volume accumulated, the local flow distributions lay on subsequent curves of increasing lung volume and the tidal volume distribution was a weighted sum of the different flow distributions. During cyclic breathing, however, the flow rates changed during a breath. Instead of following a vertical line on Fig. 3.9, the local flow distributions described a loop, with low flow rates occurring at low volumes, higher flow rates at intermediate volumes, and low rates again at the highest volumes attained during the

breath. Even for the relatively constant flows generated using a triangular waveform, there was a decrease in the flow as inspiration continued (Fig. 3.8b). The tidal volume ratio thus produced differed from that at a constant rate of flow.

3.4.5 WAVEFORMS

The difference between the tidal volume distributions generated with sinusoidal and triangular pleural pressure swings was minor (Fig. 3.7) because the differences in the instantaneous flow rates (Fig. 3.8a, b) averaged out. The square wave flow, however, was dominated by the impulse at the start (Fig. 3.8c). The effect of resistance was more important than that of compliance in determining the distribution of the very high initial flows. Although the later flows were distributed more by the ratio of the compliances, the spikes contributed significantly to the total tidal volumes, and thus the distributions were different from those generated with sinusoidal pressure swings (Fig. 3.7).

Because high flows of short duration were generated with the square wave pleural pressure swings, the tidal volume distribution pattern from this waveform followed a trend similar to that seen for bolus distribution. The flow pattern, a series of short fast gasps, is not, however, physiologically normal. Natural tidal breathing lies somewhere between the sinusoidal and triangular pressure swing patterns, resembling the sinusoidal pattern more on inspiration and the triangular pattern more on expiration. These pleural pressure driving forces should be the ones used to simulate tidal breathing.

3.5 CONCLUSIONS

For tidal breathing with pleural pressure as the driving force, the magnitude of the pleural pressure swings for any of the three waveforms considered had little effect on the distribution of the tidal volume. When the derivative of the pressure swings at FRC was finite, the distributions of tidal volumes were influenced by the regional compliance. When the derivative of the pressure swing at FRC was an impulse which generated a flow spike, the resistance of the compartments became important in determining the distribution of tidal volume.

With sinusoidal changes in pleural pressures, both the ratio of the amplitudes of the pleural pressure swings and the starting volume affected the distribution of tidal volume strongly. Phase differences between the pressure swings had a greater effect on the distribution than did the magnitude of the individual pressure variations. Conversely, large differences between the pleural pressure swings generated phase differences in flow.

The distribution of the pleural pressure, the driving force for breathing, appears to be the primary determinant of the distribution of ventilation. However, the air flow is controlled by the instantaneous values of compliance and resistance. Under physiological conditions, major changes in ventilation distribution probably are determined by changes in pleural pressure distribution and phase while the resistances and compliances exert secondary effects. Indeed, in measurements with the isotope, krypton-81m (Chapter 5), changes in tidal volume and frequency had no effect on the distribution of tidal air in the lungs.

CHAPTER 4

A MODEL OF KRYPTON-81m DYNAMICS IN THE LUNG

4.1 INTRODUCTION

When a radioactive tracer is used in the lungs, the quantity measured directly is the activity of the gas in the lung regions. To interpret the results in terms of ventilation or volume, a model is used. For steady state measurements, because the time variations of breathing are not considered, the models can be fairly simple. However, when the variations with time are to be studied, more detailed analysis is necessary. For the krypton-81m activity in the lung during cyclic breathing, the time scales of decay and of transport are sufficiently similar that both must be considered.

4.2 THE MODEL DEVELOPMENT

Consider the lung to be composed of conducting airways in which the sole transport mechanism for krypton-81m is convection, in series with a respiratory zone where all transport is by molecular diffusion. Define the inspiratory flow as positive. The axial coordinate x has its origin at the trachea. Let the cross-sectional area of each lung region increase exponentially with distance. In the conducting zone, the area varies with time, while in the respiratory zone, because there is no bulk flow, there can be no expansion. Transport throughout the lung occurs in the axial direction only, because even where the cross-section is very large, it is composed of multiple narrow airways in parallel.

4.2.1 THE CONDUCTING AIRWAYS

4.2.1.1 *The Equation*

In the conducting airways, the mass balance for krypton-81m gives

$$\frac{\partial(CA)}{\partial t} = -\frac{\partial(CQ)}{\partial x} - \lambda CA \quad (4.1)$$

On expansion, this becomes

$$\frac{\partial C}{\partial t} = -\frac{Q}{A} \frac{\partial C}{\partial x} - \lambda C - \frac{C}{A} \left[\frac{\partial Q}{\partial x} + \frac{\partial A}{\partial t} \right] \quad (4.2)$$

where $C(x,t) = \frac{\text{(local krypton concentration)}}{\text{(inlet krypton concentration)}}$

$Q(x,t)$ = the volumetric flow rate

$A(x,t)$ = the cross-sectional area of the airways.

and $\lambda = 3.2 \text{ min}^{-1} = 0.053 \text{ s}^{-1}$
= the decay constant of krypton-81m

Because the airways are elastic, the cross-sectional area A is a function of both distance and time. When the airway cross section varies, the change in volume is reflected in the distance dependence of the volumetric flow Q . Flow is unidirectional down the airways. Thus, from the equation of continuity for the system,

$$\frac{\partial Q}{\partial x} = -\frac{\partial A}{\partial t} \quad (4.3)$$

and the Eqn. 4.2 simplifies to

$$\frac{\partial C}{\partial t} = -\frac{Q}{A} \frac{\partial C}{\partial x} - \lambda C \quad (4.4)$$

4.2.1.2 *Boundary Conditions*

The concentration at the trachea is constant during inspiration.

$$C(0,t) = 1 \quad 0 < t < T_1 \quad (4.5)$$

where $t = 0$ at the onset of inspiration and $t = T_1$ at the end of

inspiration.

The concentration must be continuous from cycle to cycle.

$$C(x,0) = C(x,T_t) \quad \forall x \quad (4.6)$$

where T_t is the time at end expiration.

At the distal end of the airways, the concentration matches that in the respiratory zone.

$$C(x_L,t) = C_{Resp}(0,t) \quad \forall t \quad (4.7)$$

where x_L is the coordinate of the end of the airways, the origin for the coordinate system in the respiratory zone. For the symmetric lung model of Weibel (1963), x_L for a tidal volume of 500 ml travelling in plug flow will be only 2 mm from the distal end of the normal human lung (Scheid and Piiper, 1980).

4.2.2 THE RESPIRATORY ZONE

4.2.2.1 The Equation

The equation for the concentration of krypton-81m in the respiratory zone is

$$\frac{\partial C}{\partial t} = \frac{D}{L^2} \frac{\partial^2 C}{\partial x^2} - \lambda C + \frac{D}{AL^2} \frac{(\partial C)}{(\partial x)} \frac{(\partial A)}{(\partial x)} \quad (4.8)$$

where $D = 0.134 \text{ cm}^2 \text{ s}^{-1}$

= the molecular diffusivity of krypton-81m in air,

$x = (x - x_L)/L$ where x_L is the end of the conducting airway,

and L = the length of the respiratory zone,

The product of derivatives in Eqn. 4.8 may be removed if the cross-sectional area A is assumed to increase exponentially with distance down the lung.

$$\text{Let } A(x,t) = A_L \exp(bx) \quad (4.9)$$

From the geometry of Weibel (1963) as presented by Schied and Piiper (1980), b is approximately 8.5.

Then Eqn. 4.8 becomes

$$\frac{\partial C}{\partial t} = \frac{D}{L^2} \left(\frac{\partial^2 C}{\partial x^2} + \frac{b \partial C}{\partial x} \right) - \lambda C \quad (4.10)$$

4.2.2.2 Boundary Conditions

The concentration is continuous at the boundary between the respiratory and conducting zones.

$$C(0,t) = C_{\text{conducting}}(x_L,t) \quad \forall t \quad (4.11)$$

The krypton-81m does not reach the distal boundary.

$$C(1,t) = 0 \quad \forall t \quad (4.12)$$

The concentrations are continuous from cycle to cycle.

$$C(x,0) = C(x,T_t) \quad \forall x \quad (4.13)$$

where T_t is the time at the end of expiration.

4.3 THE CONCENTRATION IN THE CONDUCTING AIRWAYS

4.3.1 INSPIRATION

Neglect the formation of the velocity profiles in the airways and assume plug flow. A front of fresh gas moves down the airway during inspiration, arriving at each point x_0 at time t_0 . The front arrives when

$$\int_0^{x_0} A(x,t_0) dx = \int_0^{t_0} Q(x_0,t) dt \quad (4.14)$$

The contribution of the residual activity in the dead space has been neglected.

Behind the front in the region of fresh gas, the concentration of krypton-81m from Eqn. 4.4 is given by

$$C(x,t) = \exp(-\lambda\Delta t) \quad (4.15)$$

where $\Delta t = t - t_1$ is the transit time from the trachea to the point x .

The transit time Δt is a function of x and t .

The gas which is at point x at time t passed the origin at time t_1 , defined by the equation:

$$\int_0^x \lambda(x) dx = \int_{t_1}^t Q(t) dt \quad (4.16)$$

Downstream of the gas front, the krypton-81m present is that which remained at the end of expiration, but it has continued to decay.

$$C(x,t) = C(x_2, T_1) \exp[-\lambda(t + T_1 - T_1)]$$

for $t > t_{1\min}$ (4.17)

where $t_{1\min}$ is the earliest time at which fresh gas from the origin could reach point x and where x_2 is the coordinate where the gas which is now at x was situated at the end of expiration.

4.3.2 EXPIRATION

During expiration, the concentration of krypton-81m depends on the gas which entered during the previous inspiration. There is no stratification of gas composition (Scheid and Piiper, 1980).

$$C(x,t) = C(x_2, T_1) \exp[-\lambda(t - T_1)] \quad (4.18)$$

where T_1 is the end-inspiratory time and x_2 represents the position that the gas which is now at x occupied at the end of inspiration.

4.4 THE RESPIRATORY ZONE CONCENTRATION

The solution procedure for Eqn. 4.10 with boundary conditions Eqns. 4.11 - 4.13 is the following:

1. Set the time derivative in Eqn. 4.10 to zero and solve the steady-state equation for a step change in the concentration at the origin.
2. Find the transient solution for a step change in concentration at the origin. The equation and boundary conditions obtained by subtracting the steady-state solution from the entire problem may be solved by the method of the separation of variables.
3. By applying Duhamel's Theorem for superposition, replace the step change at the origin by the concentration from the conducting airways.

The intermediate results will be summarized.

4.4.1 THE STEADY STATE SOLUTION

The solution to the ordinary differential equation obtained by setting the time derivative in Eqn. 4.10 to zero and applying the boundary condition $C(0) = 1$ is:

$$C_{ss}(x) = \frac{(b/2 \sinh[m_1(1-x)] - m_1 \cosh[m_1(1-x)])}{m_1 \sinh(m_1) - b/2 \cosh(m_1)} \exp(-b/2 x) \quad (4.19)$$

$$\text{where } m_1 = (L/2D)(b^2 D^2/L^2 + 4D\lambda)^{1/2} \quad (4.20)$$

The first term dominates for krypton-81m in the lung.

4.4.2 THE TRANSIENT SOLUTION

$$\text{Let } v(x,t) = C(x,t) - C_{ss}(x).$$

The equation for v is identical to Eqn. 4.10 with new boundary conditions:

$$\frac{\partial v}{\partial t} = \frac{D}{L^2} \left(\frac{\partial^2 v}{\partial x^2} + \frac{b \partial v}{\partial x} \right) - \lambda v \quad (4.21)$$

$$v(0,t) = 0 \quad v(x,0) = -C_{ss} \quad v(l,t) = 0$$

After separation of variables, the solutions are:

$$v_k = K_k \exp[-(a^2 + \lambda)t] \exp[-(b/2)x] \sin(m_2 x) \quad (4.22)$$

$$\text{where } m_2 = (b^2/4 - a^2 L^2/D)^{1/2}$$

The constants K_k and a are determined from the boundary conditions.

$$\text{As } m_2 = k\pi, \quad k = 1, 2, 3, \dots$$

$$\text{then } a^2 = (b^2/4 - k^2 \pi^2) (D/L^2)$$

Because a is a real number, the only allowable value of k is $k = 1$.

$$K = \frac{\pi [b \sinh(m_1) - 2m_1 \cosh(m_1) + 2m_1]}{4m_1 \sinh(m_1) - 2b \cosh(m_1)} \quad (4.23)$$

where m_1 was defined in Eqn. 4.20. Thus, for a step change in the concentration at the start of the respiratory zone,

$$C(x,t) = K \exp[-(a^2 + \lambda)t] \exp[-(b/2)x] \sin(m_2 x) + C_{ss} \quad (4.24)$$

In the limit of large m_1 , $m_1 = b/2$ and $K = \pi$.

4.4.3 SUPERPOSITION OF THE BOUNDARY CONDITIONS:

SOLUTION FOR CONCENTRATION

The boundary condition at $x = 0$ is not a unit step but the concentration at the distal end of the conducting airways. Denote this by $h(t)$. Let the concentration with time-varying boundary conditions $C(0,t) = h(t)$ be represented by $C(x,t)$. Then, by Duhamel's theorem,

$$C(x,t) = \int_0^t h(\tau) \frac{\partial C}{\partial t}(x,t-\tau) d\tau \quad (4.25)$$

The differentiation of Eqn. 4.24 with respect to time gives

$$\frac{\partial C}{\partial t}(x,t) = \Lambda(x) \exp[-(a^2 + \lambda)t] \quad (4.26)$$

$$\text{where } \Lambda(x) = -K(a^2 + \lambda) \exp[-(b/2)x] \sin(m_2x)$$

4.4.3.1 Inspiration, Behind the Front

After the front has arrived at the point $x = x_L$,

$$h(t) = \exp(-\lambda \Delta t)$$

from Eqn. 4.15. If the transit time $\Delta t(x_L)$ to x_L is 2.5 s, the maximum possible during sinusoidal breathing at 12 breaths min^{-1} , then the value of $h(t)$ is 0.875. Therefore, a maximum 12.5% error is made if $\Delta t = 0$ is assumed. The value of Δt lies between 0 and 2.5 s and depends on the instantaneous flow rate and airway cross-section, but it will be treated here as constant with respect to time.

Then from Eqns. 4.25, 4.26, and 4.15:

$$C(x,t) = K \exp[-(a^2 + \lambda)t] \exp[-(b/2)x] \sin(m_2x) \quad (4.27)$$

$$\text{for } \Delta t < t < T_1$$

4.4.3.2 Expiration

On expiration, $h(t)$ is obtained from Eqn. 4.18 evaluated at x_L . At the distal end of the conducting airways, the flow must be zero, the expansion of the more proximal airways having accounted for all the entering volume. Thus, the gas at x_L does not move.

Substituting from Eqn. 4.15:

$$h(t) = \exp(-\lambda\Delta t) \exp[-\lambda(t-T_1)] \quad \text{for } T_1 < t < T_c \quad (4.28)$$

and the concentration is obtained from Eqns. 4.25, 4.26, and 4.28:

$$C(x,t) = A(x)/a^2 (\exp(-\lambda t) - \exp[-(a^2 + \lambda)t]) \exp[-\lambda(\Delta t - T_1)] \quad (4.29)$$

4.4.3.3 Inspiration, Before the Front

During inspiration before the fresh gas arrives, the concentration is analogous to that during expiration.

$$C(x,t) = A(x)/a^2 (\exp(-\lambda t) - \exp[-(a^2 + \lambda)t]) \exp[-\lambda(\Delta t - T_1 + T_c)] \quad (4.30)$$

4.5 REGIONAL ACTIVITY

Let the regional activity, the amount of krypton-81m present, be represented by $n(t)$. It is the integral of the product of concentration and area.

4.5.1 THE CONDUCTING AIRWAYS

4.5.1.1 Inspiration

On inspiration in the region swept out by the front of fresh gas, from Eqn. 4.15:

$$n(t) = \int_0^{x_0} \exp(-\lambda\Delta t) A(x,t) dx \quad (4.31)$$

The area is given by

$$A(x,t) = A_0 \exp[\beta(t)x] \quad (4.32)$$

Note that the volume of the conducting airways at any time is the integral of this expression from $x = 0$ to $x = 1$. Let the volume at any time be $V(t)$.

$$V(t) = (A_0/B) [\exp(\beta L) - 1] \quad (4.33)$$

Therefore, if the distance dependence of Δt is neglected,

$$n(t) = (A_0/B(t)) \exp(-\lambda \Delta t) [\exp(\beta(t)x_0) - 1] \quad (4.34)$$

after the front has passed. The point x_0 is the location of the front.

Before the front, the activity found from Eqns. 4.15 and 4.17 is:

$$n(t) = (A_0/B) \exp[-\lambda(\Delta t + t - T_1 + T_t)] [\exp(\beta L) - \exp(\beta x_0)] \quad (4.35)$$

The expression for x_0 is derived from Eqn. 4.14:

$$x_0 = (1/\beta) \ln[(\beta/A_0) \int_0^t Q(t) dt + 1] \quad (4.36)$$

Thus, the activity in the conducting zone as a function of time during inspiration is:

$$n(t) = \exp(-\lambda \Delta t) (\exp[-\lambda(t - T_1 + T_t)]) [V(t) - \int_0^t Q dt] + \int_0^t Q dt \quad (4.37)$$

4.5.1.2 Expiration

On expiration, from Eqn. 4.18,

$$n(t) = \int_0^L C(x_2, T_1) \exp[-\lambda(t - T_1)] \Lambda(x, t) dx \quad (4.38)$$

But $C(x, T_1) = \exp(-\lambda \Delta t) \quad \forall x, 0 < x < L$

Therefore,

$$n(t) = (A_0/B) \exp[-\lambda(\Delta t + t - T_1)] [\exp(\beta L) - 1] \quad (4.39)$$

4.5.2 RESPIRATORY ZONE

In the respiratory zone, the activity is given by

$$n(t) = \int_0^1 C(x, t) \Lambda(x) dx \quad (4.40)$$

During inspiration, after the arrival of the front, from Eqns. 4.27 and 4.9, the integral becomes

$$n(t) = KB \exp[-(a^2 + \lambda)t] \quad (4.41)$$

where

$$B = \frac{2\lambda L \pi \exp(b/2)}{b^2/4 + m_2^2} \quad (4.42)$$

On expiration, from Eqns. 4.29 and 4.9, the expression is

$$n(t) = KB(1 + \lambda/a^2) (\exp(-\lambda t) - \exp[-(a^2 + \lambda)t]) \exp[-\lambda(\Delta t - T_1)] \quad (4.43)$$

4.6 THE NORMALIZED DERIVATIVES OF ACTIVITY

4.6.1 INSPIRATION

The derivation neglects the loss of krypton-81m by diffusion out of the conducting airways, resulting in an overestimate of the activity in that region. However, the isotope in the respiratory zone of the model is that which has moved out of the conducting zone by molecular diffusion. When the total activity in the lung is of interest, the error of neglecting the diffusional losses from the conducting zone therefore is compensated for by considering the conducting regions alone.

Note that the derivative with respect to time of $V(t)$ is $Q(t)$, although the integral of $Q(t)$ is the tidal volume, not the total volume.

The derivative of Eqn. 4.37 is:

$$dn/dt = -\lambda n + \exp(-\lambda \Delta t) [Q(t) + \lambda_0 \int^t Q(t) dt] \quad (4.44)$$

Thus, the normalized derivative is

$$\frac{dn}{dt} = \frac{Q(t) - \lambda V_0 \exp[-\lambda(t-T_1+T_c)]}{\int_0^t Q(t) dt + V_0 \exp[-\lambda(t-T_1+T_c)]} \quad (4.45)$$

$$\text{where } V_0 = V(t) - \int_0^t Q(t) dt$$

But $\lambda \exp[-\lambda(t-T_1+T_c)]$ is small, about 0.04 s^{-1} for a frequency of 12 breaths per minute, and the exponential is approximately 0.9. The expression becomes

$$\frac{dn}{dt} = \frac{Q}{\int_0^t Q(t) dt + V_0} = \frac{Q(t)}{V(t)} \quad (4.46)$$

4.6.2 EXPIRATION

On expiration, the neglect of the diffusional transfer of material out of the conduction zone causes an overestimate of the amount of krypton-81m removed and thus an underestimate of the residual regional activity. The tracer that moves into the respiratory zone is not removed by convection during the expiratory phase. Hence, both the conduction and respiratory zones must be considered in the total lung activity during expiration. The activity to consider is the sum of Eqn. 4.39 and Eqn. 4.43, minus Eqn. 4.41 evaluated at $t = T_1$. But, since the exponent a , given in Eqn. 4.23; is large for krypton-81m in the lung regions with zero flow, $\exp(-a^2 t)$ tends to zero. The expression for the activity then becomes:

$$n(t) = V(t) \exp[-\lambda(\Delta t + t - T_1)] - KB \exp[-\lambda(t + \Delta t - T_1)] \quad (4.47)$$

and the derivative is:

$$dn/dt = -\lambda n(t) + Q(t) \exp[-\lambda(\Delta t + t - T_1)] \quad (4.48)$$

The normalized derivative then is:

$$\frac{dn}{dt} \frac{1}{n} = \lambda + \frac{Q(t)}{V(t) + KB} \quad (4.49)$$

$$\text{and } Q/V = [(1/n)(dn/dt) + \lambda] [(V+KB)]/V \quad (4.50)$$

on expiration.

4.7 DISCUSSION

A simple analytical result has been obtained for flow per unit volume in a lung region as a function of the krypton-81m activity. However, a number of assumptions were made and should be examined.

The lung was partitioned into a convective zone and a diffusion zone. The convective region was assumed to have plug flow and an advancing front of krypton-81m with a constant concentration. In the physical situation, velocity profiles develop and the concentration front is spread by diffusion while the tracer decays. However, the full convective diffusion equation in an expanding cross-section could not be solved analytically, even for plug flow. The advancing front approximation is adequate because, as was shown, the possible differences in transit times in the lung during normal breathing could not alter the activity of the krypton-81m by more than 12.5%. The intermediate concentration profile results are affected by the neglect of diffusion, but the final expressions for the total activity as a function of time are not, at least on inspiration, because of the integration over distance.

Because the cross-sectional area in the conduction zone changed with time and that in the respiratory zone did not, the model dimensions were discontinuous. This was not significant because each region was treated independently, with one setting the boundary concentrations for the other. It would be of importance, however if the flux of krypton-81m across the boundary between the regions were considered. Indeed, to improve the model, the boundary condition of matching concentrations at the junction should be replaced by a matching flux condition.

The volume $V(t)$ that appears in the expressions is not the total lung volume, but the volume of the convection zone. In the real lung this translates into the fact that krypton-81m measures only those regions that the gas enters by convection. The ventilation per unit volume measured is thus that of the regions of high specific ventilation.

CHAPTER 5

KRYPTON-81m EXPERIMENTS

5.1 INTRODUCTION

The predictions of the pleural pressure-driven lung model (Chapter 3) were investigated experimentally using krypton-81m as a tracer. Krypton was selected because of its short half-life, its good imaging properties, and its safety and ease of handling. Subjects were studied in the left lateral decubitus posture to permit the comparison of the lungs to the two compartments of the model. Also, in this position both the hydrostatic gradient of static pleural pressure and the dynamic pressure swings were maximized, making the two compartments dissimilar.

The interpretation of steady-state krypton-81m scans introduced by Fazio and Jones (1975) was used to obtain the ratios of average ventilation of the two regions for comparison with the pleural pressure model. The results of the model of krypton-81m dynamics (Chapter 4) were applied to study the time variations in the ventilation per unit volume and the sequence of flows in the lungs. An average breath divided into a series of sixteen images was examined for each experiment.

5.2 MATERIALS AND METHODS

5.2.1 EXPERIMENTAL PROTOCOL

Nine healthy volunteers (5 male, 4 female) were studied in one series. Two others (1 male, 1 female) participated in a second set of experiments with slight differences in protocol which will be described later. The subjects breathed air mixed with krypton-81m through a mouthpiece and two one-way valves. A pneumotachograph on the inspiratory side of the valves monitored the flow which, integrated electronically, was displayed on an oscilloscope to the subjects.

Krypton-81m was eluted from the rubidium-81 parent with a steady stream (0.5 L s^{-1}) ($5 \times 10^{-4} \text{ m}^3 \text{ s}^{-1}$) of humidified oxygen through the generator (MRC Cyclotron, Hammersmith Hospital, London, England).

To maintain the inspired concentration of krypton-81m as constant as possible throughout each breath, it was diluted with a constant flow of air (or air plus carbon dioxide) into a mixing chamber (gas bag) from which the subject breathed. The flow of air into the bag was adjusted during the set-up phase before the krypton was added so that the bag was just emptied at the end of inspiration. Further adjustments were made if necessary during the experiment. The bag refilled from the air supply and the krypton-81m generator while the subject breathed out through the expiratory valve (Fig. 5.1). The loss of krypton-81m activity caused by the residence time in the gas reservoir was compensated for by longer recording times.

Four manoeuvres were performed by each participant. The subject first breathed air through the mouthpiece at 12 breaths per minute until a steady, comfortable volume, the baseline tidal volume V_{T12} was established. He or she was instructed to maintain this tidal

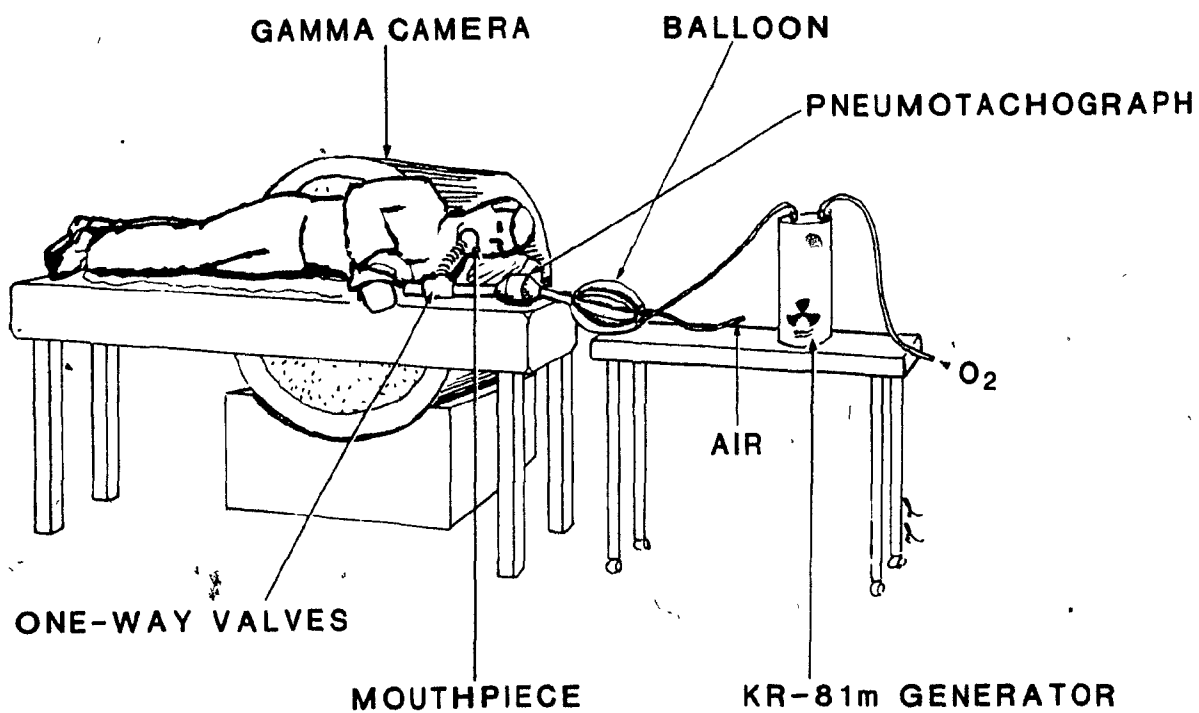


Fig. 5.1 A sketch of the experimental set-up. The subject is shown in the left lateral decubitus position, his back against the gamma camera. Note the reservoir in which the air and the krypton-81m are combined.

volume with the help of the oscilloscope display, and the krypton-81m was added to the inspiratory circuit. For a second acquisition the subject breathed at the same frequency with a tidal volume twice the baseline value. Carbon dioxide was added to the inspiratory air. The procedure was repeated at 24 breaths per minute, where the tidal volume V_{T24} was half the baseline volume. Thus, similar minute volumes were used at both frequencies. Although the rates of inspiration and expiration were uncontrolled, the ratio of inspiratory time to total cycle time (T_I/T_{TOT}) was held at 0.5 by having the subject begin inspiration on one metronome beat and start expiration on the next. (Under normal breathing conditions, T_I/T_{TOT} is less than 0.5.)

The activity rate over the chest was recorded with a large-field gamma camera (Acticamera, CGR, LeBuc, France) placed against the subject's back. The data were stored and processed on a Simis 3 computer (Informatek, Orsay, France), in list mode with a 10 msec time increment. In list mode, separate x-y co-ordinates are stored for the activity accumulated during each time interval. The activity at each co-ordinate could be summed to produce the steady state image or the information for a particular time period could be selected. A minimum of 300,000 counts was collected during each manoeuvre.

The number of decay events during scintillation counting is generally assumed to follow a Poisson distribution. This is true as long as the concentration of the tracer does not change appreciably during the counting period (Knoll, 1979). Because fresh gas enters the lung at each breath, the assumption is acceptable, if not perfect, for krypton-81m, half-life 13 s and effective counting period of the order

of 5 s. The standard deviation of the number of counts is thus the square root of the mean.

In the second set of experiments also, the subjects breathed krypton-81m and air from a mixing chamber while lying on their left sides. The frequencies were 9, 12, and 24 breaths per minute for one subject and 9 and 12 breaths per minute for the other, with the tidal volumes that were comfortable for the subjects. Data were recorded with one head of a dual head scintillation camera (Unicon) and processed on a VAX 780 computer (Digital Equipment Corporation, Maynard, Mass.). The pneumotachograph signals were sampled and recorded simultaneously. Following a steady state acquisition of 1,000,000 counts, a one minute krypton-81m washout was recorded for the same frequency and tidal volume. The decay of the isotopes was monitored over the chest field to determine the regional washouts, not at the mouth for the overall value. After decay correction the washout data were fitted to monoexponential functions on a pixel by pixel basis for a 32 x 32 matrix.

5.2.2 THE GAMMA CAMERA

A gamma camera consists of a detector, a collimator, and an array of photomultipliers and associated electronics. The detector is a large sodium iodide crystal contaminated with 0.1 mole percent Thallium. The collimator is a plate of lead with multiple parallel holes to permit only normally incident gamma particles to reach the detector. When a photon (gamma particle) produced by the decay of krypton-81m strikes the crystal it scatters an electron. Each Compton particle produced in this way displaces many valence electrons in its path, imparting 3 eV to each. When these excited electrons encounter

an imperfection caused by a thallium atom, they drop back into the valence band "trap", releasing their surplus energy in a burst of blue-violet light (wavelength 4.2×10^{-5} m) to which the sodium iodide crystal is transparent.

For each gamma particle absorbed by the detector, many photons of light are produced. Each scintillation event (detected decay) thus is sensed by several of the photomultipliers mounted behind the crystal. The location of the event is determined by weighting the energy output by the photomultiplier position and summing the values to obtain the coordinates. The more photons produced by an incident gamma particle, the better the positional resolution. Similarly, the greater the concentration of the tracer, the shorter the time to form the image and the lesser the blurring caused by movements of the subject.

5.2.3 THE MIXING CHAMBER

Although the use of the mixing chamber greatly reduces the activity of the gas delivered to the lungs, its necessity was confirmed in a test performed with one seated subject. Two scans were done in immediate succession, one using the mouthpiece and mixing chamber arrangement and the other a face mask with a continuous supply of krypton-81m but with air flow only on demand. Although the krypton-81m eluted during expiration was contained in the large bore tube through which the air flowed during inspiration, the mixing was poor. The difference between the activity profiles produced with the two delivery systems is striking (Fig. 5.2). With the mask and tube, the distribution was more apical and central than it was with the reservoir system. The early part of the breath was weighted disproportionately by the krypton-81m that accumulated in the tube during expiration,

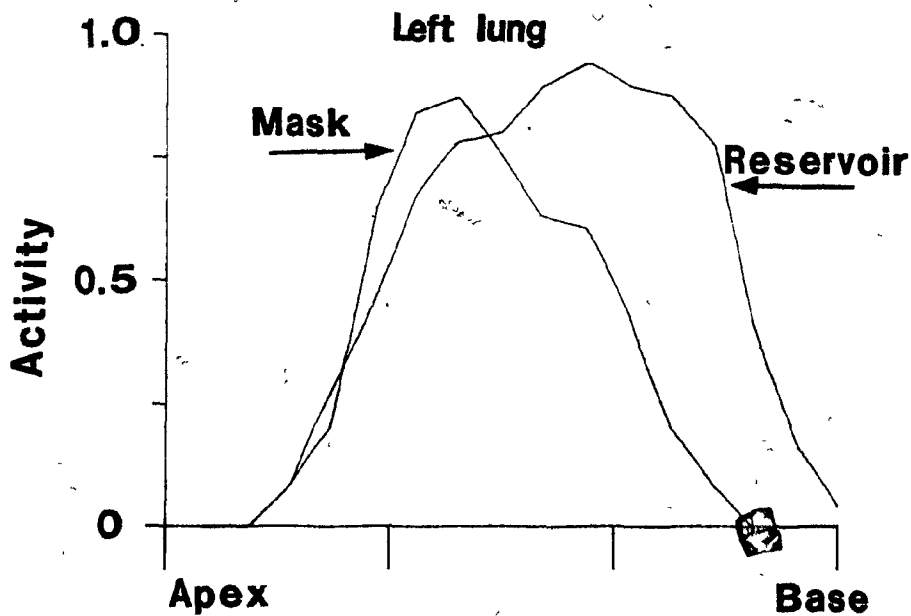
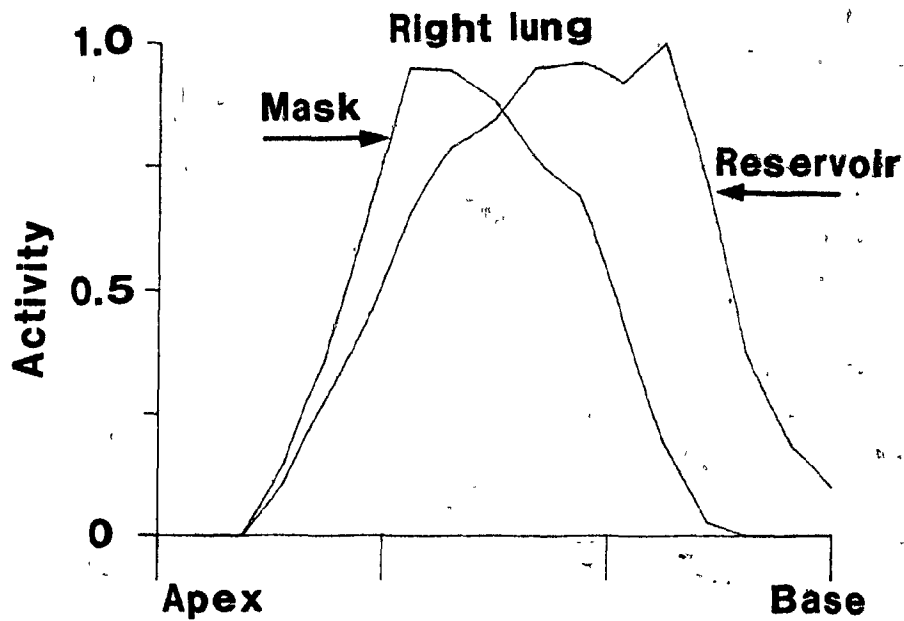


Fig. 5.2 Activity profiles generated with and without the mixing chamber. The normalized activity as a function of position down the lungs of a seated subject (subject J) is shown for krypton-81m delivered with the mixing chamber and a constant flow of air (reservoir) or with a mask and tube in which the air flow was intermittent (mask).

while the later portions of the inspire contained much lower concentrations. The central and apical regions, known from bolus studies to receive the earlier portions of a breath (Grant et al, 1974), appeared better ventilated than the more basal regions which receive the later part of the tidal volume. A larger lung volume was displayed as well ventilated when the mixing chamber (reservoir) was used.

When the pneumotachometer signal is available, the average inlet krypton-81m concentration obtained with the reservoir in place may be found by dividing the counts over the trachea during the inspiratory phase of a reconstructed breath by the simultaneous flow at the mouth. The counts represent the number of moles of the isotope present and the flow gives the volume delivered in each time interval. Hence, the ratio is proportional to the inspired concentration, but under the conditions of low flow at the beginning and end of inspiration, the division by a very small quantity introduces an artifact. The concentration during most of inspiration is seen to be constant (Fig. 5.3). Thus, as Amis and Jones (1980) and Hughes (1979) suggest, a mixing chamber in the inspiratory line helps keep the inspired concentration constant even though the volume of gas with very low concentration contained in the dead space contaminates the start of inspiration.

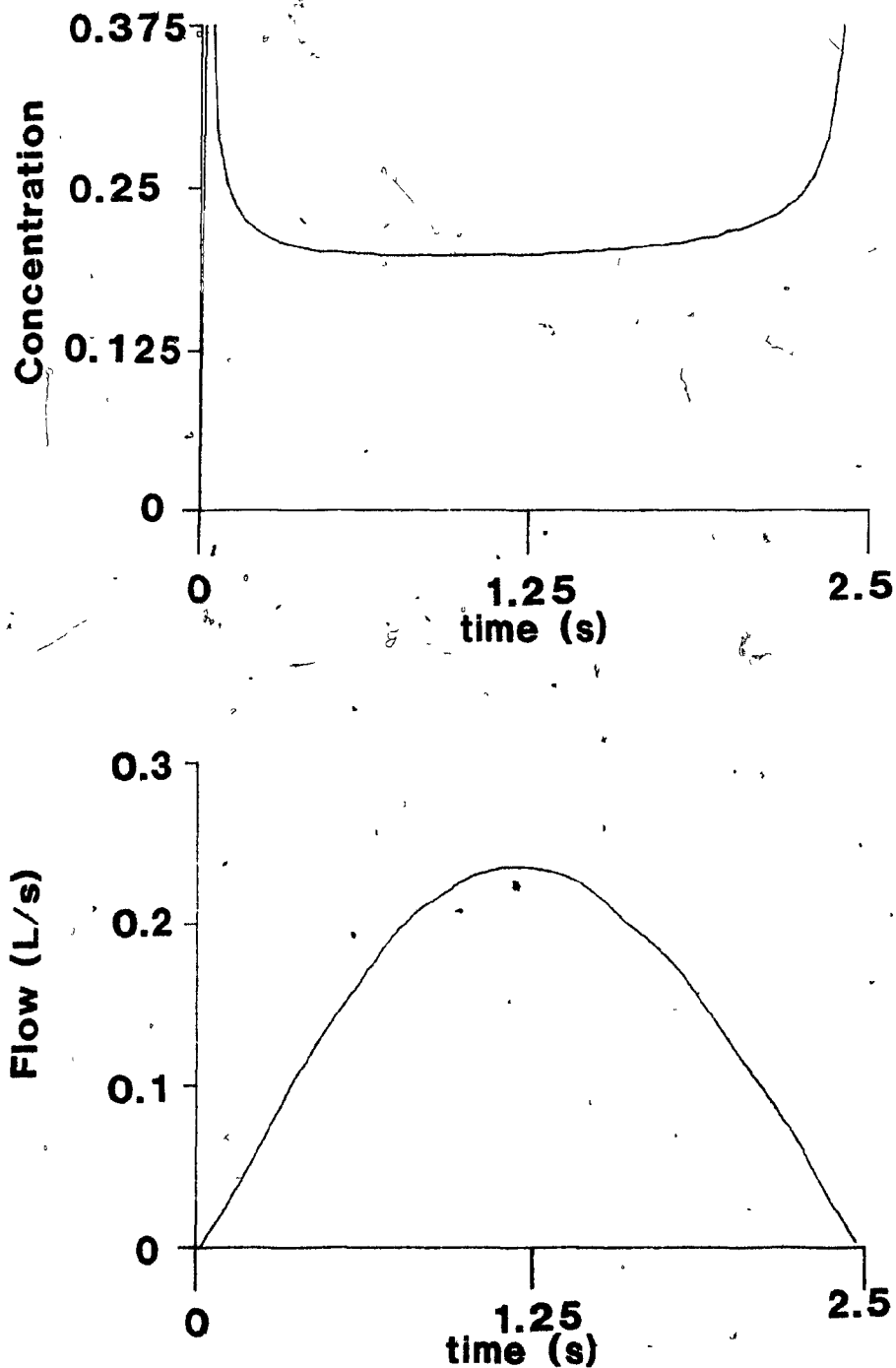


Fig. 5.3 The concentration at the mouth during inspiration. The concentration of krypton-81m over the trachea during inspiration from the mixing chamber is shown in the upper panel, the flow at the mouth in the lower panel.

5.2.4 METHODS OF ANALYSIS

5.2.4.1 Steady State

The steady state scans were interpreted using the overall mass balance presented by Fazio and Jones (1975) in which the lung is modelled as a single well-mixed compartment. Because krypton-81m solubility is low, the amount that dissolves in the lung tissue during a breath may be neglected.

Over a number of tidal breaths, if the concentration of krypton-81m does not change,

$$Q_{IN}C_I = Q_{EX}(n/V) + \lambda n \quad (5.1)$$

Therefore
$$n = (QC_I)/(Q/V + \lambda) \quad (5.2)$$

where Q , the flow, is assumed to be equal on inspiration and expiration (steady state assumption), C_I is the constant inlet concentration of krypton-81m, n is the number of moles of krypton-81m present in the lung, V is the volume of the lung compartment, and $\lambda = 3.2 \text{ min}^{-1}$ is the decay constant of the isotope. The ratio of count rates between two regions is then the ratio of the regional ventilation (Q_1/Q_2) multiplied by the correction factor,

$$\frac{(Q_2/V_2 + \lambda)}{(Q_1/V_1 + \lambda)} \quad (5.3)$$

(Harf et al, 1978). If Q/V is nearly the same for both regions or if it is much smaller than λ in both, the correction factor is approximately unity.

The digitized steady state scans for each experiment were displayed on a colour screen. The two lungs, outlined by eye on the images, were divided into caudal and cephalad regions of approximately

equal surface areas and masks for the regions were stored. Over the selected regions, the ratios of the counts were computed for non-dependent to dependent zones (right to left lung), and for cranio-caudal distributions within each lung.

Activity profiles were constructed from the scans both across both lungs at approximately the middle of the activity field and down each lung. The cephalo-caudal profiles for both lungs were normalized using the maximum number of counts per pixel in the profile of the left lung. The profile from left to right in the middle of the chest was normalized by the maximum activity in that slice. No attempt was made to scale for body size.

5.2.4.2 *The Average Breath*

To study the time-course of a breath, averaging is required, because too little krypton-81m is delivered during a single breath of krypton-81m in air to show the sequence of filling. A representative breathing cycle, an average breath, must be reconstructed from the addition of multiple cycles. Although this may be done with the aid of a pneumotachograph or other device to signal end inspiration or end expiration (Alderson et al, 1979; Alderson and Line, 1980; DeLand and Mauderli, 1972; Line et al, 1980), it requires that the gating signal be acquired simultaneously with the activity record. However, a signal other than the recorded activity is not necessary (Kaplan et al, 1982). As the computer used in the main study had no recording channel other than that from the gamma camera, only the krypton-81m activity information was used (Fig. 5.4). (In the later series when the pneumotachograph signal was available, it was used for the reconstruction.)

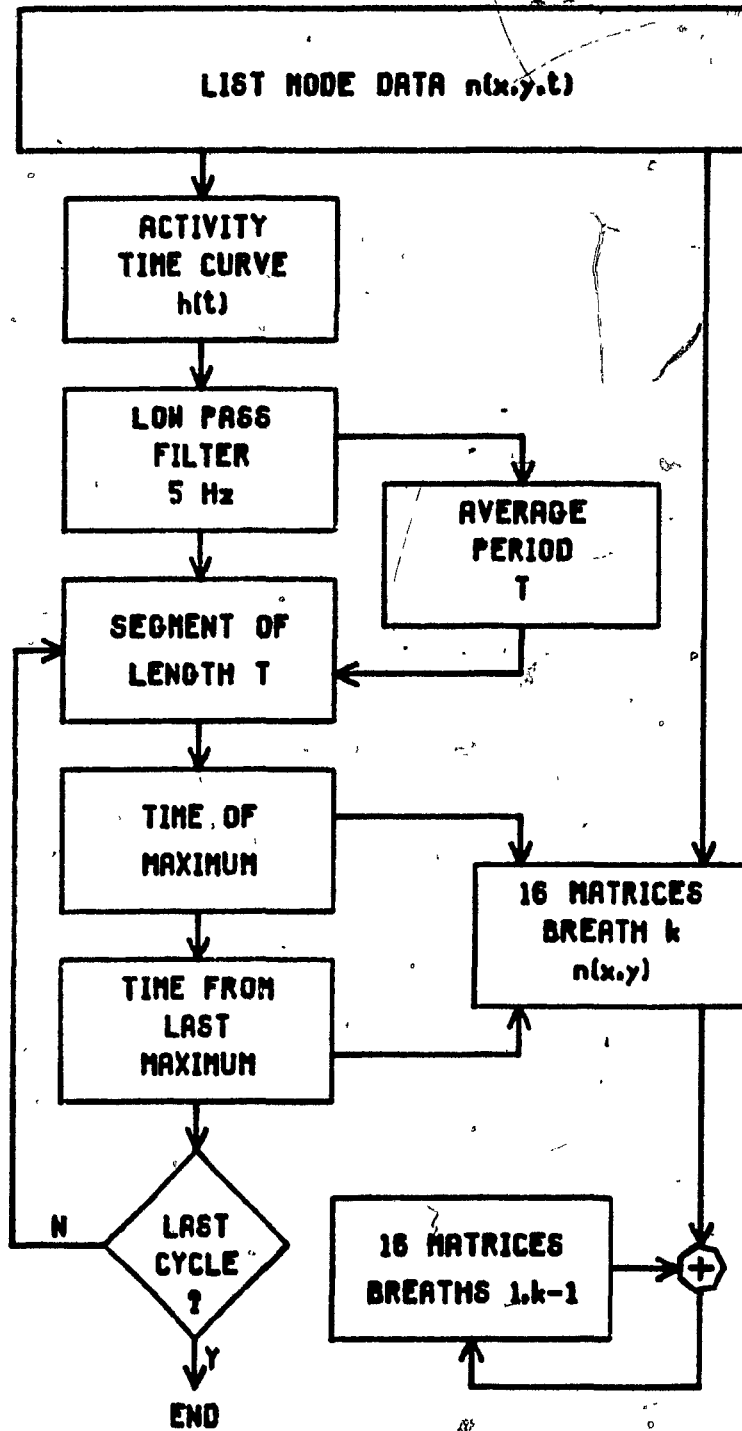


Fig. 5.4 The calculation of a representative breath (dynamic series of images) from list mode data. Only the recorded activity was used.

The period of each cycle was found from the time-activity curve for the entire lung field. Cycles deviating from the mean period by more than twenty percent were rejected. The periods of the individual breaths were divided into sixteen equal time segments. These were used to extract the matrices corresponding to the first sixteenth, second sixteenth, etc. of each separate breath from the filtered data. Matching breath fractions were added to produce a sixteen frame sequence (a dynamic series) of a representative ("average") cycle. Activity-time curves were constructed over the representative breath for the regions corresponding to the individual lungs as outlined on the steady state images. The gated images themselves were not analysed.

The interpretation of the time-varying krypton-81m activity during a breath is more complicated than that of the steady state image. Clearly, the activity is not directly proportional to the flow of air entering the region. To interpret the curves, it was necessary to examine the mass balance of krypton-81m in the lungs. Solution of the equations (Chapter 4) permitted the derivation of the flow per unit lung volume as a function of time:

$$Q(t)/V(t) = (1/n(t)) \cdot dn(t)/dt + g(t) \quad (5.4)$$

where $V(t) = V_0 + \int_0^t Q(t) dt$ represents the volume of the well ventilated region, and $g(t)$ is a correction term including diffusion and decay effects.

The flow rates per unit volume for the left and right lungs were found from Eqn. 5.4 using the signal processing interpreter Nexus (Hunter and Kearney, 1983) on a PDP 11/70 computer (Digital Equipment

Corporation, Maynard, Mass.). The curve for each cycle was concatenated with itself three times. Cubic spline interpolation was used to decrease the interval between points to 0.1 s and to smooth the curves before differentiation. The curves were smoothed to account for 95% of the variance, the derivatives were taken, they were divided by the smoothed activity-time curves, and the middle cycle was extracted, thereby eliminating the portions distorted by the end effects during smoothing and differentiating.

5.3 RESULTS

5.3.1 STEADY STATE

5.3.1.1 *Count Ratios*

The ratios of accumulated (steady state) counts for the non-dependent over the dependent lungs (right over left) are presented in Table 5.1. The variation among subjects is large but the change with the different manoeuvres for individual subjects is small. The analysis of variance shows that the mean ratios do not differ significantly with the changes of frequency and tidal volume. More importantly, the difference between the baseline ratio at 12 breaths per min and the normal tidal volume, and any other condition is insignificant as shown by a paired Student's t test. The cranio-caudal changes of count distribution in the lungs (Tables 5.2 and 5.3) also do not differ significantly from zero.

The steady state scans presented here may be interpreted according to Eqn. 5.2. However, in the lateral decubitus position, the ventilation per unit volume can be assumed neither negligible relative to the decay of constant of krypton-81m nor uniform between the lungs.

TABLE 5.1

RATIOS OF COUNTS: NON-DEPENDENT/DEPENDENT LUNG

SUBJECT	12 BREATHS/MIN		24 BREATHS/MIN	
	V_{T12}	$2 \cdot V_{T12}$	V_{T24}	$2 \cdot V_{T24}$
A	1.25	0.98	1.34	1.00
B	1.08	1.13	----	1.11
C	1.01	1.07	1.09	1.08
D	0.88	1.04	1.14	1.11
E	1.07	1.08	0.93	0.99
F	0.84	0.95	0.92	0.95
G	1.17	----	2.09	1.17
H	0.68	0.78	0.77	0.92
I	0.62	0.61	0.47	0.60
J	1.23	1.21	----	----
K	1.59	1.73	1.94	----
mean	1.04	0.95	1.19	0.99
sd	0.28	0.18	0.53	0.17

* Frequency = 9/min, Tidal volume = $2 \cdot V_{T12}$

ANALYSIS OF VARIANCE

	Sum of Squares	d.f.	Mean Squares	F
Among	0.29	3	0.097	1.04
Within	3.08	33	0.093	

$F_{3,33}(0.05)=8.6$

Not significant.

DIFFERENCE FROM 12 BREATHS/MIN, V_{T12}

	12 BREATHS/MIN		24 BREATHS/MIN	
	$2 \cdot V_{T12}$		V_{T24}	$2 \cdot V_{T24}$
mean	-0.025		-0.175	-0.036
sd	0.135		0.322	0.152
n	8		9	9
t	0.52		1.63	0.71

Not significant.

Note: Data for subjects J and K are from the later experiments.

TABLE 5.2

RATIOS OF COUNTS: CEPHALO/ CAUDAL REGIONS, DEPENDENT LUNG

SUBJECT	12 BREATHS/MIN		24 BREATHS/MIN	
	V_{T12}	$2 \cdot V_{T12}$	V_{T24}	$2 \cdot V_{T24}$
A	1.00	1.12	0.90	0.96
B	1.25	1.17		1.26
C	0.99	1.06	0.83	0.95
D	1.18	1.25	0.77	1.03
E	0.85	0.86	0.93	0.89
F	0.92	0.79	1.05	0.83
G	1.11	----	0.84	1.27
H	1.00	0.69	1.01	1.01
I	1.02	0.91	0.83	1.18
J	1.25	1.09*	----	----
K	0.75	0.74*	0.77	----
mean	1.03	0.98	0.93	1.04
sd	0.16	0.20	0.14	0.16

* Frequency = 9/min, Tidal volume = $2 \cdot V_{T12}$

DIFFERENCE FROM 12 BREATHS/MIN, V_{T12}

	12 BREATHS/MIN		24 BREATHS/MIN	
	$2 \cdot V_{T12}$	V_{T24}	$2 \cdot V_{T24}$	
mean	0.039	0.043	-0.012	
sd	0.148	0.132	0.102	
n	8	9	9	
t	0.745	0.977	0.353	

Not significant.

Note: Data for subjects J and K are from the later experiments.

TABLE 5.3

RATIOS OF COUNTS: CEPHALO/CAUDAL REGIONS, NON-DEPENDENT LUNG

SUBJECT	12 BREATHS/MIN		24 BREATHS/MIN	
	V_{T12}	$2 \cdot V_{T12}$	V_{T24}	$2 \cdot V_{T24}$
A	0.79	0.88	0.79	0.92
B	1.01	1.06		1.12
C	0.86	1.23	0.84	1.04
D	0.74	0.75	0.74	0.65
E	0.74	0.75	0.74	0.65
F	0.68	0.69	0.77	0.65
G	0.90	0.82	1.00	0.85
H	0.89		0.73	0.95
I	1.35	0.71	1.23	0.81
J	0.99	0.93 [*]		
K	0.63	0.64 [*]	0.64	
mean	0.88	0.85	0.84	0.87
sd	0.20	0.20	0.18	0.16

* Frequency = 9/min, Tidal volume = $2 \cdot V_{T12}$

DIFFERENCE FROM 12 BREATHS/MIN, V_{T12}

	12 BREATHS/MIN		24 BREATHS/MIN	
	$2 \cdot V_{T12}$	V_{T24}	$2 \cdot V_{T24}$	
mean	0.046	0.013	0.033	
sd	0.288	0.085	0.213	
n	8	9	9	
t	0.45	0.46	0.46	

Not significant.

Note: Data for subjects J and K are from the later experiments.

In a bronchspirometric study of awake subjects, Lillington et al. (1959) found nitrogen clearance rates in the left lateral decubitus position of 0.018 s^{-1} (1.1 min^{-1}) and 0.009 s^{-1} (0.57 min^{-1}) in the dependent and non-dependent lungs respectively for quiet breathing. Although the limits proposed by Arnot et al (1981) and by Papanicolaou and Treves (1980) for the assumption that the number of counts is directly proportional to the arriving flow is 0.025 s^{-1} (1.5 min^{-1}), the values of Lillington et al. (1959) are probably exceeded by most subjects. Even with their values, neglect of the correction factor would cause a 14% error. Thus, krypton-81m scans for subjects in the lateral decubitus position must be interpreted by including the factor of ventilation per unit volume, obtained either from a washout measurement as was done for children (Ciofetta et al, 1980), or by other means.

5.3.1.2 Profiles

The profiles of the steady-state activity across the chest from right to left and down the lungs from apex to base for three subjects are shown in Fig. 5.5 - 5.7. The left (dependent) lungs showed considerably more activity than the right. The cranial regions of the left lung had higher concentrations of krypton-81m than the caudal regions while the distribution of the tracer in the right lung was more uniform or slightly preferential to the basal zones. The profiles changed little with different experimental conditions.

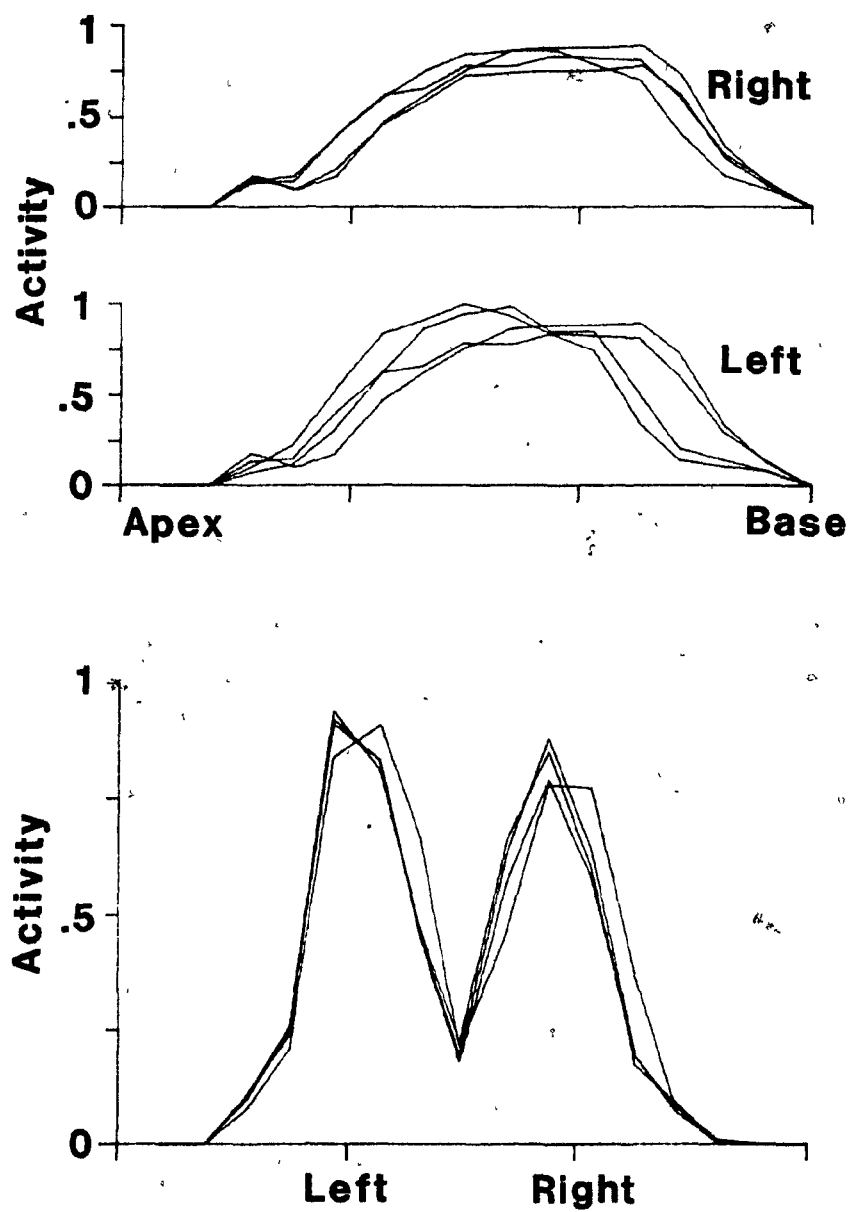


Fig. 5.5 Steady state activity profiles. Normalized activity profiles are shown for the left and right lungs, apex to base (upper curves) and across the lungs from left to right in the centre of the lung field. Subject C, left lateral decubitus.

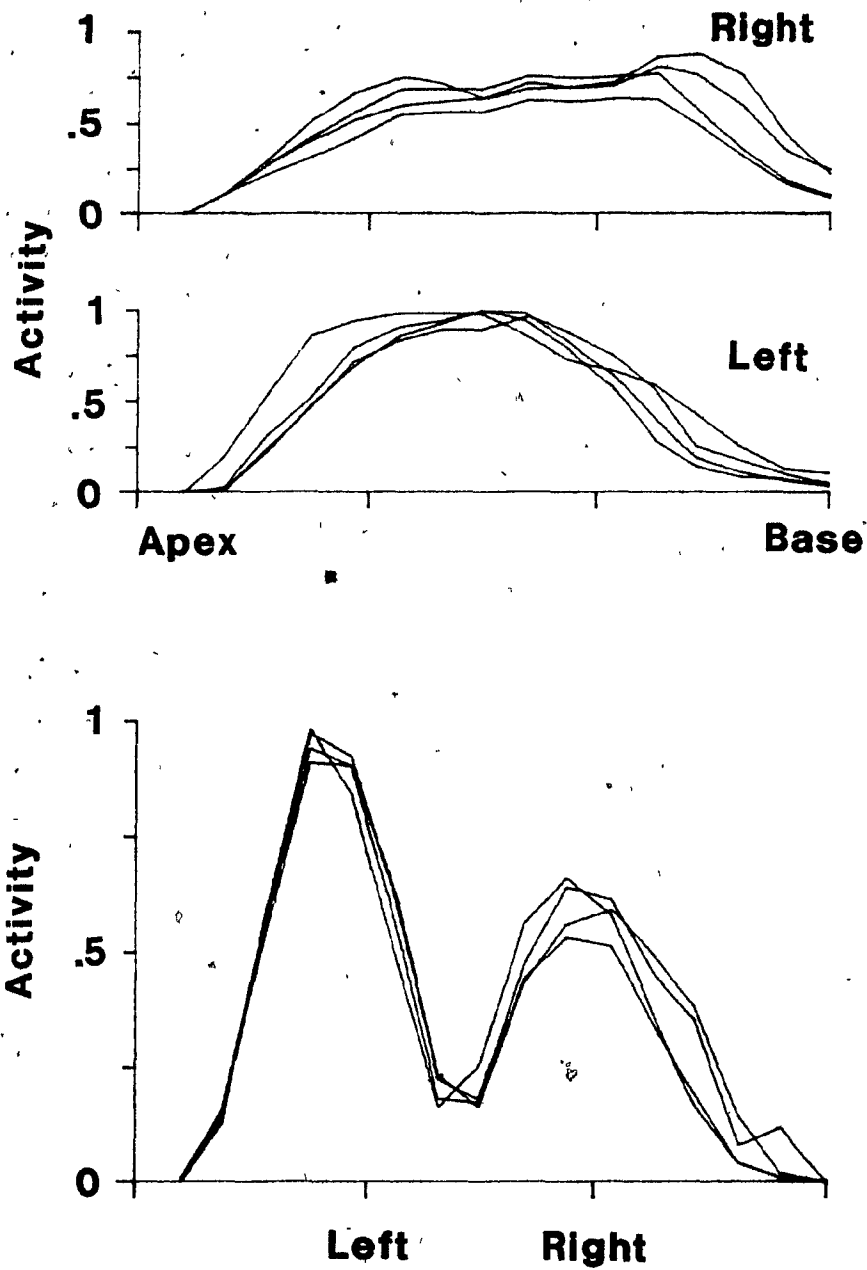


Fig. 5.6 Steady state activity profiles. Subject D.

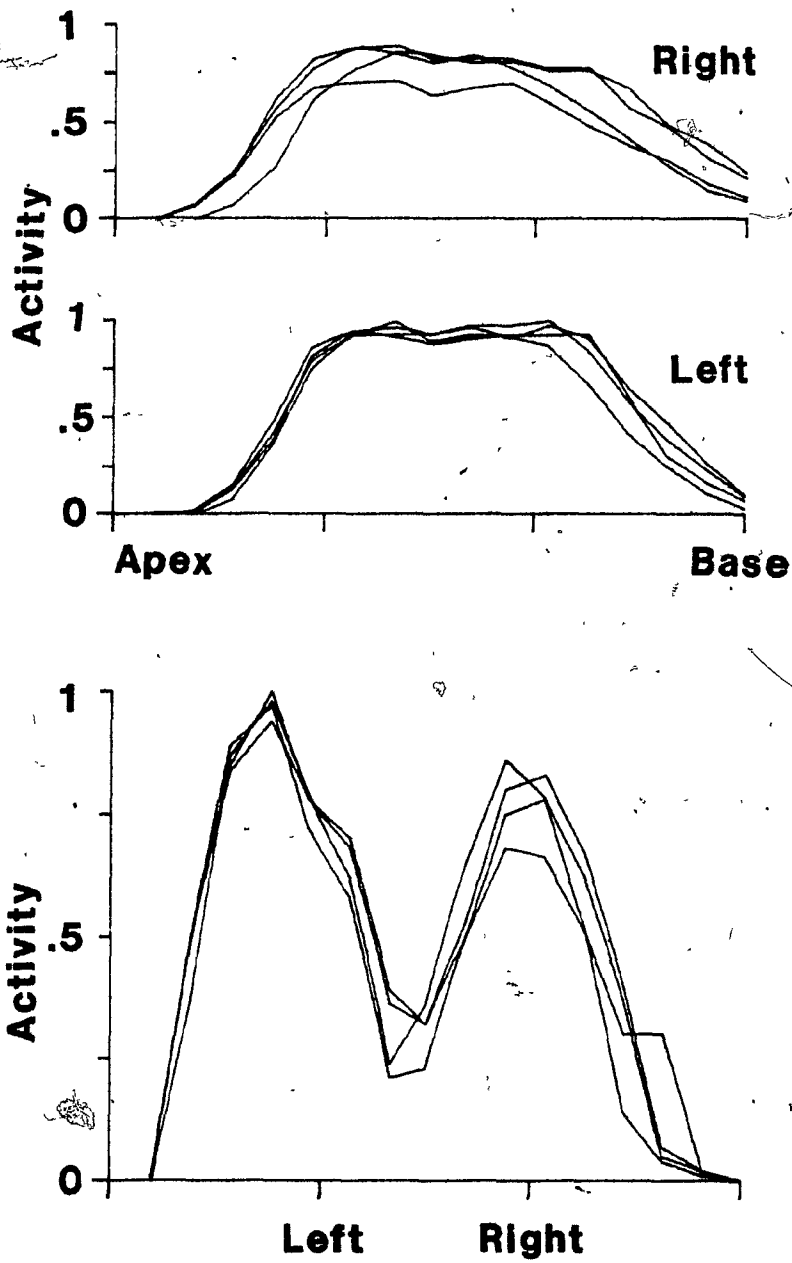


Fig. 5.7 Steady state activity profiles. Subject F.

5.3.2 WASHOUTS

Ventilation per unit volume was measured by the washout of krypton-81m in two subjects. For subject K (Fig. 5.8), the mean values over all pixels during the first 15 seconds (3 breaths) at 12 breaths min^{-1} were 0.03 s^{-1} and 0.06 s^{-1} (1.92 min^{-1} and 3.57 min^{-1}) (Table 5.4) in the right and left lung, respectively. The value does not represent the mean clearance rate, as the washout slopes have not been weighted by the volumes measured by the pixels and the point to point variability is large.

The washouts using krypton-81m involved significant experimental and computational uncertainties because of the rapid decay of the isotope and the resulting low number of counts. After three breaths, the activity was very near the background level. The variability involved in estimating over so few breaths renders the absolute measurements doubtful. The pattern of Fig. 5.8 therefore is presented only for internal comparison. The trends seemed similar in the other cases which are summarized in Table 5.4. The washout was locally inhomogeneous. This range of the local values in two normal subjects suggests that the well-mixed assumption for tracer behaviour must be reconsidered. The difference in size of the dependent and non-dependent lungs was evident.

5.3.3 DYNAMIC CYCLE

For the two subjects of the second series, the pneumotachograph measurements were compared with the activity-time curves over the entire field of both lungs. The instantaneous activity

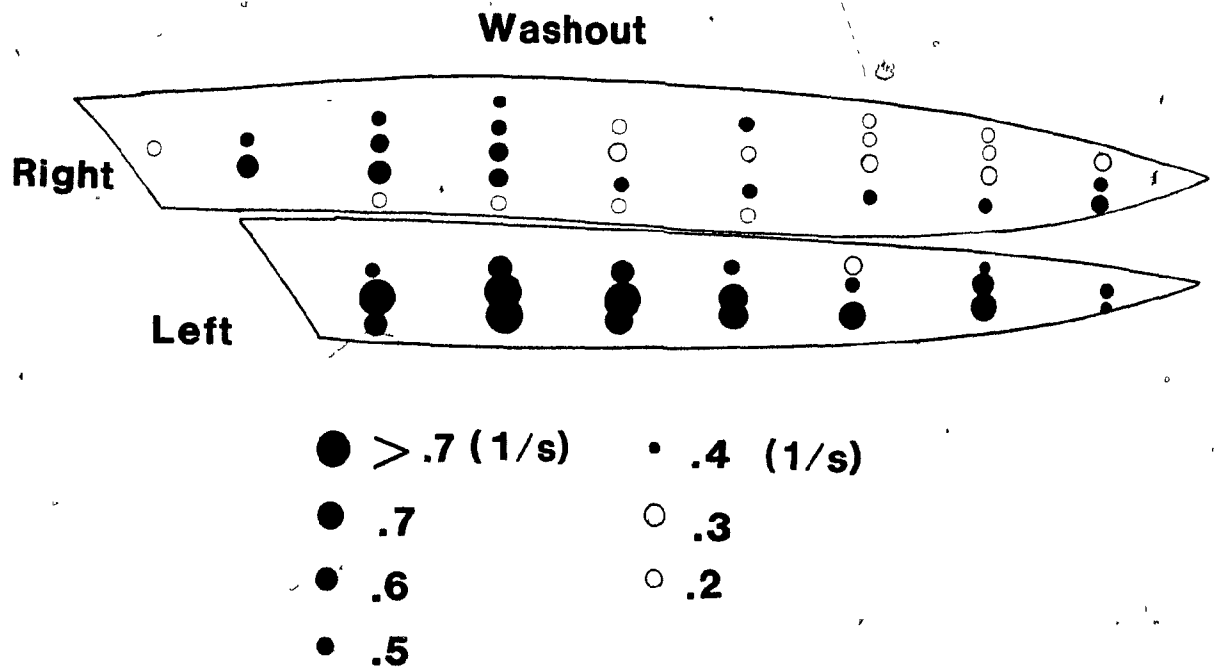


Fig. 5.8 Local washout of krypton-81m. The ventilation per unit volume was calculated from the slope of the logarithm of concentration as a function of time on a regional basis. Denser colour indicates faster washout. The lung outline is approximate. Subject K, 12 breaths min^{-1} .

TABLE 5.4

MEAN VALUES OF THE WASHOUT SLOPES

Frequency	Subject	Right Lung		Left Lung	
		Mean (s^{-1})	s.d.	Mean (s^{-1})	s.d.
KRYPTON-81m					
12/min	J	-0.010	0.005	-0.026	0.012
12/min	K	-0.032	0.014	-0.060	0.027
24/min	K	-0.034	0.018	-0.048	0.023
9/min	K	-0.019	0.013	-0.020	0.012

was seen to vary much like the tidal volume, while the derivative of the counts normalized by the count rate was similar to the volumetric flow (Fig. 5.9).

A multiple linear regression was performed to compare the data to Eqn. 5.4. The equation was rewritten to make the flow Q a linear combination of the normalized derivative term $(1/n)(dn/dt)$, of the integral of flow ΔV , and of the product $\Delta V(1/n)(dn/dt)$. The coefficients are given in Table 5.5. The fit accounted for more than 98% of the variance at 9 and 12 breaths per minute. The coefficient b of the normalized derivative (mean for 4 cases = 4.2 L) corresponds to the maximum lung volume in Eqn. 5.4, because the origin was chosen at end inspiration. The volume divisor of the flow is the term $(b + c\Delta V)$. The expression $(a + d\Delta V)/(b + c\Delta V)$, of the order of magnitude of 10^{-2} , then represents $g(t)$ in the equation. The normalized derivative curves thus represent the flow per unit volume for the region over which they are measured.

5.3.3.1 Flow per Unit Volume Curves

The flow per unit volume curves for one subject are shown in Fig. 5.10 for the four experimental conditions. As one period of each case is displayed, the time axes are scaled differently in each panel. The curves for the left and right lungs are presented. The magnitude was greater in the left (dependent) than in the right lung. Although the mean of the curves of flow per unit volume was zero, the curves were not symmetrical about the time axis. The magnitude of the maximum was slightly greater than that of the minimum and it occurred before the middle of the inspiratory phase.

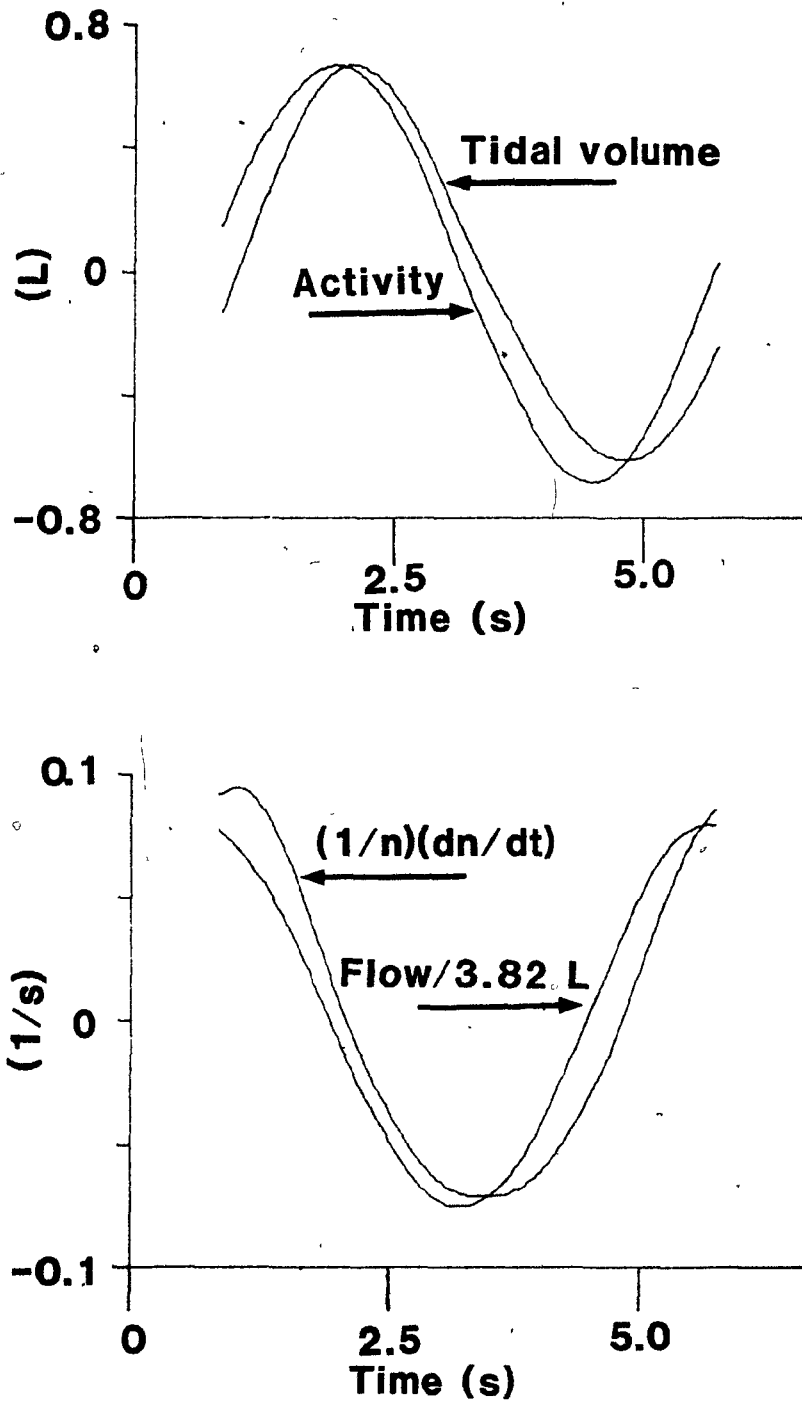


Fig. 5.9 A comparison between the activity and tidal volume and the normalized derivatives and the flow per unit volume. The activity was multiplied by the factor (maximum tidal volume/maximum activity) to enable display on the same axes. The pneumotachograph signal was divided by the slope of the regression line between itself and the normalized derivative.

TABLE 5.5

BEST FIT PARAMETERS OF EQUATION

Subject	Frequency (1/min)	Flow = a + b (1/n)(dn/dt) + c (ΔV)(1/n)(dn/dt) + d(ΔV)				VAF (%)
		a (L/s)	b (L)	c (1/L)	d (1/s)	
J	9	-0.09	5.51	0.50	-0.06	99.3
J	12	-0.03	4.54	-0.52	-0.12	99.4
K	9	-0.07	3.12	-0.98	-0.09	98.5
K	12	-0.02	3.63	-0.77	-0.15	98.6

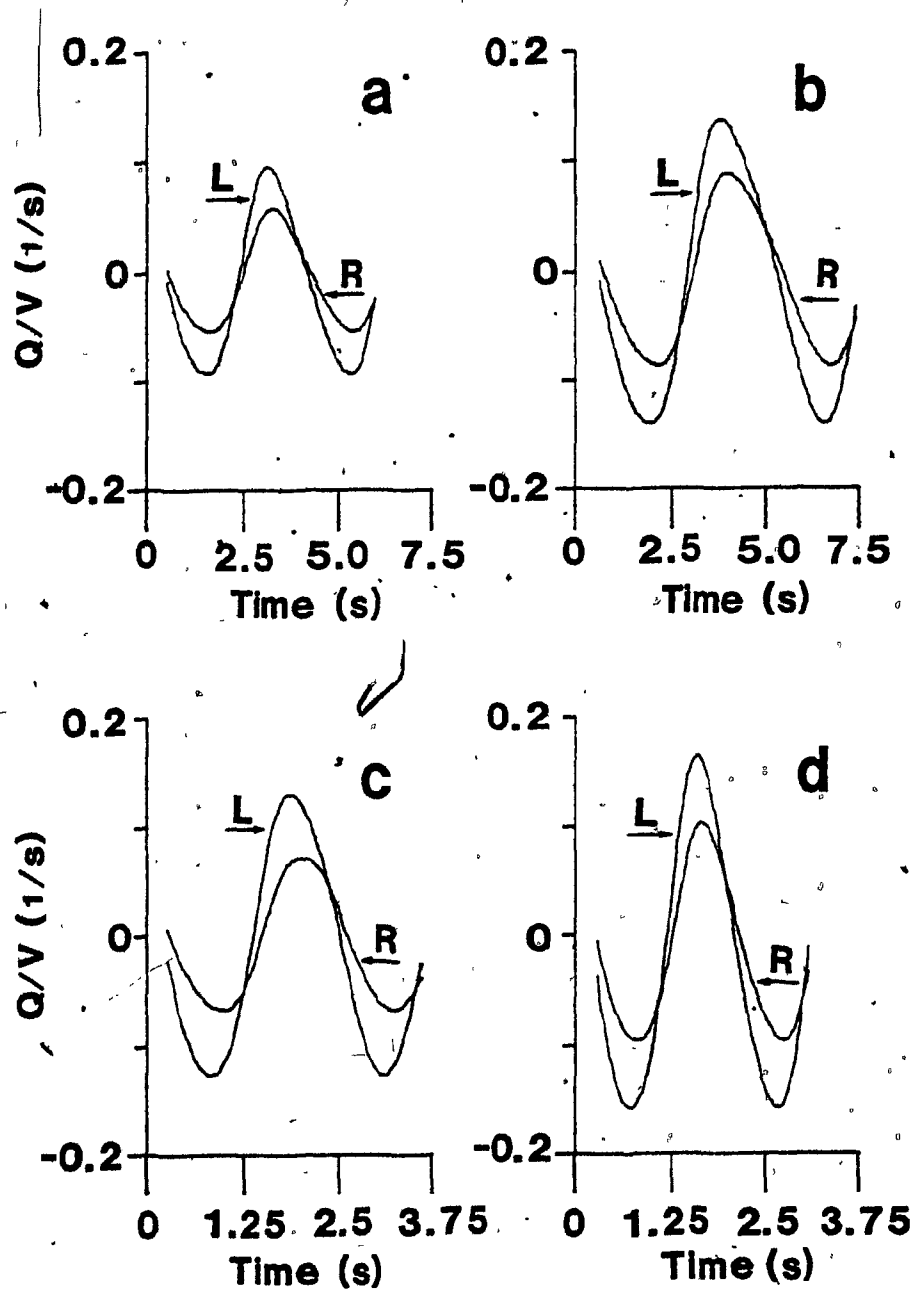


Fig. 5.10 Curves of the flow per unit volume. Subject F.
 a) 12 breaths min^{-1} , Baseline tidal volume V_{T12} . b) 12 breaths min^{-1} ,
 doubled tidal volume. c) 24 breaths min^{-1} , tidal volume V_{T24} .
 d) 24 breaths min^{-1} , doubled tidal volume.

The magnitude of these curves increased with tidal volume and with frequency, but in particular with frequency (Table 5.6). At 12 breaths min^{-1} , the average increase was 32% in the left lung, 22% in the right lung, and 24% overall when the tidal volume doubled. At 24 breaths min^{-1} , the increases were 18%, 12%, and 16% for left, right, and both lungs, respectively. When the tidal volume was constant and the frequency doubled, the values increased by 121%, 88%, and 92% in the left, right, and both lungs, respectively. When the frequency doubled with the minute ventilation held constant, the increases were 97%, 77%, and 70% for the left, right, and both lungs, respectively. In all cases, the flow per unit volume was greater in the left (dependent) than in the right (non-dependent) lung.

Washout curves provide one kind of measurement of flow per unit volume, the computed curves another. The single value of the washout slope is an average calculated from a model of constant flow into a well-mixed compartment. The computed flow per unit volume curves are correlated with the time-varying flow into a compartment of time-varying volume. Thus, the two measures are not directly comparable. The root mean square of the curves may be similar to the washout slope but will not be identical, since both measure an "average" ventilation per unit volume but the mean of the ratio of flow to volume is not the same as the mean flow divided by the mean volume. Indeed, the root mean square values are in a range between 0.03 s^{-1} and 0.18 s^{-1} for the left lung and between 0.02 s^{-1} and 0.08 s^{-1} in the right lung, while washout values of 0.024 s^{-1} and 0.0096 s^{-1} for the left and right lungs, respectively, have been reported for subjects in the left lateral decubitus position (Lillington et al, 1959). In

TABLE 5.6

VENTILATION PER UNIT VOLUME CURVES
ROOT MEAN SQUARE VALUES (1/s)

LEFT LUNG SUBJECT	12 BREATHS/MIN		24 BREATHS/MIN	
	V_{T12}	$2 \cdot V_{T12}$	V_{T24}	$2 \cdot V_{T24}$
A	0.047	0.068	0.074	0.086
C	0.046	0.061	0.077	0.126
D	0.053	0.094	0.076	0.097
E	0.032	0.033	0.103	0.104
F	0.068	0.099	0.093	0.116
G	0.066	-----	0.080	0.079
H	0.054	0.062	0.085	0.100
I	0.048	0.051*	0.180	0.156
J	0.077	0.077*	-----	-----
K	0.076	0.066*	0.144	-----

RIGHT LUNG SUBJECT	12 BREATHS/MIN		24 BREATHS/MIN	
	V_{T12}	$2 \cdot V_{T12}$	V_{T24}	$2 \cdot V_{T24}$
A	0.030	0.037	0.043	0.041
C	0.037	0.048	0.060	0.075
D	0.037	0.054	0.049	0.049
E	0.022	0.025	0.082	0.085
F	0.040	0.062	0.051	0.072
G	0.049	-----	0.066	0.058
H	0.035	0.033	0.047	0.056
I	0.040	0.038*	0.041
J	0.049	0.046*	-----	-----
K	0.052	0.047*	0.147	-----

TOTAL SUBJECT	12 BREATHS/MIN		24 BREATHS/MIN	
	V_{T12}	$2 \cdot V_{T12}$	V_{T24}	$2 \cdot V_{T24}$
A	0.037	0.052	0.056	0.064
C	0.042	0.054	0.067	0.099
D	0.045	0.073	0.061	0.071
E	0.028	0.029	0.092	0.094
F	0.055	0.080	0.072	0.094
G	0.057	-----	0.067	0.057
H	0.045	0.048	0.068	0.078
I	0.042	0.046*	0.053
J	0.061	0.060*	-----	-----
K	0.061	0.053*	0.138	-----

* Frequency = 9/min, Tidal volume = $2 \cdot V_{T12}$

----- not measured; could not be calculated.

-- continued

TABLE 5.6 -- continued
DIFFERENCE FROM 12 BREATHS/MIN, V_{T12}

	12 BREATHS/MIN		24 BREATHS/MIN	
	$2 \cdot V_{T12}$	V_{T24}	V_{T24}	$2 \cdot V_{T24}$
LEFT LUNG				
mean difference	0.017	0.047		0.056
sd	0.015	0.038		0.056
t	3.05	3.74		5.44
p	0.005	0.002		0.002
RIGHT LUNG				
mean difference	0.008	0.019		0.027
sd	0.009	0.018		0.027
t	2.29	2.96		3.61
p	0.025	0.002		0.005
TOTAL				
mean difference	0.013	0.023		0.035
sd	0.011	0.017		0.022
t	3.08	3.78		4.31
p	0.012	0.002		0.002

The root mean square values were calculated from the curves, $(1/n)(dn/dt)$, for the left lung, right lung, and both lungs. V_{T12} is the baseline tidal volume at 12 breaths/min. V_{T24} is the comfortable tidal volume at 24 breaths/min.

seated subjects, Forkert et al (1978) showed that the washout in the dependent and non-dependent regions were different, ranging, for example, from 0.112 s^{-1} in the dependent zone to 0.031 s^{-1} in the nondependent zone in one seated subject.

5.3.3.2 Flow Rate Ratios

The flow rates into and out of the individual lungs were compared using the flow per unit volume curves and an estimate of relative lung volumes. For the lateral decubitus position, the static volume of the dependent lung at FRC has been estimated to be 62% of that of the non-dependent lung (Kaneko et al, 1966). At a resting volume of (FRC + 0.1 TLC) this ratio increased to about 68%. By using 65% as a mean ratio between the dependent and non-dependent lung volumes, curves of the ratio of flow rates in the right lung to those in the left were computed (Fig. 5.11). For most of the cycle, the flow in the dependent lung was greater than that in the non-dependent lung. Only immediately before and after the change in flow direction (at end inspiration or end expiration), was the flow in the non-dependent lung larger than that in the dependent one. The negative ratios indicate a time when one lung was filling while the other was emptying.

Because of the estimation used for the volume ratios, it was not possible to determine the time at which the flows were equal. Different values of the ratio of the volume of the left lung to the right in the lateral decubitus position have been given by different investigators. Lillington et al. (1959) found 0.49 at FRC for conscious, intubated subjects, but the data of Hedenstierna et al. (1981) yield 0.39 in anaesthetized adults. The use of different

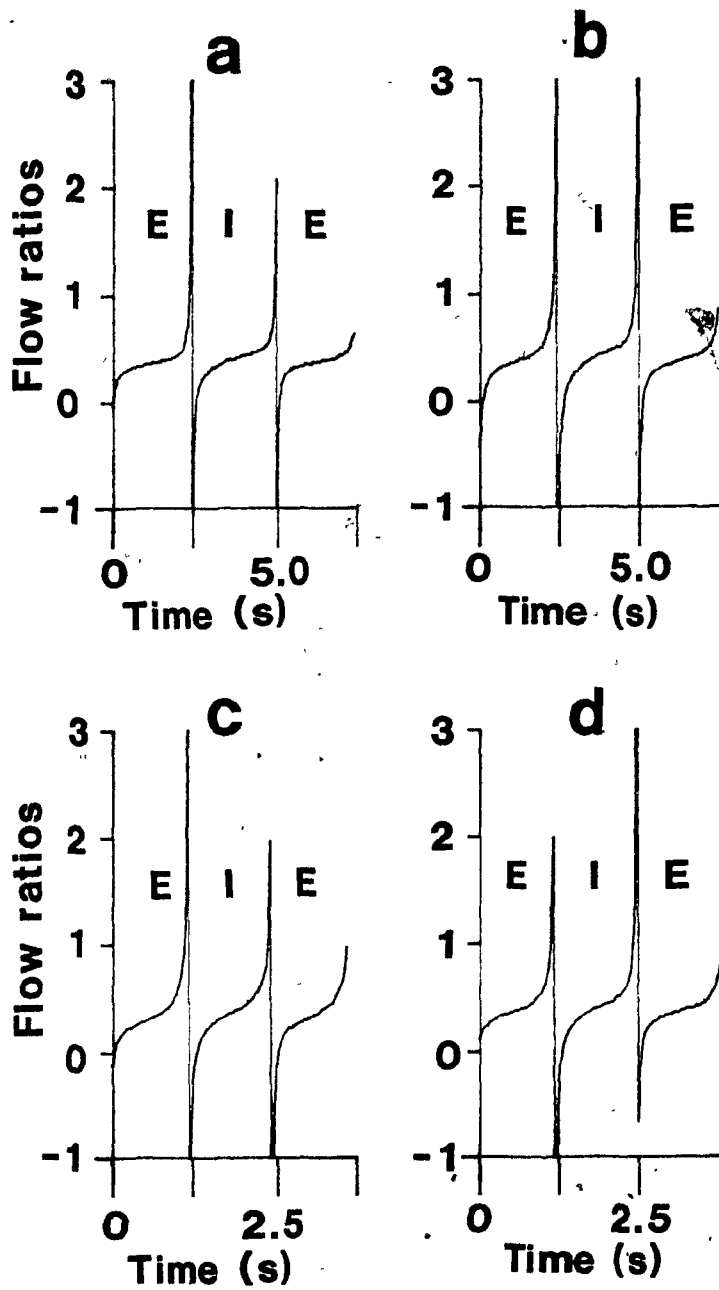


Fig. 5.11 Ratios of flows, right to left lung. Subject F. The four panels correspond to those of Fig. 5.10. E marks expiration and I, inspiration. The large spikes occur when the flow in the left lung is approximately zero.

TABLE 5.7

RATIOS OF FLOWS: NON-DEPENDENT/DEPENDENT LUNG

SUBJECT	12 BREATHS/MIN		24 BREATHS/MIN	
	V_{T12}	$2 \cdot V_{T12}$	V_{T24}	$2 \cdot V_{T24}$
A	1.06	0.75	0.89	0.69
C	0.92	0.95	0.95	0.83
D	0.80	0.75	0.90	0.73
E	0.80	0.92	0.94	0.97
F	0.64	0.72	0.65	0.70
G	1.83	----	0.98	1.00
H	0.60	0.58	0.53	0.68
I	0.57	0.54 [*]	0.37
J	0.97	0.92 [*]	----	----
K	1.29	1.45 [*]	1.97	----

DIFFERENCE FROM 12 BREATHS/MIN, V_{T12}

mean	-0.03	0.13	0.15
sd	0.14	0.32	0.35
t	-0.49	1.13	1.15

Not significant.

* Frequency = 9/min, Tidal volume = $2 \cdot V_{T12}$

---- not measured; could not be computed.

values for the volume ratio would change the scale of the flow ratio curves and the time at which the flows become equal. If the dependent lung was in fact less fully inflated proportional to the non-dependent lung than the estimated 65%, the flows to the individual lungs would have been more similar in magnitude and the flows would have been equal earlier in the cycle.

The steady state count ratios for the lung (Table 5.1) were converted to average flow rate ratios using the root mean square values (Table 5.6) of flow per unit volume in the denominator term (Table 5.7). The flow ratios were smaller than the count ratios because of the greater flow per unit volume in the dependent lung. The flow ratios were almost all less than one, indicating the higher flow that existed to the dependent zone. A paired Student's t test showed that the flow ratios at none of the other conditions varied significantly from those at the 12 breaths per minute, normal tidal volume baseline.

The steady state flow ratios and the flow ratio curves are measures of related variables, but cannot be compared directly. The steady state values are the ratios of the mean flows while the curves are the ratios of the instantaneous values. Because the mean of the ratios is not equivalent to the ratio of the means, one measurement cannot be converted into the other.

TABLE 5.8

PHASE ANGLES, LEFT LUNG LEADING

SUBJECT	12 BREATHS/MIN		24 BREATHS/MIN	
	V_{T12}	$2 \cdot V_{T12}$	V_{T24}	$2 \cdot V_{T24}$
A	34°	7°	41°	40°
C	7°	0°	45°	30°
D	14°	16°	14°	44°
E	15°	48°	13°	0°
F	29°	37°	60°	43°
G	0°	--	0°	0°
H	25°	54°	43°	43°
I	-17°	31°	-15°	--
J	0°	--	--	--
K	0°	--	0°	--

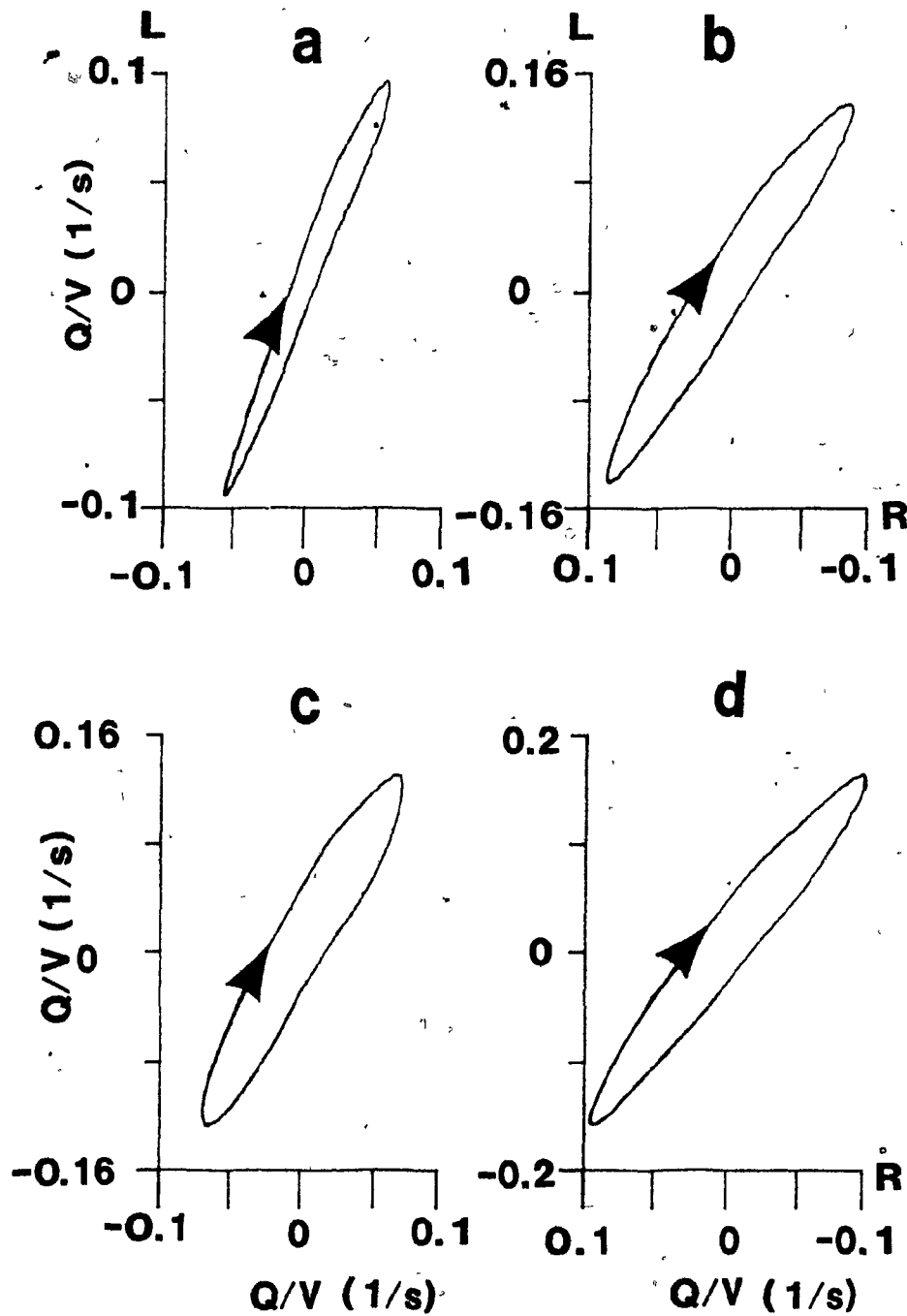


Fig. 5.12 Flow per unit volume, left lung plotted against flow per unit volume, right lung. Subject F. The panels correspond to those of Fig. 5.10. The direction of looping is indicated by the arrows. The left lung leads.

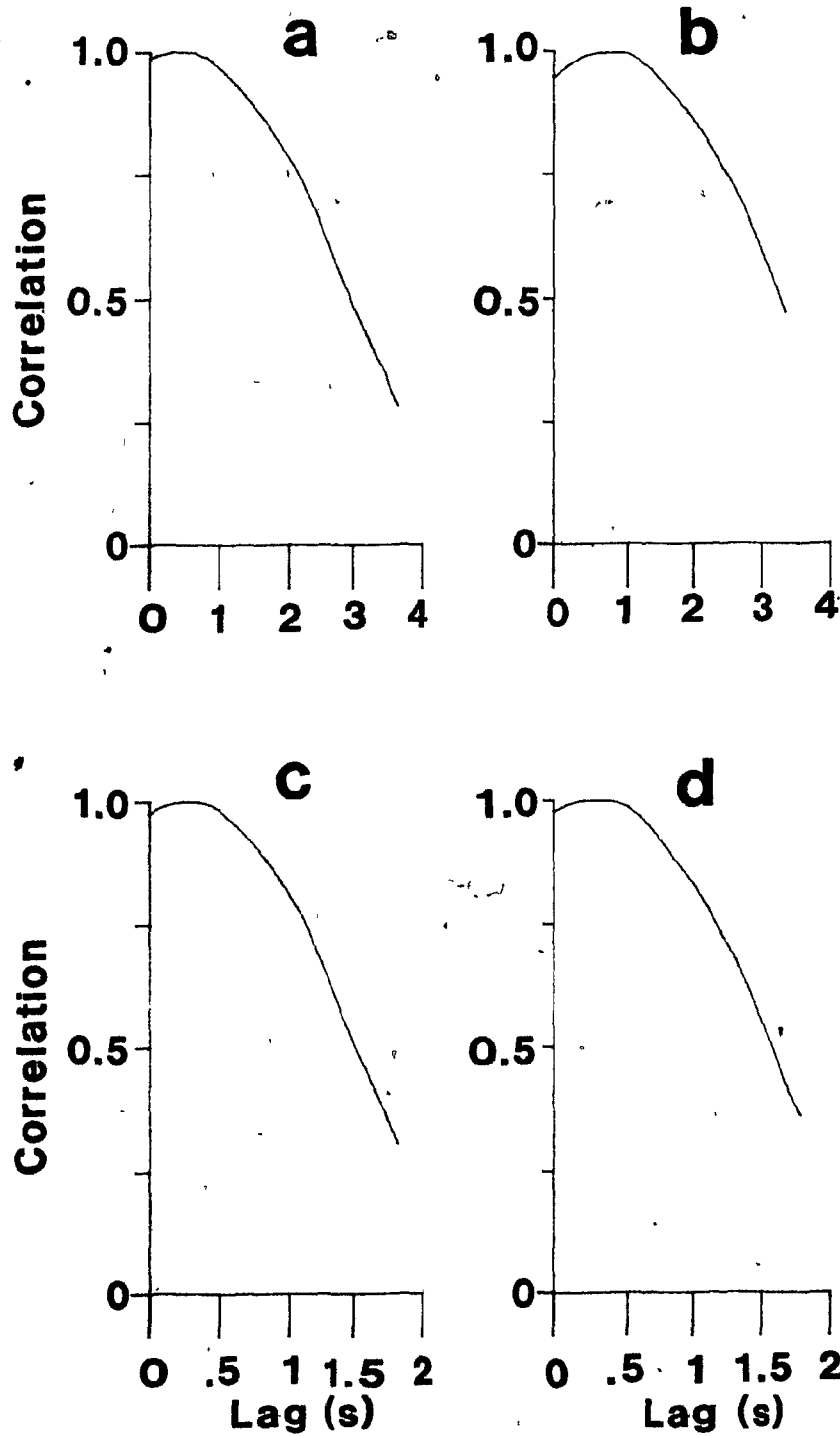


Fig. 5.13 Cross-correlations between the left and right flows per unit volume. Subject F. Panels correspond to those in Fig. 5.10. The maximum correlation occurs when the right lung lags the left.

5.3.4 PHASE

There were phase differences evident between the flows per unit volume in the left and right lungs, in most cases with the left lung leading the right (Table 5.8). Although this may be seen on the curves of Fig. 5.10, it is clearer in Fig. 5.12 where the flow rate per unit volume of one lung is plotted against that of the other. The corresponding cross-correlations are shown in Fig. 5.13. The largest phase angles, measured from the cross correlations, were seen at 24 breaths min^{-1} , although large phase differences were found for all of the experimental manoeuvres. Neither the depth of breathing nor the frequency had systematic effect on the phase angle. It is important to note that the resolution of the angles was coarse, with one lag point representing approximately 7° at 12 breaths min^{-1} and 14° at 24 breaths min^{-1} .

5.4 DISCUSSION

5.4.1 STEADY STATE SCANS

5.4.1.1 *Non-dependent to Dependent Ratios*

The steady state activity ratios (Table 5.1) remained essentially unchanged by variations of frequency and tidal volume within the normal, physiological range. The average flow ratios (Table 5.6) obtained from the activity ratios using the average flow per unit volume ratios in the correction term, Eqn. 5.3, showed similar invariance with the changes in manoeuvre. Although the ventilation per unit volume itself changed significantly with frequency and tidal volume (Table 5.6), the changes in the correction term (Eqn. 5.3) were small.

The constant ratios of mean volumetric flows and therefore of tidal volumes were in accord with the pleural pressure-driven model (Chapter 3) for pressure swings over the dependent and nondependent lungs which changed in proportion to each other. The ratios were generally less than one, showing the preferential ventilation of the dependent zones expected for the region with the larger pleural pressure swing. No effects of the regional time constants could be seen in the steady state scans. The range of flows used could not show the secondary effects of frequency and tidal volume that were evident in the simulation (Chapter 3) given the measurement uncertainty caused by the low count rates.

The stability of the ratios suggested that each subject chose a pattern of muscle use for breathing and maintained it for all four manoeuvres; it has been shown (Roussos et al, 1977; Chevrolet et al, 1979) that the contraction of particular respiratory muscles strongly influences the distribution of inspired air. Conversely, the intersubject variability may have represented in part the unconscious choice of different muscle contraction patterns by different individuals. Different lung volumes among subjects, shown in the model (Chapter 3) to affect tidal volume distributions and by Engel and Prefaut (1981) to alter bolus distribution in the supine position, also may have played a role. The body position, the resistance of the valves in the airway, and the efforts to maintain a constant breathing frequency and tidal volume certainly caused modifications in the pattern of breathing from that at rest. Without the ability to monitor respiratory muscle activity or functional residual capacity, the sources of the differences remained an open question.

5.4.1.2 Apico-Basilar Ratios

The cranio-caudal distribution of activity (Tables 5.2 and 5.3) also remained constant with changes in flow rate and frequency. The ventilation per unit volume was not computed for these regions because the activity of the krypton-81m generators was low enough that the acquisition of sufficient counts for the construction of sixteen images over regions smaller than one lobe was impractical. The count ratios themselves were studied.

In the non-dependant lung, the activity was greater in the basal than in the apical regions, while in the dependant lung, it was approximately uniform. The profiles down the lungs (Fig. 5.5 - 5.7) show this clearly. The activity, although not directly proportional to the average volumetric flow, was related to the ventilation, the sequential nature of which has been demonstrated in the cranio-caudal axis in supine subjects during inspiration at a constant flow rate (Engel and Prefaut, 1981). The lung volume at which a bolus of xenon-133 was inspired was shown to be a very significant factor in its distribution, it being preferentially to the caudal zones at high lung volume but preferentially cephalad at lower lung volumes (near FRC). The authors attributed this to airway closure in the paradiaphragmatic lung regions caused by the hydrostatic pressure of the abdomen on the dependant portions of the lungs. In the left lateral decubitus position the higher krypton-81m activity in the caudal region in the non-dependant lung but nearly uniform activity in the dependant lung may have resulted from a similar effect. The non-dependant lung was at a volume greater than its supine functional residual capacity while the dependant lung was at a volume similar to or slightly smaller (Lillington et al, 1959). If airway closure may be postulated in the

dependent paradiaphragmatic lung regions in normal supine man, then it is even more likely in lateral decubitus subjects, for whom the hydrostatic pressure on the dependent lung is higher. The uniform activity along the cranio-caudal axis of the dependent lung probably represented preferential flow to the cranial zones at the beginning of inspiration because of airway closure in the caudal area followed by preferential flow to the caudal zones after the airways opened and the large swing in the pleural pressure over the dependent paradiaphragmatic lung took effect. The distribution of the average flow may have been less uniform than that of the activity because high ventilation per unit volume following airway opening would have increased the magnitude of the denominator of Eqn. 5.2 for the basal region. In contrast in the non-dependent lung, the alveoli were inflated well above their closing volumes, the ventilation per unit volume was lower, and probably the count ratios were close to the ratios of the average flows and intraregional filling was nonsequential.

The measured cranio-caudal distributions in the dependent lung were affected by some measurement error. Because the lung regions of interest were selected on the total image, the lung margins used in drawing them were those of full inspiration. During expiration, however, the large change in position of the dependent hemi-diaphragm pushed the lung base in the cephalad direction. The region designated "basal" then contained only a portion of the lung base and included zones with no lung at all. The part of the lung base that had moved cephalad was counted as part of the apical region during the later parts of expiration. Thus, the distribution was biased twice in favour of the apical zones. This error could be reduced in future studies by

the use of the separate images from the dynamic series instead of the steady-state scan, drawing the regions on each one, and adding them. However, the correct choice of the regional boundaries would be difficult and the computation lengthier.

5.4.2 CURVES OF FLOW PER UNIT VOLUME

The ventilation per unit volume varied with time in an almost sinusoidal pattern for normal breathing. For subjects in the left lateral decubitus position, the values in the dependent lung were larger than in the nondependent lung, reflecting both the larger fraction of the flow to and from the dependent lung and its lower lung volume. The substantial displacement of the diaphragm described by Roussos et al. (1976) affected both the static and the dynamic pleural pressures in the lateral decubitus postures.

The calculated ventilation per unit volume increased with both tidal volume and frequency. Of the two, the frequency exerted the more pronounced effect, with the average increase of ventilation per unit volume being 97% and 77% in the left and right lungs, respectively, when the frequency was doubled and the tidal volume halved to maintain normal minute ventilation. When the minute ventilation was twice the normal value, the average changes with frequency were slightly less, or 91% and 64% in the left and right lungs, respectively. Doubling the tidal volume at 12 breaths min^{-1} caused average increases of only 32% and 22% for the left and right lungs, while doubling the frequency at the same tidal volume produced changes of 121% and 88% for the left and right lungs, respectively. These changes with frequency and depth of breathing of the measured ventilation per unit volume might be caused by variations of the

pleural pressure swings, by stratification of the tracer concentration in the lungs, or by intraregional inequalities of resistance and compliance.

A change in the pleural pressure swings large enough to more than double the ventilation per unit volume when the frequency was doubled without a redistribution of the pressures over the chest seems unlikely, yet the steady-state flow ratios did not change as would be expected for a different ratio of pleural pressure swings. Furthermore, the reduction in the effect of frequency changes at larger tidal volume and the effect of frequency at constant minute ventilation are difficult to explain as pressure effects alone.

Stratification of the gas within the lung would increase the measured ventilation per unit volume by decreasing the volume into which the tracer was dispersed. At higher frequencies, the isotope concentration arriving would be slightly higher (shorter transit time) but the residence time in the lung would be much less. At higher tidal volumes and constant frequencies, however, the residence time would be unchanged and the volume delivered increased so that the ventilation per unit volume might increase only slightly, depending on the amount of stratification that existed at that frequency with the lower tidal volume. The changes would not of necessity be the same for both lungs. This explanation is consistent with the data, but Forkert et al. (1978) showed that stratification was not the cause of the frequency dependence of regional washouts. The speed of inspiration of a bolus of xenon-133 affected the frequency dependence of its washout even if the residence time in the lung was the same after fast and slow inhalations. Because xenon-133 equilibrates in the lungs and krypton-81m does not, however, the possibility that stratification of

krypton-81m within the lungs contributes to the changes of ventilation per unit volume with flow rate cannot be excluded.

The distribution of ventilation among regions experiencing the same pleural pressures is determined by the regional resistances and compliances. At low flows, the resistive pressure drop is small and the distribution follows the regional compliances. At higher flow rates, the resistance accounts for a larger fraction of the total pressure drop and affects the distribution more. A similar mechanism can explain the intraregional changes in ventilation per unit volume with increases in frequency and tidal volume. Forkert et al. (1978) considered regional inhomogeneities of time constants to be the principal cause of the frequency dependence of regional xenon-133 washouts.

In the dependent lung in the lateral decubitus position at functional residual capacity, airway closure is likely (Roussos et al, 1976). Indeed, a nonhomogenous pattern of open and closed airways has been seen in lung sections at moderate levels of inflation (Gil and Weibel, 1972) and recruitment and derecruitment of alveoli has been measured with aerosols (Smaldone et al, 1983). Thus, local differences exist in resistance and compliance. At lower flow rates, the contribution of the resistive pressure drop is small and more of the driving pressure is available for the expansion of partially opened airways. The arriving air thus enters a diffuse region of the lung. When the frequency increases, however, the higher flow rates generate greater frictional losses and the air enters only the low resistance passages. The volume of the lung receiving the tracer decreases, but the portions of the lung it enters experience high volumetric flows. The increase of flow rate caused by doubling the tidal volume has

similar effects, but with the difference that the larger volume requires larger inflation of the lung. More of the airways attain diameters large enough for low resistance flow and the increase in the ventilation per unit volume with flow rate is lessened.

5.4.2.1 *The volume considered*

The volume that was under consideration in the flow per unit volume curves that were derived from krypton-81m dynamic scans was not necessarily the entire gas volume of the lung. It was that volume which the tracer could enter either by bulk flow or diffusion before it decayed. Thus, both trapped gas volume and zones for which the transit time from the central airways was long relative to the half-life of the isotope, if they existed, were omitted from the measurements. The degree of obstruction necessary before a region would be unrepresented would be a function of the concentration gradient, determined by the strength of the krypton-81m source. Slowly ventilated regions are somewhat underrepresented in krypton-81m scans even when they appear (Amis and Jones, 1980). The curves show ventilation per well-aerated volume.

5.4.3 THE SEQUENCE OF FLOWS

The curves representing the ratios of the flows in the two lungs (Fig. 5.11) show that the dependent lung emptied and filled faster than the non-dependent lung over most of the cycle. The flow associated with the non-dependent lung dominated only at the end of expiration and for a brief part of the cycle at the beginning of inspiration. Therefore, a large proportion of the air in the dead space at the end of expiration came from the non-dependent lung, and a large proportion of it re-entered that lung at the onset of

inspiration. Because of the lower krypton-81m concentration in the dead space, the activity measured in the non-dependent lung in the early part of inspiration underestimated of the flow to that lung by an unknown amount. However, the volume of air containing krypton-81m at the inlet concentration is the same volume that contains oxygen at 21%. The more significant portion of the inspire in terms of gas exchange is that which was followed with the tracer.

Frazier et al. (1976) measured the function of the individual lungs in awake man intubated with a double lumen endotracheal tube. In the lateral decubitus position they found asynchronous emptying of the lungs and asynchronous onset of flow limitation. During constant rate expiration from total lung capacity to residual volume, the dependent lung showed higher, though gradually decreasing, flow rates for about two thirds of the expiration, after which the increasing flow from the non-dependent lung began to dominate even before closing volume was reached in the dependent lung. The onset of flow limitation in the dependent lung coincided with a large increase in flow from the non-dependent lung. A similar cross-over of the flow rates was seen during the cyclic breathing of krypton-81m in air above FRC. Roussos et al (1976) noted the onset of phase IV of nitrogen washouts in the lateral decubitus posture at 58% VC during normal breathing, suggesting that airway closure may occur at high lung volumes in this position, and Engel and Prefaut (1981) found evidence suggestive of closure in the dependent, paradiaphragmatic regions even of supine man at FRC. It is not unreasonable to suppose that some flow limitation occurred during these experiments.

5.4.4 PHASE

A phase difference between the flow per unit volume curves for the right and left lungs existed in most subjects for most manoeuvres (Table 5.7). It provided further evidence of the sequential pattern of ventilation in the left lateral decubitus position. A phase difference between the pleural pressure swings on the lungs could have caused one lung to fill before the other (Chapter 3), but even without a lag in the pleural pressure swings, a lag in the flow is predicted for pleural pressure swings of substantially different magnitude (Fig. 3.6d). Under those conditions, the compartment with the larger pressure swing leads the other and also receives the greater tidal volume. The phase difference is caused by the nonlinear volume-compliance relationship of the lung. In the experiments, the pleural pressure swings may have been in phase during inspiration and out of phase during expiration. On expiration, the abrupt change in pleural pressure on the left (dependent) lung as the abdominal contents recoiled against the newly relaxed diaphragm probably caused a phase advance in the pressure swings.

5.4.5 PROBLEMS OF METHODOLOGY

During the analysis of the data, some problems of methodology became evident. It is useful to consider them in conjunction with the experimental findings. They should be corrected in any future work.

The principal experimental problem was the weakness of the krypton-81m generator. Because the activity arriving in the lungs was low, many breaths were needed for adequate representation of the breathing pattern. Subjects found it difficult to remain still and to breathe in a regular pattern for more than a few minutes. The range of

frequencies and tidal volumes was restricted to those not too different from normal since the control of carbon dioxide levels for lengthy periods of hyperventilation is difficult without gas mixing apparatus. Moreover, the resolution of the images deteriorated as the count rate approached the background levels, and the count rate dropped when the flow of air increased. To extend the measurements to higher frequencies and tidal volumes, and to measure over smaller regions, more powerful sources of the isotope are necessary.

Many untested hypotheses remain because physiological parameters could not be measured in conjunction with the activity from the lungs. For further investigation of the dynamics of breathing, more experiments with simultaneous pneumotachograph recordings are needed. To test the effects of pleural pressure changes and muscle activity, oesophageal pressures and electromyographic signals from the diaphragm should be recorded also, synchronized with the activity to allow construction of an average breath cycle of these parameters. Unfortunately, such experiment could be performed in only the very few centres equipped with a gamma camera linked to a computer with multiple analog to digital channels.)

Some information that might have been of interest was lost during the reconstruction of the average breath. In addition to the matrix of the total activity for each one-sixteenth of a breath, the standard deviation of the resultant activity-time curve could have been retained as a measure of the intercycle variability at each point. Although this would not alter the basic interpretation of the curves, it would help in determining how best to fit the curves to other physiological parameters.

5.5 CONCLUSIONS

Steady-state krypton-81m measurements in the left lateral decubitus position supported the predictions of the pleural pressure-driven model (Chapter 3). There was no evidence that changes in the overall distribution of a tidal breath were caused by the variations of flow rate generated by increasing the tidal volume and frequency within the measured range. Because the range of the measurements was narrow and the intersubject variability high, the results did not constitute proof of the model; nevertheless, they supported its predictions.

The use of a gas reservoir for mixing krypton-81m and air was shown to be both necessary and effective for the maintenance of a nearly constant inlet concentration. Its major drawback was the decrease of the activity of the krypton-81m arriving at the mouth.

Dynamic information was obtained from average breaths measured with krypton-81m. The magnitude of the curves of the regional ventilation per unit volume increased significantly with both frequency and tidal volume. The flow was seen to favour the dependent lung over most of the cycle but to be preferential to the non-dependent lung at the onset of inspiration and of expiration. The nondependent lung was thus observed to receive most of the deadspace gas. The sequential nature of ventilation in the left lateral decubitus position was evident.

Although representative breaths previously had been reconstructed from list mode data (Kaplan et al., 1982), the cycles had not been interpreted physiologically. Through the use of the model of krypton-81m dynamics, the activity was re-expressed in terms of the

ventilation per unit volume of a region, which was presented as a function of time. Information about the sequential nature of ventilation in the left lateral decubitus position, available previously only from intubated subjects, was obtained noninvasively from a lung scan.

CHAPTER 6

LUNG SOUND MEASUREMENTS

6.1 INTRODUCTION

For many people the stethoscope is the instrument most symbolic of clinical medicine. Physicians routinely listen to the sounds of breathing to obtain instant, useful, qualitative information. With even limited experience some differences in the sounds from healthy and diseased lungs are apparent. Physicians learn to distinguish among "coarse and fine crackles", "wheezes" and "rhonchi", or perhaps "coarse rales", "crepitations", and "sibilant or "sonorous rhonchi" (Murphy, 1981). The causative physics and physiology may be unknown, but the sounds can be associated with different states of health.

More quantitative interpretations of lung sounds have been sought. The intensity of the sounds of normal breathing has been reported to reflect the distribution of pulmonary ventilation (LeBlanc et al., 1970; Ploysongsang et al., 1977, 1978, 1982) but other work (O'Donnell and Kraman, 1982; Kraman and Austrheim, 1983) has cast doubt on this interpretation. Few of the reported results can be interpreted easily.

This study was undertaken in an attempt to quantify the effect of airflow on breath sounds and to consider the potential of sounds for the measurement of the distribution of ventilation. The problem addressed was the definition of the relationship between the airflow at the mouth and the breath sounds detected over the chest.

6.2 MATERIALS AND METHODS

6.2.1 MEASUREMENT

Sounds of normal adult breathing were recorded from three sites, two on the posterior thorax and one on the right anterior chest. The recording sites were used in pairs, the right anterior-posterior pair while the subjects were seated and the right and left dorsal locations while the subjects were in the left lateral decubitus position.

Three identical piezoelectric microphones (General Radio type 1560-P5, General Radio, West Concord, Mass.) detected the lung sounds. The listed bandwidth for the microphones was 20 Hz to 20 kHz; in a test in an anechoic chamber, the response of one of the microphones was flat ± 4 dB from 250 Hz to 2 kHz, and flat ± 1 dB to 500 Hz. The microphones, mounted in aluminum housings, were fixed to the chest with a silicon adhesive (Hollister, Chicago, Ill.) reinforced with adhesive tape. The surface of the housing in contact with the skin was an annulus of outside diameter 4.6 cm surrounding the opening to the cavity (diameter 1.8 cm) in which the microphone was recessed. The height of the entire housing was 4.3 cm, composed of a cylinder of diameter 3.5 cm and height 3.7 cm which flared to form the mounting ring of height 0.62 cm and diameter 4.6 cm. The mass of the microphone assembly was 125 g.

Each microphone was air coupled to the chest through a cylindrical space 1.8 cm in diameter and 0.95 cm deep. Because the cavity was small relative to the wavelengths of the sounds that were present, it could be modelled as a Helmholtz resonator (Kinsler et al., 1982). The resonant frequency for a cylinder of this volume is

3.96 kHz, outside the signal bandwidth. The cavity was kept at mean atmospheric pressure by a 20-gauge needle that provided a low frequency pressure leak to the room.

As the lung parenchyma has been reported to act as a band-pass filter between 100 Hz and 1 kHz (Rice et al., 1983), and as in test measurements with the experimental apparatus, no power was seen above 500 Hz, a measurements bandwidth from 100 to 800 Hz was selected. The output from the microphones was passed through a fourth-order Butterworth high-pass filter with the corner frequency set at 100 Hz, (Rockland model 452, Rockland Systems Corp., West Nyak, New York), amplified 1000 times (Gould 4600 Preamplifier, Gould Inc., Cleveland, Ohio), then low-pass filtered at 800 Hz with an eight-pole Bessel filter (902LPF, Frequency Devices, Haverhill, Mass.) before being sampled by a 12-bit analogue-to-digital converter (LPA 11-K, Digital Equipment Corp., Maynard, Mass.) at 2 kHz (Fig. 6.1).

The flow of air at the mouth was measured using a capillary pneumotachograph (Fleisch number 3) and a pressure transducer (DP45 ± 1 in H₂O) and demodulator system (CD101, Validyne, Northridge, California). The flow signal also was low pass filtered at 800 Hz with an eight-pole Bessel filter before being sampled at 2 kHz simultaneously with the sounds (Fig. 6.1).

The microphones on the back were placed approximately halfway between the spine and the mid-axillary line, 5 cm below the edge of the scapula to record sounds from the lower lobes. The one on the anterior chest was located over the third intercostal space, midway between the axilla and the sternum to detect the sounds generated in the upper lobe. The microphone coupling was checked by observing the breath

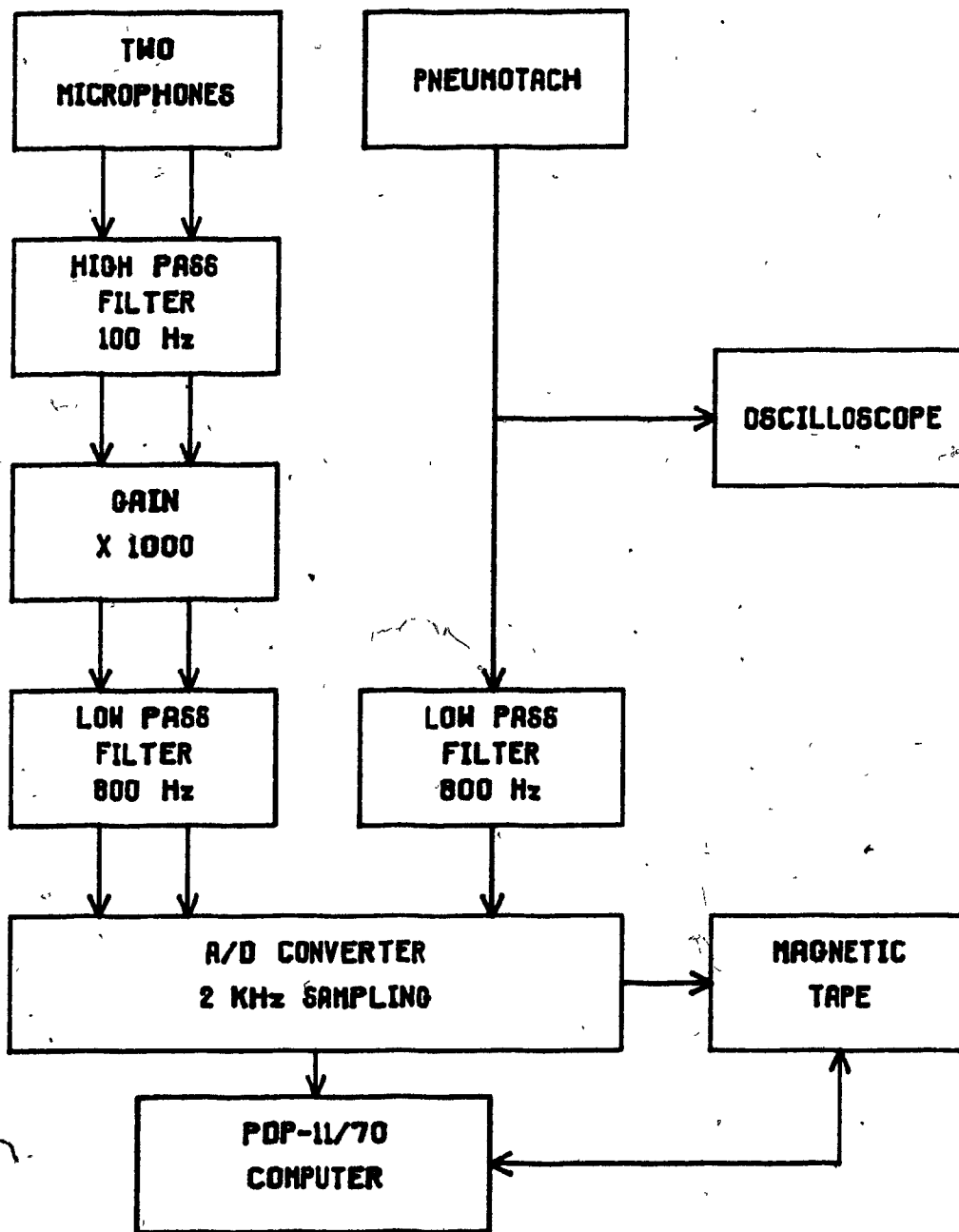


Fig. 6.1. Data acquisition. The flow of information during the experiments is shown.

sound pattern on the oscilloscope; the signal to noise ratio was sensitive to the adhesion of the microphone assembly but the signal itself appeared unchanged if the microphone was moved a few centimeters in any direction.

The recorded sounds evidently were related to the flow (Fig. 6.2). Although similar-looking signal bursts could be produced on an oscilloscope at zero flow by arm motions or by contracting the respiratory muscles against a closed glottis, when the sounds were monitored simultaneously on the oscilloscope and through a pair of earphones, signals of this shape corresponded to normal breath sounds.

Pertinent characteristics of the eight subjects who participated in the study are given in Table 6.1. For the first set of three data acquisitions the subjects sat leaning slightly forward, hands resting on knees. For the second set, they lay on their left sides, their heads resting on a pillow and their left arms comfortably bent. The goal in the arm positioning was to keep the muscle activity beneath the microphones to a minimum. Subjects observed their flow signal on an oscilloscope.

The different experimental cases are summarized in Table 6.2. The first recording in each position was of 20 seconds of rhythmic breathing. The subject attempted to maintain a moderate flow with a regular two second inspiratory period and two second expiratory period. For the second record, 30 seconds in length, a stimulus (Fig. 6.3) consisting of randomly ordered flow rates, constant for two seconds and with magnitudes of 0, 0.75, 1.0, 1.5, 2.0, and 2.5 L/s, was displayed to the subject. Each inspiratory flow was followed immediately by an expiratory flow of the same magnitude in the hope that the subject

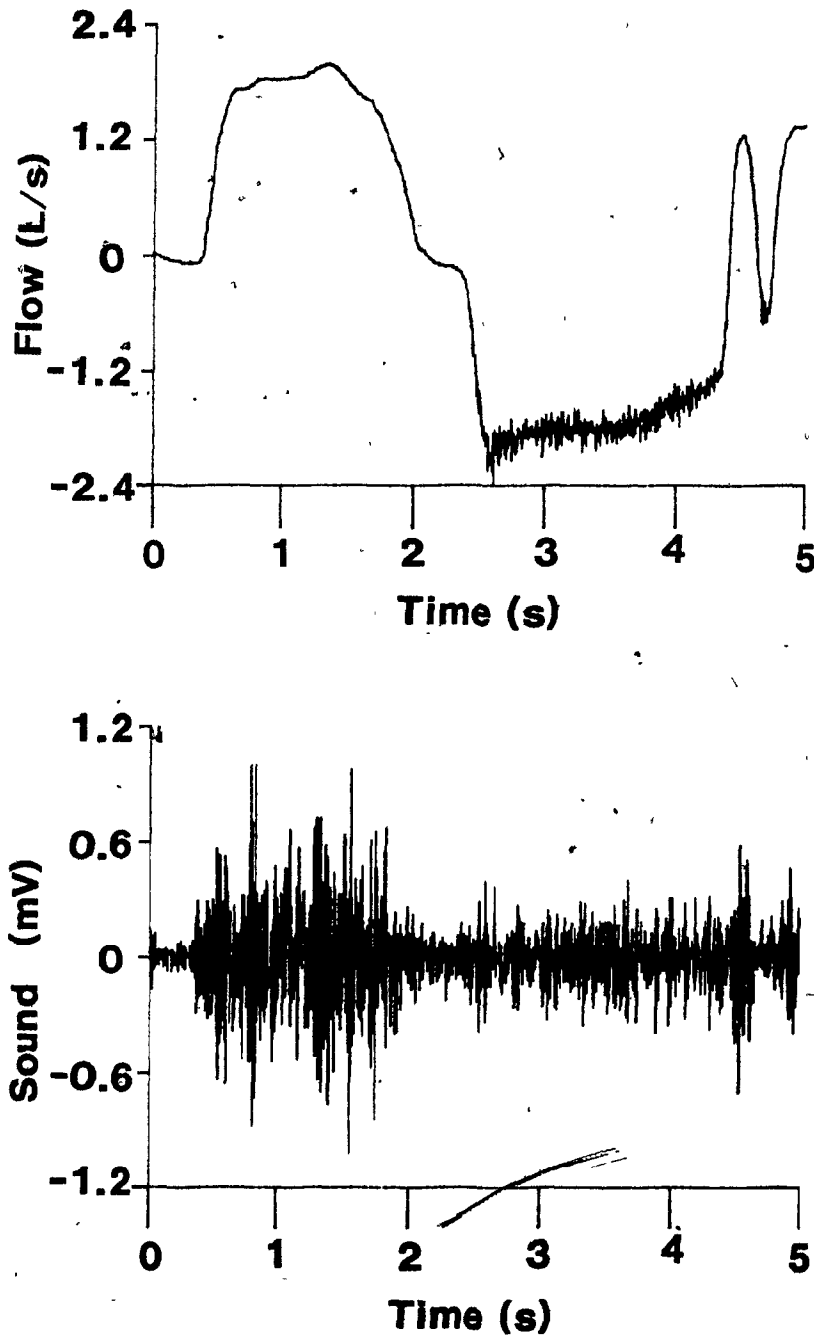


Fig. 6.2. A sample breath with the sound it produced. The flow signal from one breath is shown above the sound signal that was recorded simultaneously.

TABLE 6.1

PHYSICAL CHARACTERISTICS OF SUBJECTS

Subject	Age	Height (m)	Weight (kg)	Sex
1	24	1.75	82	m
2	29	1.83	102	m
3	27	1.88	88	m
4	27	1.78	55	m
5	28	1.65	65	m
6	28	1.66	65	f
7	32	1.57	56	f
8	28	1.83	75	m

TABLE 6.2

EXPERIMENTAL CASES

Case 1:	Seated	Regular deep breathing Period of each breath = 4 s
Case 2:	Seated	Tracking given flow rates and patterns Length of each flow segment = 4 s
Case 3:	Seated	Tracking given flow rates and patterns Resistance added at the mouth piece Length of each flow segment = 4 s
When seated:		
Microphone 1	Right anterior chest (Upper lobe, non-dependent)	
Microphone 2	Right posterior chest (Lower lobe, dependent)	
Case 4:	Left Lateral Decubitus	Regular deep breathing Period of each breath = 4 s
Case 5:	Left Lateral Decubitus	Tracking given flow rates and patterns Length of each flow segment = 4 s
Case 6:	Left Lateral Decubitus	Tracking given flow rates and patterns Resistance added at the mouth piece Length of each flow segment = 4 s

When in the left lateral decubitus position:

Microphone 1 Left posterior chest (Lower lobe, dependent)

Microphone 2 Right posterior chest (Lower lobe, non-dependent)

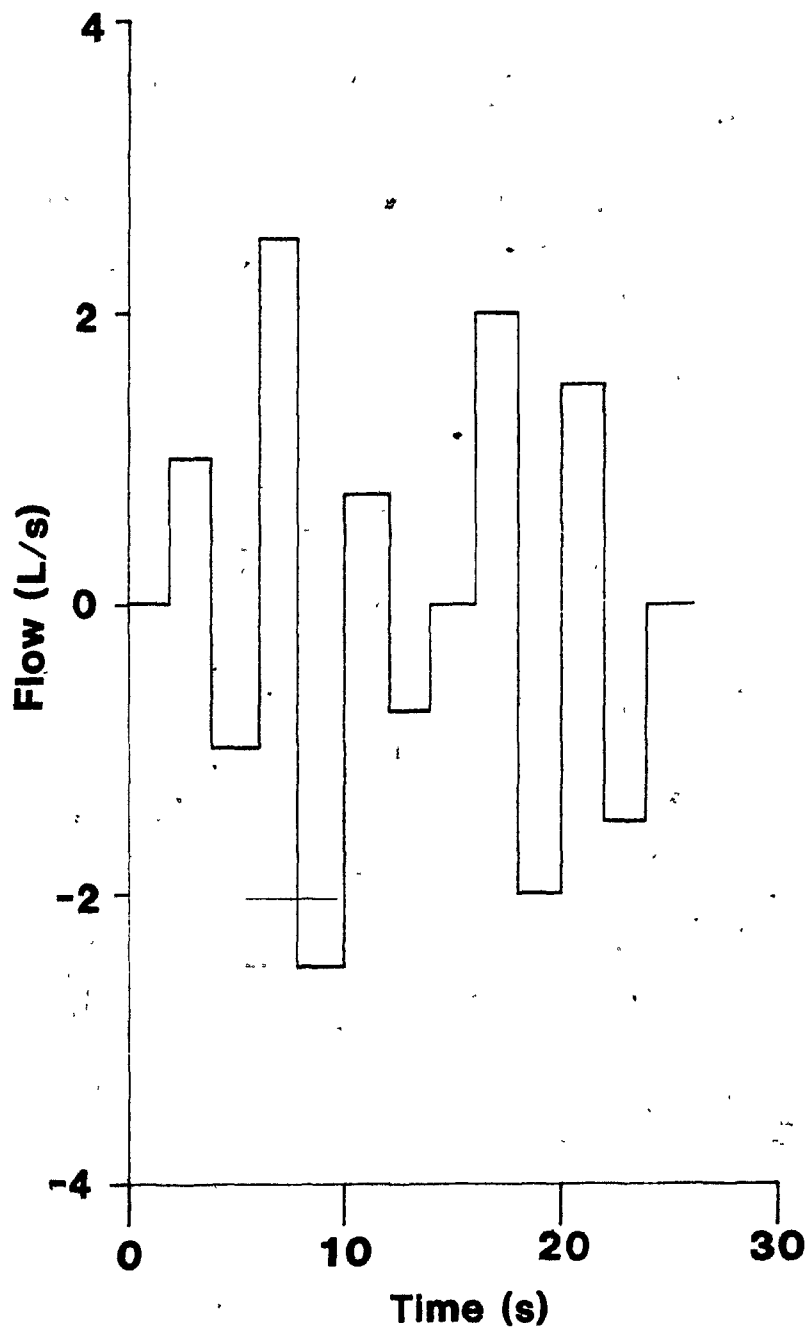


Fig. 6.3. The tracking stimulus. This pattern was displayed during experiments 2,3,5, and 6. Subjects were instructed to attempt to match the pattern with the breathing signal from the pneumotachograph.

would maintain a steady functional residual capacity. The pattern repeated every 26 seconds. Because it was impossible for subjects to maintain the constant flow for a full two seconds, particularly at the higher flow rates, they were instructed to try to reach the target flow and to hold it for as long as possible, then to allow their flow rate to drop to zero but to wait for the stimulus before their next deviation from zero flow. The third recording of each sequence differed from the second only in having a resistive load of $3.5 \text{ cm H}_2\text{O/L/s}$ ($350 \text{ kPa m}^{-3} \text{ s}^{-1}$) added between the mouthpiece and the pneumotachograph. Samples of the flow patterns generated by one subject are shown in Fig. 6.4.

6.2.2 ANALYSIS

The stored sound and flow signals were treated using the signal processing language, Nexus (Hunter and Kearney, 1984), first by considering the envelopes of the sound signals, i.e., the root mean square sounds, and secondly by examining the sound spectra.

6.2.2.1 Smoothed Root Mean Square Sound Envelope

To study the variations of the sound amplitude with the flow the sound signals were demodulated (Fig. 6.5). The standard deviation of the sound was taken over 10 msec intervals to obtain the root mean square signal at a reduced sampling rate. Because the averaging involved in calculating the standard deviation low-pass filtered the signal by eliminating fluctuations of period less than 10 msec, the number of points could be reduced without risk of distorting the lower frequency information. Further filtering was accomplished by

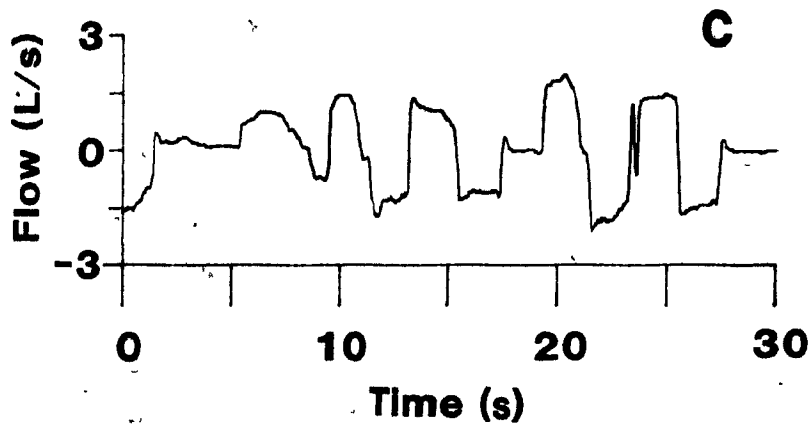
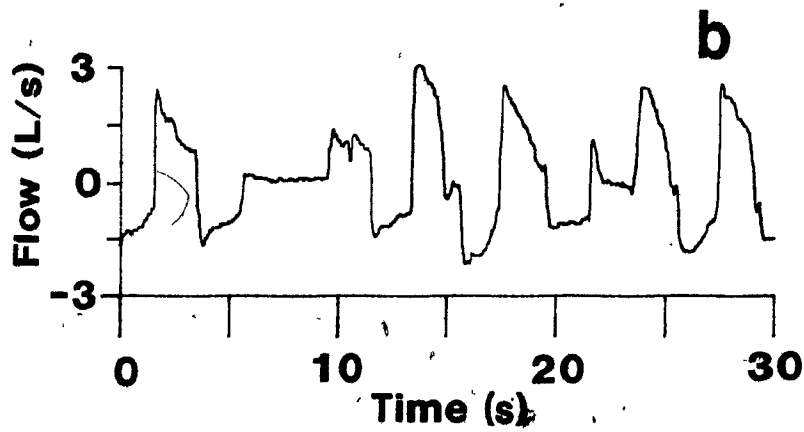
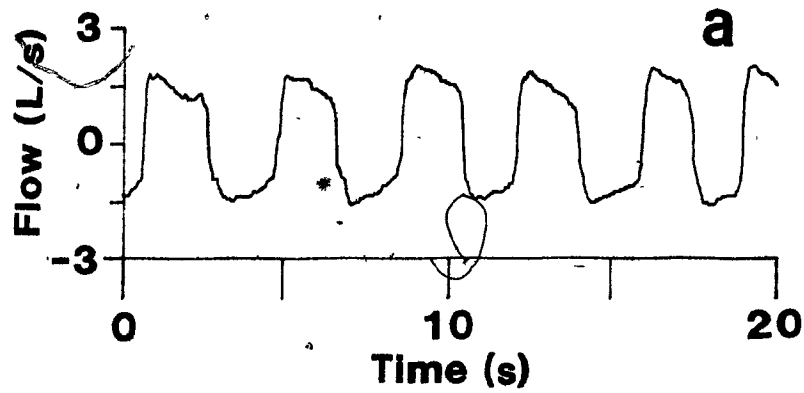


Fig. 6.4. Sample flow patterns. a) Regular breathing (Case 1). b) Tracking (Case 2). c) Tracking through the resistor (Case 3). Subject 3, seated.

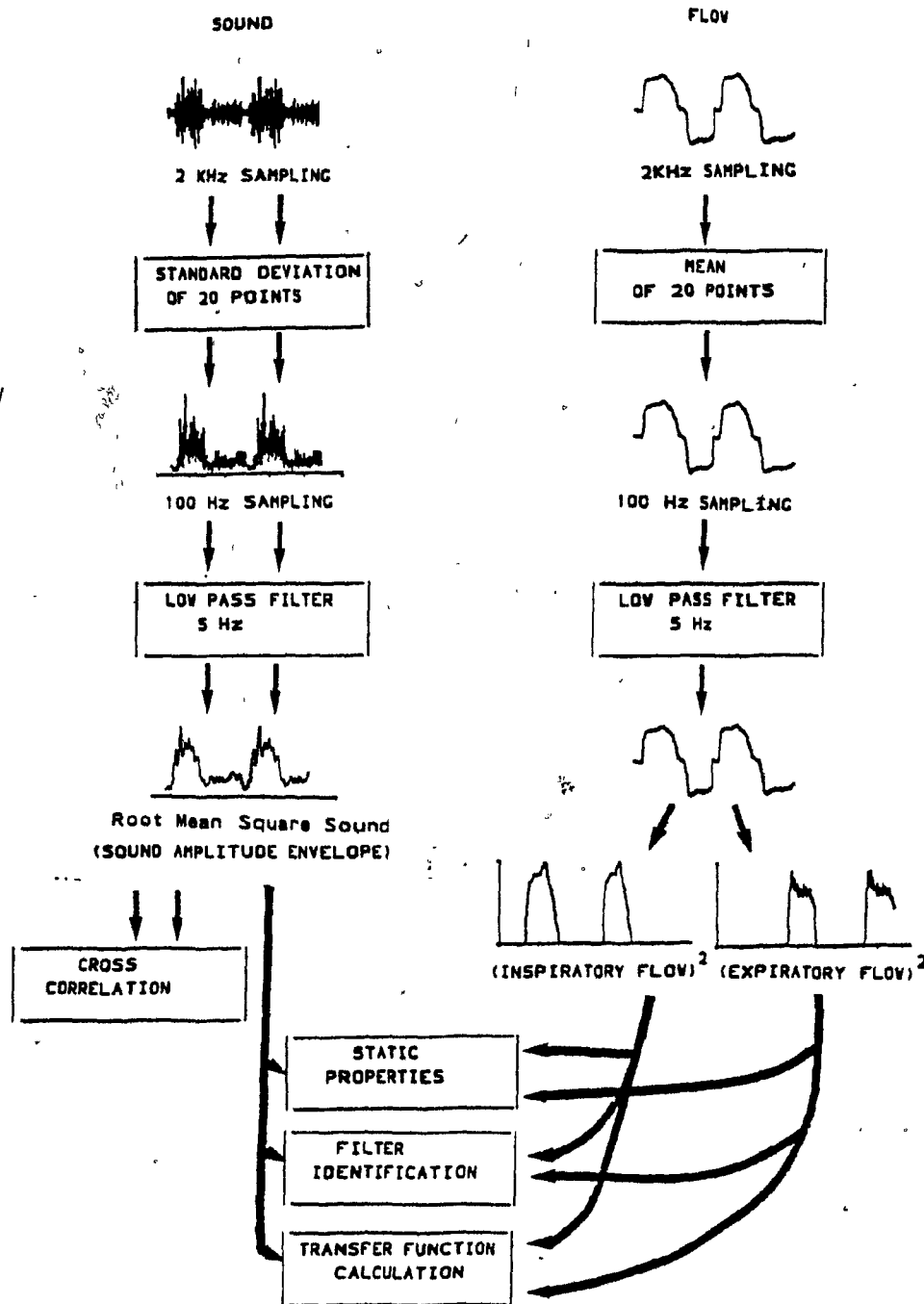


Fig. 6.5. Signal treatment for amplitude analysis. The steps followed to obtain the sound amplitude envelope and the square of the flows from the sampled signals are shown. The analyses performed on the resultant signals are indicated.

convolving the signal with a finite impulse response filter with a 5 Hz cut-off frequency. This frequency was set slightly higher than the bandwidth of the flow to remove the fluctuations that were not the output of a linear system acting on the flow but to avoid distorting those that could have been. The flow signals were segmentally averaged over 10 msec intervals and then convolved with the same finite impulse response low-pass filter.

Statics

Preliminary analysis of the data showed that the sound amplitude varied with the square of the flow, but that inspiration and expiration followed different functional relationships. Therefore the proportionality between the flow squared and the sounds occurring simultaneously, the static component of the relationship, was studied separately for each flow direction (Fig. 6.6). For the inspiratory cycle, the sounds that occurred during negative flow were dropped from the signal, as were the negative flows themselves. A linear regression was performed between the squared inspiratory flow and the corresponding sound. For expiration, the negative flows and matching sounds were treated similarly, with the inspiratory segments removed.

Dynamics

The lung sounds were considered to be the sum of the outputs of two linear time-invariant systems in which the inputs were the inspiratory and expiratory flow rates raised to the second power (Fig. 6.7). The systems were studied sequentially. Inspiratory flow was isolated by setting all negative flows to zero. The expiratory flow was defined as the difference between total flow and inspiration.

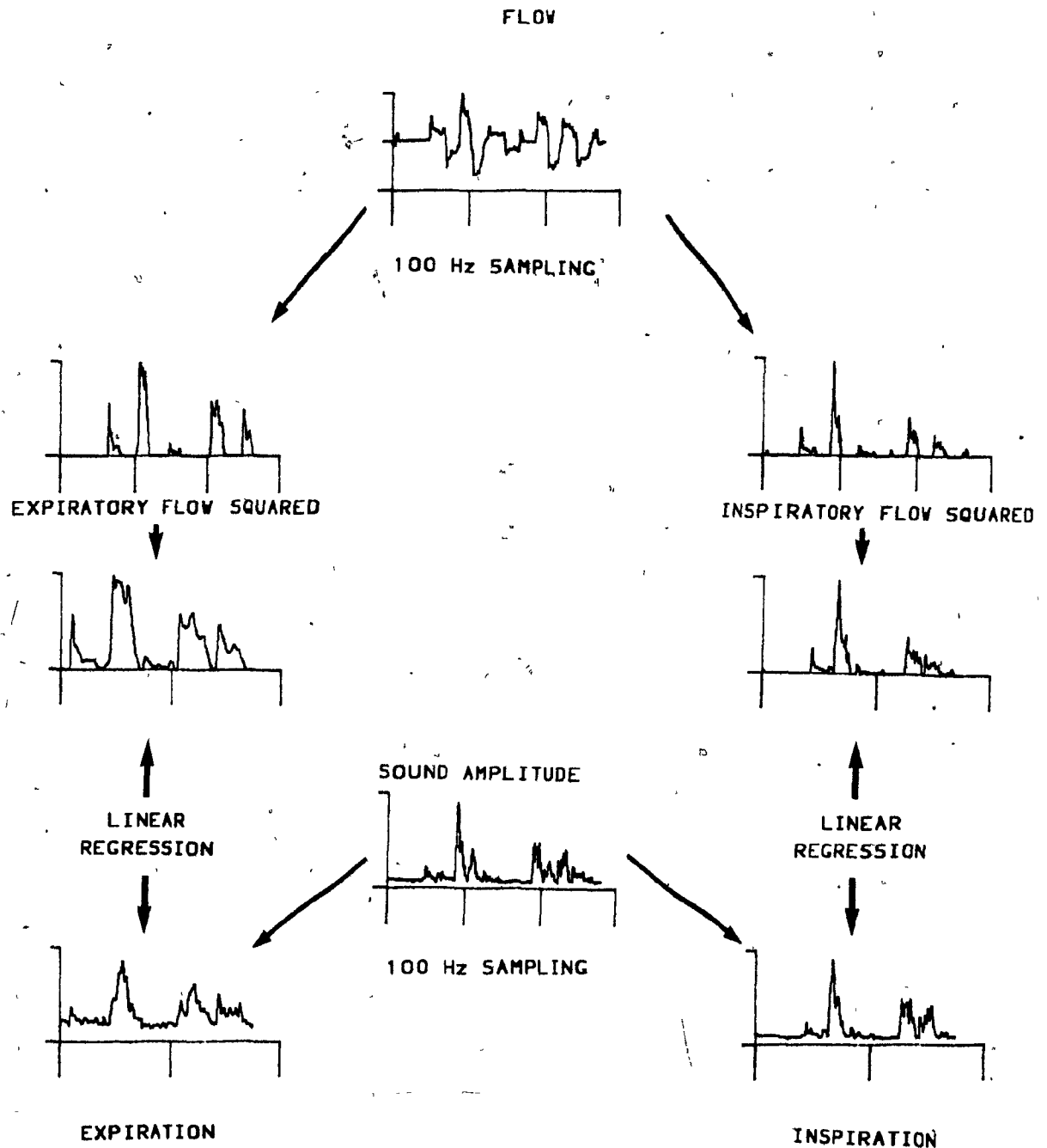


Fig. 6.6. The regression between the sound amplitude and the square of the simultaneous flow. The second power of flow for use in the static analysis was obtained by separating the positive and negative flows before squaring them. The time axis was compressed, removing the times corresponding to the other phase of the flow. The corresponding sound amplitude signal was extracted for each phase and a linear regression performed. $n = 1800$ (Cases 1 and 4) or $n = 2800$ (Cases 2, 3, 5, and 6).

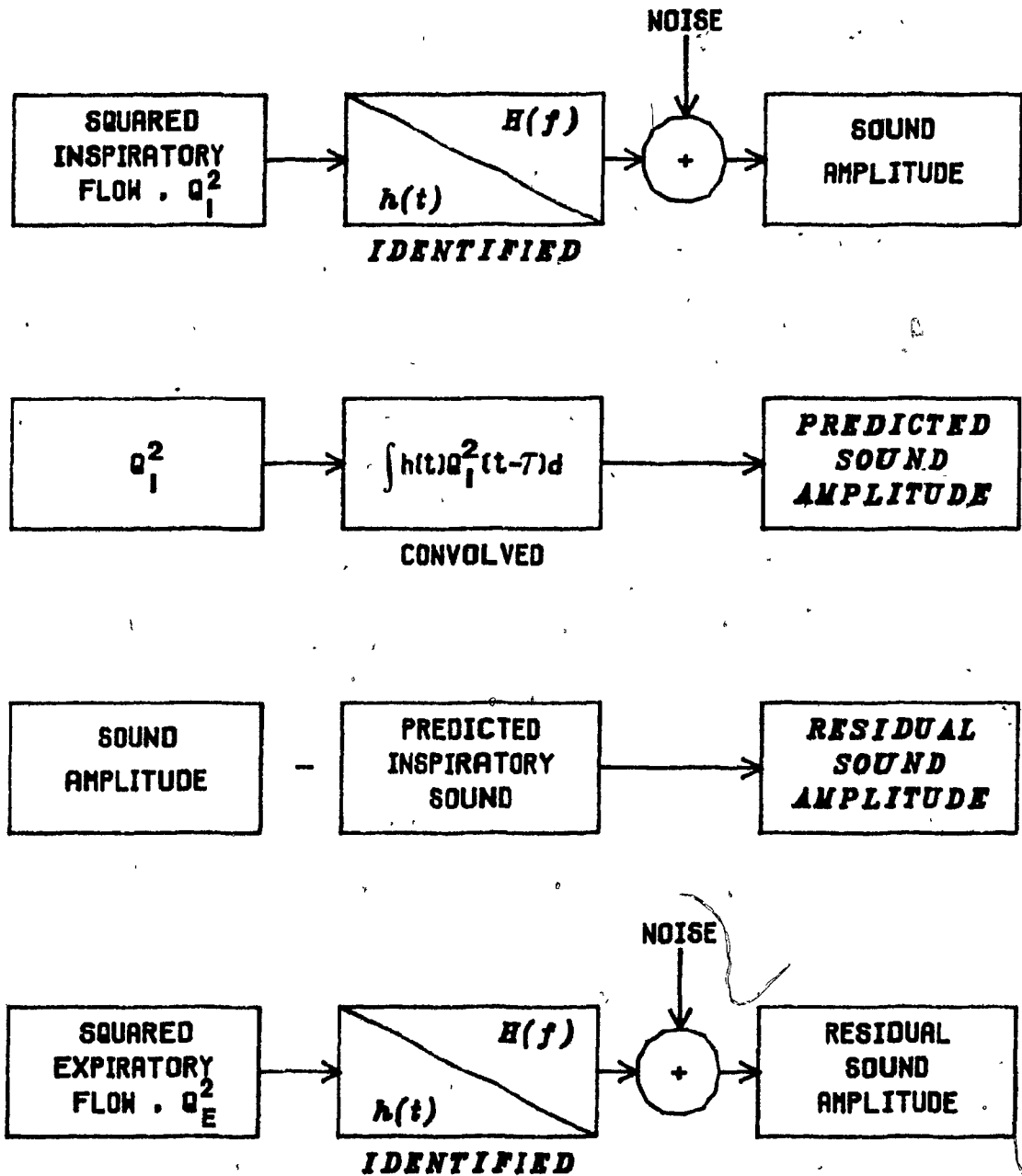


Fig. 6.7. The linear dynamic systems analysis. Italics indicate the quantities calculated in each step. Roman type shows data or quantities calculated in the previous steps. $H(f)$ represents the transfer function, $h(t)$ the impulse response function, and Q the airflow.

First, the square of the inspiratory flow was used as the input and the total measured sound was considered to be the system output plus noise consisting of the sound generated by the expiratory flow plus the other experimental noise. The filter between the square of inspiratory flow and sound was found and was convolved with the input. The linear prediction of the inspiratory sound so generated was subtracted from the measured sound and the linear relationship found between the residuals and the square of the expiratory flow. The gain, phase and coherence transfer functions between the squared flows and the sound were calculated as an alternative method of portraying the best linear models of the relationships. The cross-correlations between pairs of sound signals also were computed.

6.2.2.2 Frequency Spectra

To study the sound spectra at different flow rates, portions of the tracking studies where the flow was nearly constant were selected and the power spectra of the sounds from each microphone computed (Fig. 6.8). The raw signal, not the demodulated amplitude envelope, was used. The power from each microphone was calculated in 60 Hz bandwidths. Because the static relationship between flow and sound amplitude was seen to be a power law, the constants in the assumed relationship, $P = a Q^b$ were determined for each frequency band by finding the coefficients of the regression between the logarithms of power and mean flow. A least-squares fit was used despite the logarithmic transformations since the principle of least squares may be invoked to find the minimum variance estimates of parameters without assuming normal distributions (Guttman, Wilks and Hunter, 1971). The exponents of the power law expression were computed similarly for the

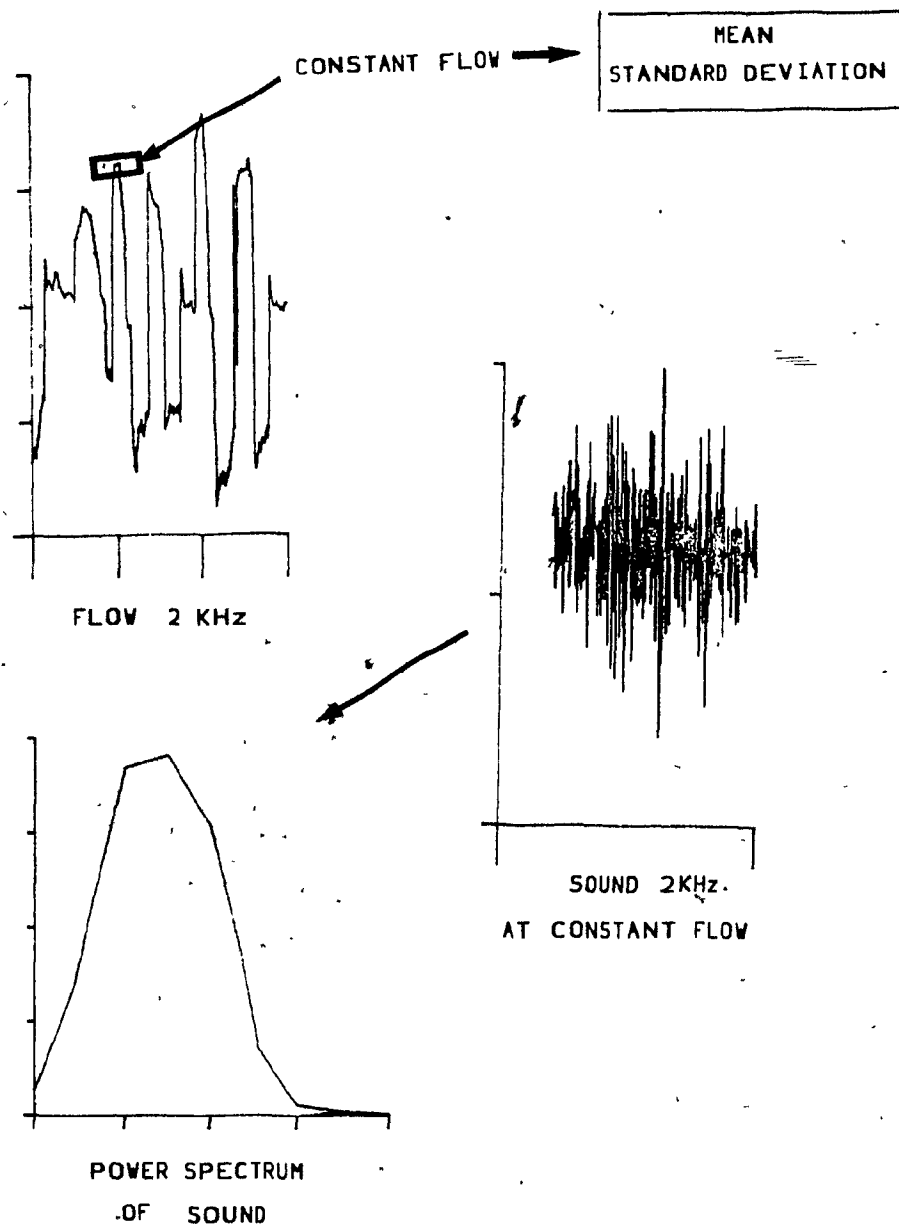


Fig. 6.8. Spectral analysis. A region of constant flow was selected by scanning the flow curves. The raw sound signal (2KHz sampling) occurring at that time was extracted and its power spectrum computed. It was characterized by the mean and standard deviation of the flow.

total power at each flow rate, where the power was found as the variance of the raw signal.

6.3 RESULTS

6.3.1 SYSTEM STATICS: THE ALGEBRAIC EQUATION

The gains (slopes), offsets ('y' intercepts), and percentage of the variance accounted for by the linear relationships between flow squared and the simultaneously occurring sound are given in Table 6.3. The points lost because of poor microphone coupling as defined by aberrantly low signal power are indicated by dashes. Low values of the variance accounted for do not mean bad data, but records where the static linear model was inadequate.

As each record represented 20 to 30 seconds of breathing, good correlations (high variance accounted for) indicated breath to breath reproducibility as well as linearity. During inspiration the relationship was generally very good, accounting for high percentages of the variance in the sound amplitude. The reproducibility between trials was moderately good, also, as shown by the repeat measurements on subject 7. Some inspiratory records showed a poor linear relationship between flow squared and sound. In one of these cases (subject 3), a distinct threshold was seen above which clean sound signals were recorded.

With few exceptions, the straight-line fit during expiration was a very poor representation of the data. Since the amplitudes of the expiratory sounds were often low, one reason may have been poor signal to noise ratio. However, because clear signals were visible in many cases, a non-linear relationship was also likely.

TABLE 3

INSPIRATION		STATIC GAIN BETWEEN SECOND POWER OF FLOW AND SOUND AMPLITUDE						
		Microphone 1			Microphone 2			
Subject	Case	Gain	Offset	ZVAF	Gain	Offset	ZVAF	
1	1	---	---	--	---	---	--	
	Seated	2	0.85	0.67	83	0.56	0.80	84
		3	0.76	0.66	74	0.59	0.85	75
	Left	4	---	---	--	---	---	--
	Lateral	5	0.73	0.74	73	1.26	1.02	87
	Decubitus	6	0.56	0.73	76	0.82	1.13	81
2	1	---	---	--	1.60	0.25	72	
	Seated	2	0.46	0.79	85	0.63	0.81	80
		3	0.47	0.72	89	0.65	0.72	85
	Left	4	---	---	--	1.87	0.78	54
	Lateral	5	0.26	0.97	56	1.54	1.27	85
	Decubitus	6	0.45	0.87	77	1.97	1.06	84
3	1	0.90	0.47	75	0.40	1.51	23	
	Seated	2	0.96	0.76	83	0.65	1.07	70
		3	0.81	0.88	84	1.23	1.10	32
	Left	4	0.78	0.61	64	1.17	2.25	67
	Lateral	5	0.59	0.77	84	1.35	1.55	89
	Decubitus	6	0.56	0.92	64	1.95	1.49	89
4	1	1.87	0.40	83	---	---	--	
	Seated	2	1.53	0.93	88	---	---	--
		3	1.83	1.01	84	---	---	--
	Left	4	1.17	0.48	79	4.47	0.49	79
	Lateral	5	1.43	0.73	83	3.03	1.01	94
	Decubitus	6	1.33	0.81	83	2.78	1.10	92
5	1	1.52	0.00	65	1.87	0.00	76	
	Seated	2	---	---	--	1.35	0.56	75
		3	---	---	--	1.64	0.73	83
	Left	4	2.42	0.36	70	1.35	0.99	76
	Lateral	5	1.33	1.03	76	1.75	0.66	85
	Decubitus	6	1.11	0.72	69	1.79	0.74	81
6	1	---	---	--	5.36	0.81	95	
	Seated	2	1.19	0.83	65	3.57	1.47	93
		3	2.07	0.69	73	2.74	1.19	79
	Left	4	1.25	0.99	78	2.74	1.19	79
	Lateral	5	2.11	0.76	90	3.66	1.46	80
	Decubitus	6	1.83	0.92	89	5.94	0.91	81
7	1	1.13	0.93	75	3.19	0.89	89	
	Seated	2	1.12	0.81	73	3.49	0.92	83
		3	1.36	0.74	66	3.47	0.87	67
	Left	4	2.16	0.94	85	3.51	1.09	88
	Lateral	5	2.00	0.87	87	3.23	1.04	83
	Decubitus	6	1.62	1.15	75	1.16	1.33	26
8	1	0.35	0.94	70	0.78	1.21	81	
	Seated	2	0.36	0.79	68	0.71	1.07	47
		3	0.50	0.82	59	1.55	1.20	49
	Left	4	0.41	0.58	85	1.23	0.98	86
	Lateral	5	0.48	0.74	70	1.20	0.87	87
	Decubitus	6	0.46	0.68	43	0.95	0.80	84

-- continued

TABLE 3 -- CONTINUED

EXPIRATION	Subject	Case	Microphone 1			Microphone 2			
			Gain	Offset	ZVAF	Gain	Offset	ZVAF	
1	Seated	1	----	----	--	----	----	--	
		2	0.83	1.42	35	0.43	1.08	45	
		3	0.12	0.91	6	0.41	0.91	2	
	Left	4	----	----	--	----	----	--	
		Lateral	5	0.39	0.72	67	0.39	1.18	64
		Decubitus	6	0.11	0.88	0	0.17	1.23	36
2	Seated	1	----	----	--	0.89	0.78	2	
		2	0.23	0.73	72	0.11	1.00	35	
		3	0.11	0.74	62	0.10	0.73	43	
	Left	4	----	----	--	0.13	1.37	0	
		Lateral	5	0.28	1.07	3	0.20	1.49	28
		Decubitus	6	0.15	0.97	32	0.29	1.28	63
3	Seated	1	0.31	1.06	25	0.48	1.18	33	
		2	0.55	1.01	48	0.68	1.12	54	
		3	0.17	0.95	30	0.01	1.50	0	
	Left	4	0.16	1.17	18	0.60	1.80	67	
		Lateral	5	0.54	0.72	68	1.60	1.12	77
		Decubitus	6	0.17	0.81	33	0.54	1.28	51
4	Seated	1	0.51	0.71	48	----	----	--	
		2	0.59	1.38	35	----	----	--	
		3	1.11	1.17	47	----	----	--	
	Left	4	0.30	0.64	50	1.07	0.68	61	
		Lateral	5	0.34	1.02	35	0.36	1.91	7
		Decubitus	6	0.30	0.83	33	0.50	1.44	21
5	Seated	1	-0.19	1.90	13	0.36	1.25	23	
		2	----	----	--	0.20	1.08	34	
		3	----	----	--	0.36	1.17	17	
	Left	4	-0.14	2.88	6	-0.12	2.58	2	
		Lateral	5	0.06	1.91	2	0.39	1.53	39
		Decubitus	6	0.14	1.39	1	0.33	1.89	3
6	Seated	1	----	----	--	3.98	0.81	85	
		2	0.81	0.73	86	2.50	1.51	92	
		3	0.57	0.72	57	1.43	1.74	33	
	Left	4	0.90	1.02	73	0.98	1.24	58	
		Lateral	5	0.83	1.07	92	0.87	1.08	80
		Decubitus	6	0.87	1.08	80	1.37	1.39	61
7	Seated	1	1.02	0.92	46	1.90	0.95	60	
		2	1.50	0.73	82	2.37	0.98	81	
		3	1.30	0.63	70	1.12	1.20	41	
	Left	4	0.96	1.00	60	0.50	1.04	52	
		Lateral	5	1.15	1.02	74	0.69	1.02	71
		Decubitus	6	1.12	1.20	41	0.47	1.25	41
8	Seated	1	0.10	0.83	44	0.54	1.08	84	
		2	0.15	0.94	20	0.65	1.29	39	
		3	0.16	0.70	28	0.31	0.97	23	
	Left	1	0.12	0.62	63	0.53	0.73	85	
		Lateral	2	0.44	0.67	40	0.99	0.92	46
		Decubitus	3	0.52	0.72	5	0.37	0.73	58

-- continued

TABLE 3 -- CONTINUED

INSPIRATION - REPEATED MEASUREMENTS

Subject	Case	Microphone 1			Microphone 2		
		Gain	Offset	ZVAF	Gain	Offset	ZVAF
7	1	1.70	1.50	83	----	----	--
	1	1.20	1.90	71	3.50	1.60	91
	Seated 1*	1.20	2.10	70	1.60	1.00	69
Decubitus	4	2.00	1.90	79	----	----	--

EXPIRATION - REPEATED MEASUREMENTS

Subject	Case	Microphone 1			Microphone 2		
		Gain	Offset	ZVAF	Gain	Offset	ZVAF
7	1	1.50	1.60	90	----	----	--
	1	1.50	1.50	79	4.20	1.30	96
	Seated 1*	1.50	1.60	76	0.60	0.60	87
Decubitus	4	1.20	2.00	27	----	----	--

Note: --- indicates datum unavailable because of poor microphone coupling.

* indicates seated microphone 1: Right posterior
microphone 2: Left posterior

The linear regression was performed using all points of inspiration or of expiration. The mean sound amplitude of each 100 ms was compared to the mean flow for the same 100 ms. The gains (slopes of the regression line), offsets (intercepts) and percent variance accounted for by the regression ($ZVAF = r^2 \times 100$) are reported.

Units: Gain [=] $V/(m^6/s^2) \times 10^{-2}$

Offset [=] $V \times 10^{-2}$

Both the adequacy and the shortcomings of the algebraic relationship as a model between flow and sound are evident when sound amplitude is plotted against the square of the flow for one microphone (Fig. 6.9). The loop represents one breath during which the sound amplitude had two values for the same flow depending on whether the flow was increasing or decreasing. In the example plotted, because the lower sound levels occurred during accelerating flow, a volume effect like that reported by LeBlanc et al. (1970) where the sound intensity was decreased at higher lung volume does not explain the difference. In the experiments reported here, the loops occurred in both directions during some experiments. The looping does not indicate a phase difference between sound and flow; the impulse response functions (Fig. 6.10) show no lags between flow and sound, and the cross-correlations between two sounds (Fig. 6.13) show them to be in phase.

6.3.1.1 Gains

The gains, the change in sound amplitude divided by the change in flow squared, were a flow independent measure of the sound amplitudes. They were considered to summarize the flow-sound system when the linear relation accounted for 70% or more of the variance in the data.

The relative static gains between the inspiratory flow squared and the sound amplitudes at the two microphones were calculated as the ratio of non-dependent to dependent regions (Table 6.4). Because the common effects between microphones cancelled each other in

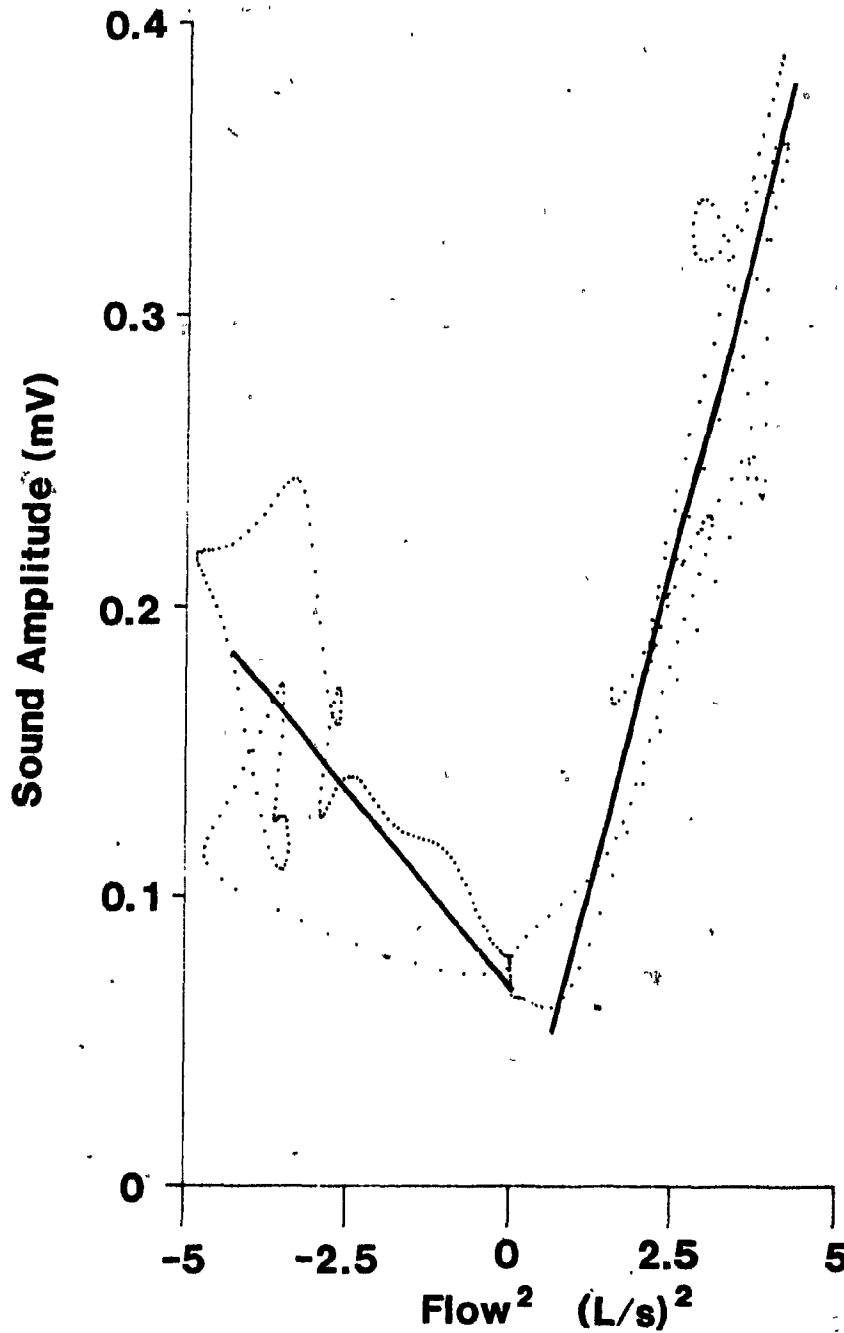


Fig. 6.9. Sound amplitude as a function of flow squared. One breath is shown. The expiratory flow squared has been multiplied by -1. Each point represents 100 ms. The straight lines on the figure were inserted by eye.

TABLE 6.4

RATIOS OF GAINS:
NON-DEPENDENT TO DEPENDENT MICROPHONES

INSPIRATION

SEATED			DECUBITUS		
SUBJECT	CASE	RATIO	SUBJECT	CASE	RATIO
1	2	0.66	1	5	0.58
	3	0.78		6	0.68
2	2	1.37	2	6	0.23
	3	1.38		3	5
3	2	0.68	3	6	0.29
	6	1.99		4	4
7	1	2.82	4	5	0.47
	2	3.12		6	0.48
7r	1	2.82	5	4	1.79
	8	2.23		5	0.76
2r ¹	1	1.55	6	4	0.45
	2	1.49		5	0.76
	3	1.40		6	0.31
3r ¹	1	1.08	7	4	1.63
				5	1.62
			8	5	0.40
				2r ¹	4
				5	0.76
				6	0.89
			3r ¹	4	0.53
				5	0.76
				6	0.89

Note: The data in the table are those for which the VAF's (Table 1) for both values under comparison are greater than or equal to 70%.

r designates a repeat measurement

r¹ designates a repeat measurement for which the flow signal was unavailable. Total mean sound amplitudes were compared.

Inspiration and expiration were lumped together.

The goodness-of-fit of the linear relationships is unknown.

the ratios of the gains, the ratios represented the data in a form that was partly subject independent. Only those data were used for which the the sound from each microphone could be represented by the gain.

The values for subjects in the seated position ranged from 0.66 (subject 1) to 3.12 (subject 7), while those for the lateral decubitus position varied from 0.23 (subject 2) to 1.79 (subject 5). Although the intersubject variability was large, it was comparable to that reported in the literature; Ploysongsang et al. (1977) found a range from about 0.8 to 2.0 in the ratios of overall sound amplitude at the base to that at the apex in seated subjects. Given the intersubject variability, the ratio proved to be surprisingly reproducible on repetition of the experiment for one subject (Subject 7). In two other subjects, the means of repeat measurements of sound (no flow recorded) were compared; the ratios were within 15% of those of the gains in three of the five cases (Table 6.4), even though expiration and inspiration were not separated and the linearity of the relationship between flow squared and sound could not be checked in the ratio of the means.

In the computation of the ratios for seated subjects, because the sounds were from the right upper lobe (anterior chest) and right lower lobe (posterior chest), differences in the thickness of the chest wall at the two sites might have affected the values. In the measurements made while the subjects were decubitus, however, the microphones were over homologous lung segments where the chest wall thicknesses should have been similar. Kraman and Austrheim (1983) reported that the average breath sound amplitude in standing subjects was nearly bilaterally symmetrical, but Kraman (1983c) found

TABLE 6.5

EFFECT OF ASSUMING DECUBITUS POSITION

CHANGES IN GAIN: RIGHT POSTERIOR MICROPHONE TRACKING			REGULAR	
SUBJECT	NO RESISTANCE	PLUS RESISTANCE	SUBJECT	
1	-41.1 %	-22.4 %	4	-34.4 %
2	-43.5 %	-4.3 %	7	+98.8 %
3	-38.5 %	----	8	+17.1 %
4	-6.5 %	-27.3 %		
6	----	-11.6 %	7r	+58.1 %
7	+78.6 %	----		+14.6 %
				+70.4 %

7r -- One decubitus trial compared to 3 seated measurements.

CHANGES IN RATIO OF GAINS: NON-DEPENDENT TO DEPENDENT MICROPHONE

SUBJECT	TRACKING	SUBJECT	PLUS RESISTANCE	SUBJECT	REGULAR
1	-12.1 %	1	-12.8 %	7	-42.2 %
2	-83.2 %	6	-84.4 %	8	-85.2 %
3	-35.3 %				
7	-48.1 %				

Note: The data in the table are those for which the VAF's (Table 1) for all values under comparison are greater than or equal to 70%.

significant differences in both directions between the sounds over the lung bases in 7 of 9 subjects, and O'Donnell and Kraman (1982) reported that the sound was louder over the left lung. In one seated subject, when sounds were recorded from both left and right posterior positions, the gain with inspiratory flow squared was 37% higher over the left lung than over the right and the gain with expiratory flow squared was 61% lower over the left lung. Since the gain measured with the left posterior microphone varied as much between two of the repeated measurements (Table 6.3), the difference was covered by the uncertainty of the measurement. These ratios thus were considered to be representative of the ratios of the sound from the lungs in the fields covered by the microphones.

6.3.1.2 Position changes

The effect of the changes in subject position on the gain between inspiratory flow squared and sound amplitude is summarized in Table 6.5, again for those records where the relationship in both positions accounted for 70% or more of the variance. No pattern was seen for the right posterior microphone which remained in place throughout the experiment. The changes in the ratios of non-dependent to dependent gains, however, showed an unequivocal decrease of varying magnitude when the subject moved from the seated to the lateral decubitus position. However, the comparisons were of different regions of the chest in the two positions and only a few measurements were sufficiently linear at both pairs of microphones for the comparisons to be made.

6.3.1.3 External Resistance

An external flow resistor was added in an attempt to decouple the effects of the flow per se from those of the muscular activity required to generate it. If the sounds recorded had been muscle noise, they would have increased when the resistive noise was added. The changes in gain caused by the addition of the resistor are given in Table 6.6, again for only those cases in which the algebraic relationship between flow and sound amplitude accounted for 70% or more of the variance. For seated subjects, the changes in the gain of the microphone over the more dependent region (right posterior) ranged from -10.6% to +19.6%, while those of the microphone over the less dependent zone (right anterior) varied from +3.2% to +15.1%. In the lateral decubitus position, the changes in the gain over the dependent lung (left posterior) lay between -44.4% and +62.3% while those for the non-dependent lung (right posterior) ranged from -23.3% to +21.5%. The changes in the ratios of the non-dependent to dependent lung also varied widely, from -47% to +18%.

6.2.3.4 Pattern of Breathing

The pattern of breathing was changed in each position from regular breathing with constant tidal volume to the flow tracking pattern. The changes in gain for the data with 70% or more of the variance explained are given in Table 6.7. The range of values for seated subjects was from -60.6% to +9.4% and for decubitus subjects, from -45.0% to +68.8%. The alterations in gain caused by the change in breathing pattern were as scattered and unsystematic in appearance as those caused by the addition of the resistance. The non-parametric Wald-Wolfowitz Run Test (Guttman, Wilks and Hunter, 1971) showed that

TABLE 6.6

EFFECT OF ADDED RESISTANCE

SEATED, R LUNG		CHANGES IN GAIN		CHANGES IN GAIN RATIO	
SUBJECT	POSTERIOR	ANTERIOR	SUBJECT	CHANGE	
1	-10.6 %	+5.4 %	1	+18 %	
2	+2.2 %	+3.2 %	2	+1 %	
3	-15.6 %	----			
4	+19.6 %	----			
6	----	+15.1 %			

LEFT LATERAL DECUBITUS		CHANGES IN GAIN		CHANGES IN GAIN RATIO	
SUBJECT	POSTERIOR R	POSTERIOR L	SUBJECT	CHANGE	
1	-23.3 %	-29.4 %	1	+17 %	
2	----	+27.9 %	3	-34 %	
3	----	-44.4 %	4	+2 %	
4	-7.0 %	-8.3 %	6	-47 %	
5	+21.5 %	+2.3 %			
6	-7.0 %	+62.3 %			
7	-19.0 %	----			
8	----	-20.8 %			

Note: The data in the table are those for which the VAF's (Table 1) for ALL values under comparison are greater than or equal to 70%.

TABLE 6.7

EFFECT OF BREATHING PATTERN
CHANGES IN GAIN: REGULAR BREATHING TO TRACKING

SEATED			LEFT LATERAL DECUBITUS		
S	POSTERIOR R	ANTERIOR R	S	POSTERIOR R	POSTERIOR L
2	----	-60.6 %	4	+22.2 %	-32.2 %
4	-18.2 %	----	5	-45.0 %	+29.6 %
6	----	-33.4 %	6	+68.8 %	+33.6 %
7	-0.9 %	+9.4 %	7	-7.4 %	-8.0 %
			8	+17.1 %	-2.4 %

Note: The data in the table are those for which the VAF's (Table 1) for both values under comparison are greater than or equal to 70%.

the differences between the changes with added resistance and those with the variation in the pattern of breathing for each microphone in each position were insignificant at the 95% confidence level, and the sign test showed no differences within either set.

6.3.2 SYSTEM DYNAMICS: DIFFERENTIAL EQUATION

The static analysis quantitated only that relation between the flow at the mouth and the sound occurring simultaneously. Neither the possible delays between events in the lung and the flow at the mouth nor potential dynamic effects (differentiation, memory) were included. These were studied by modelling the squared flow-sound amplitude relationship as a linear dynamic system (Fig. 6.7).

6.3.2.1 Impulse Response

The impulse response $h(t)$ of a linear system with input $x(t)$ and output $y(t)$ is defined by the convolution equation,

$$y(t) = \int_{-\infty}^{\infty} h(\tau)x(t-\tau)d\tau$$

In Nexus (Hunter and Kearney, 1984), it is calculated from the auto- and cross-correlations of the output and input signals. The impulse response function provides a complete characterization of a linear system as a function of time, equivalent to the output of the system after an input impulse function.

The features of the impulse response function between inspiratory flow squared and the amplitude shown in Fig. 6.10 were typical. A large spike occurred at the origin, signifying a static gain at zero lag. The oscillations to the right of the origin were too small to be identified. The impulse response accounted for no more of

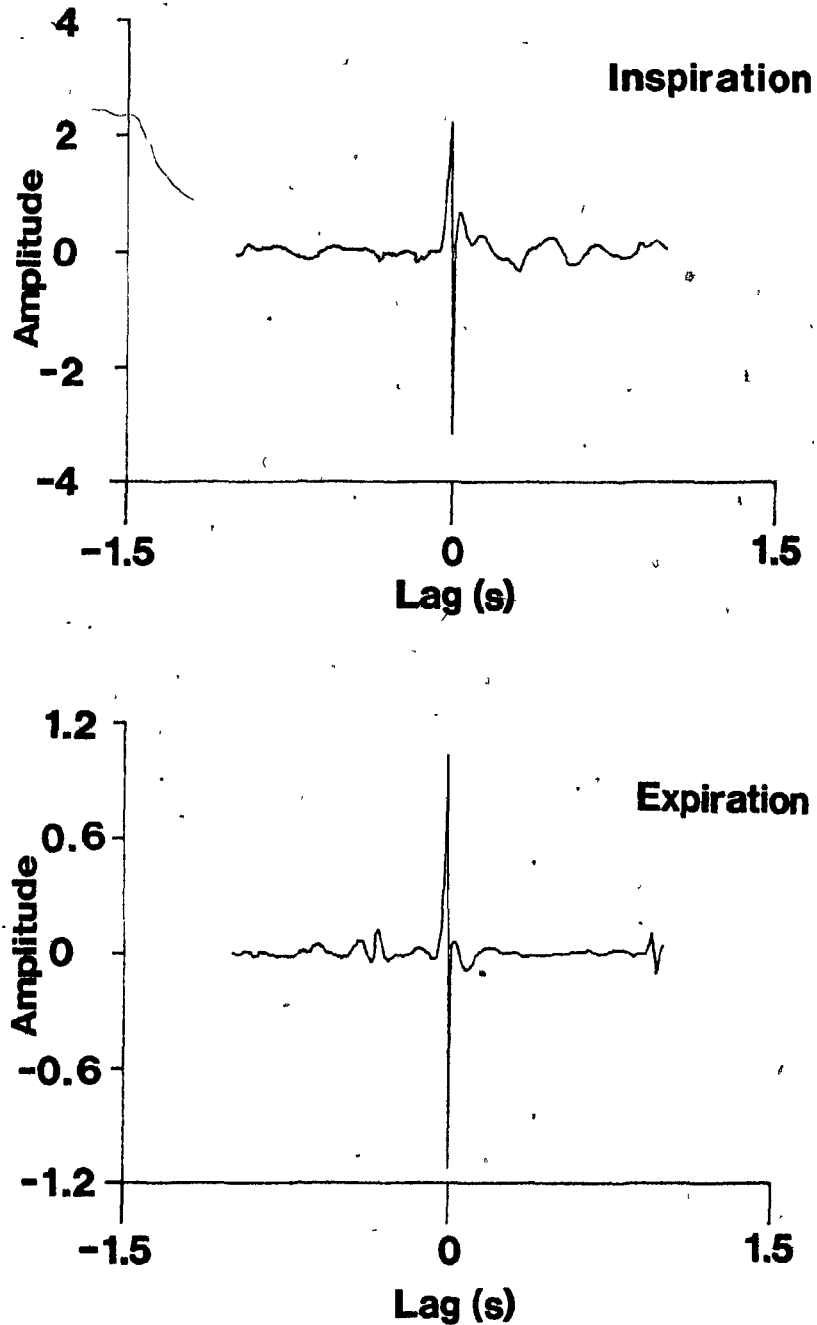


Fig. 6.10. Sample impulse responses between flow squared and sound for inspiration and expiration. Subject 3, case 2, dependent microphone.

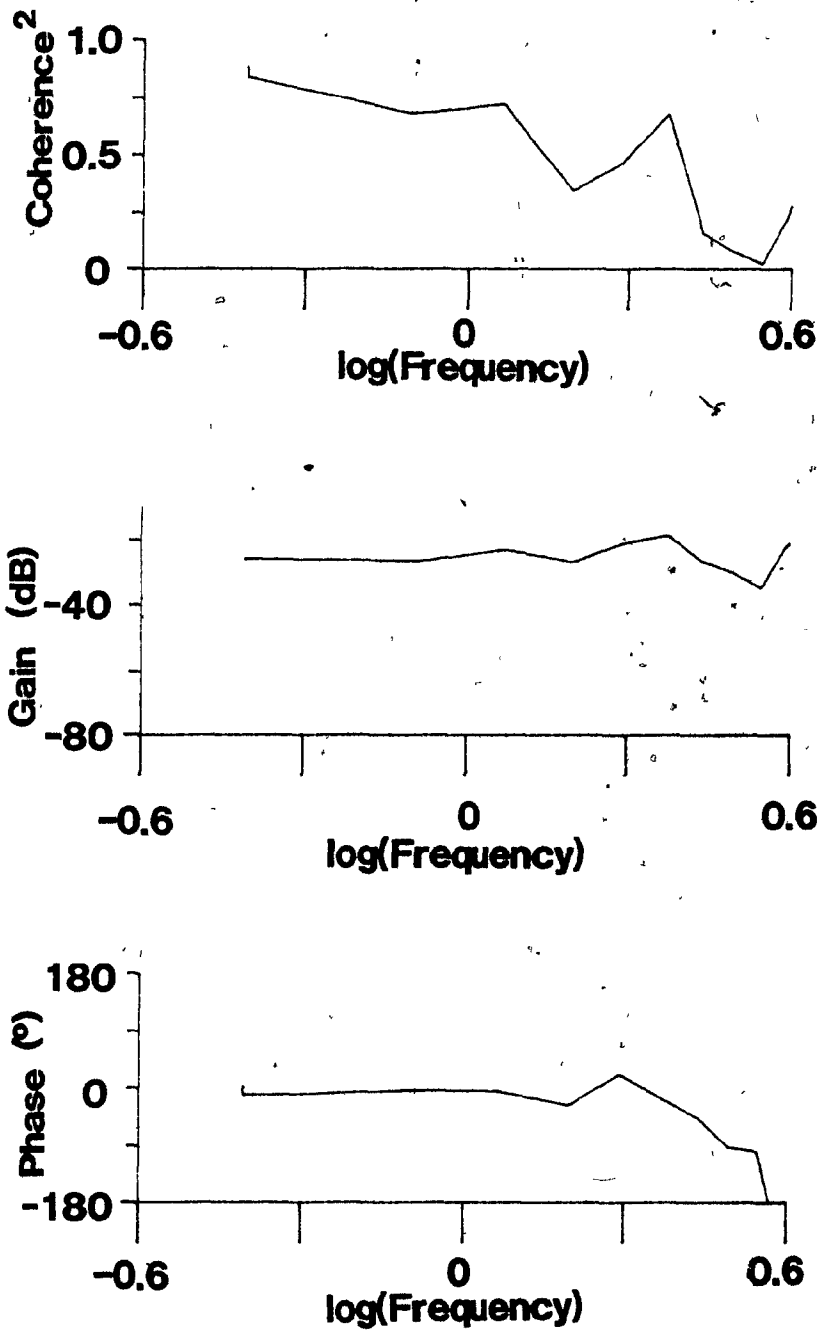


Fig. 6.11. Transfer functions. Coherence squared, gain, and phase are plotted between inspiratory flow squared and sound amplitude. Subject 3, case 2, dependent microphone. Where the coherence is high, there is a static gain and no phase shift.

the variance than did the static fit. For expiration also, the variance explained by the impulse response was only that accounted for by the static fit, i.e., the spike at the origin.

6.3.2.2 Transfer Functions

The transfer functions for a linear system with input $x(t)$ and output $y(t)$ are expressed in the Fourier transform domain as functions of frequency, ω .

$$\text{Gain} = \frac{|Y(\omega)|}{|X(\omega)|} \quad \text{Phase} = \frac{\phi(Y(\omega))}{\phi(X(\omega))} \quad \text{Coherence}^2 = \frac{|S_{XY}(\omega)|^2}{|S_{XX}(\omega)| |S_{YY}(\omega)|}$$

where ϕ represents the angle and S_{XY} , S_{XX} , and S_{YY} are the transforms of the cross correlation and auto correlations of the signals indicated by the subscripts. The gain is usually expressed in decibels, as $20 \log(\text{Gain})$ as defined above. The coherence squared is a measure of the fraction of the output at each frequency that results from the linear system acting on the input. It is analogous to the square of the correlation coefficient in linear regression.

The same information for inspiration is shown in the frequency domain in Fig. 6.11 as was given in the time domain in Fig 6.10. The value of coherence squared between inspiratory flow squared and the sound amplitude envelope was high for frequencies from 0-3 Hz, after which it dropped sharply. For that range of frequencies, there was an almost flat gain and no phase shift. The drop in coherence at 3 Hz occurred because the input had no power at higher frequencies (Fig. 6.12). Where the sound amplitude was the output of a linear system acting on the squared flow, the system showed no frequency dependence.

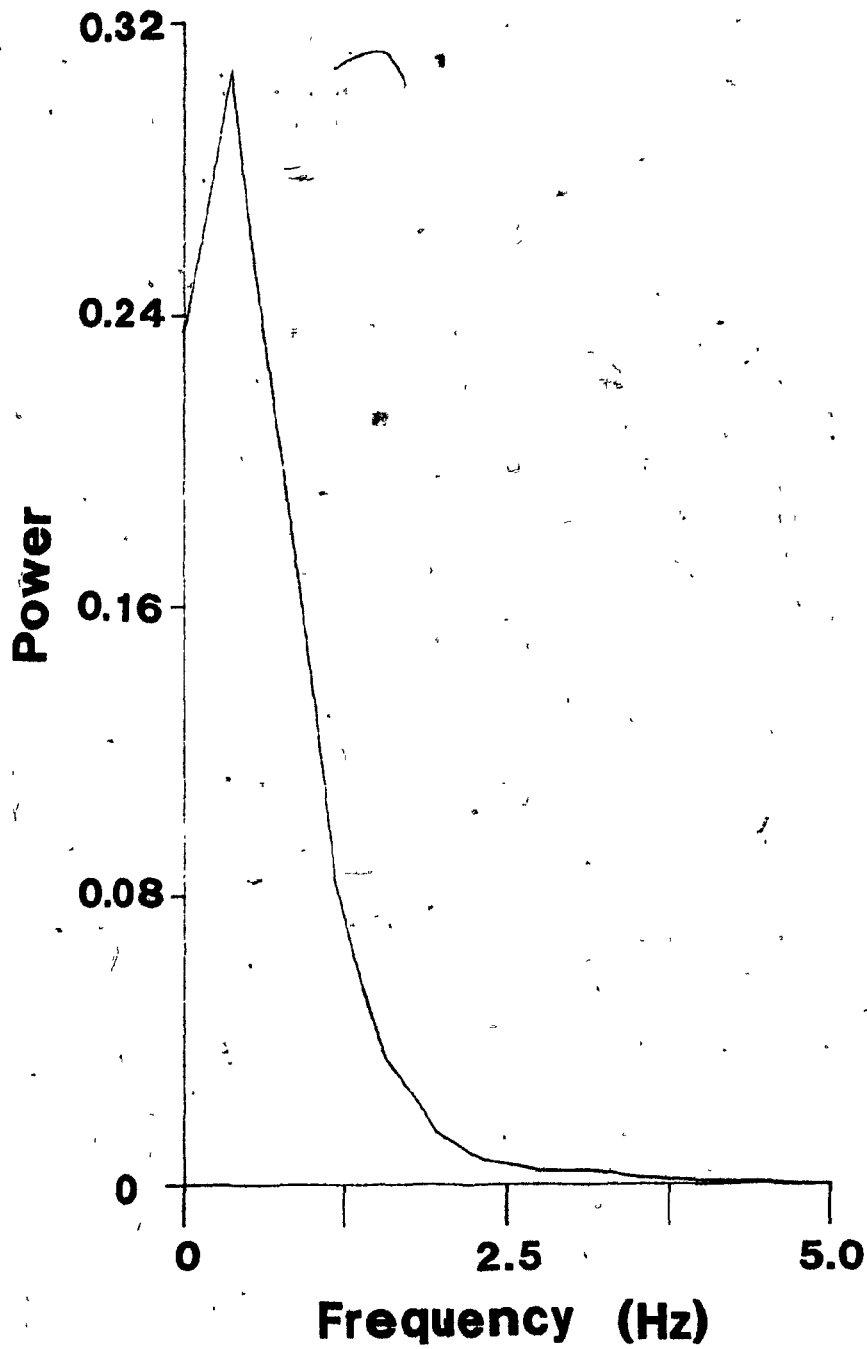


Fig. 6.12. The power spectrum of the flow. The power (in arbitrary units) of the input function, the flow, is shown as a function of frequency.

Both dynamic representations showed that the best linear system to model the relationship between inspiratory flow squared and the sound amplitude was the static algebraic function. The variance accounted for by the dynamic impulse responses were in no case more than ten percent greater than that from the statics alone. The same was true for expiration.

6.3.3 CROSS CORRELATIONS

The cross correlation $C_{xy}(d)$ between two signals $x(t)$ and $y(t)$ is defined by the equation

$$C_{xy}(d) = \int_0^{\infty} (x(t) - \mu_x) (y(t-d) - \mu_y) dt$$

(Strictly speaking, this is the cross covariance function if the values of the means are not zero.) This function is often normalized by the square root of the product of the mean square values of the signals. It indicates the degree of similarity between two signals as a function of the lag time, d , between them. If $y(t)$ is related to $x(t)$ and has been phase shifted relative to it, then C_{xy} will have a maximum value (of one, if the function has been normalized) at the lag time corresponding to the delay.

A sample plot of the cross-correlation between the sound envelopes at the two microphones is shown in Fig. 6.13. In both seated and decubitus positions, the sounds at the two microphones were in phase for all but two records, where the dependent lung led by 0.1 s. Kraman (1984) found that the sounds from two microphones on the chests of standing subjects occurred simultaneously, but large phase differences between the breath sounds at two different microphones have been reported by Druzgalski et al. (1980) in normal subjects and

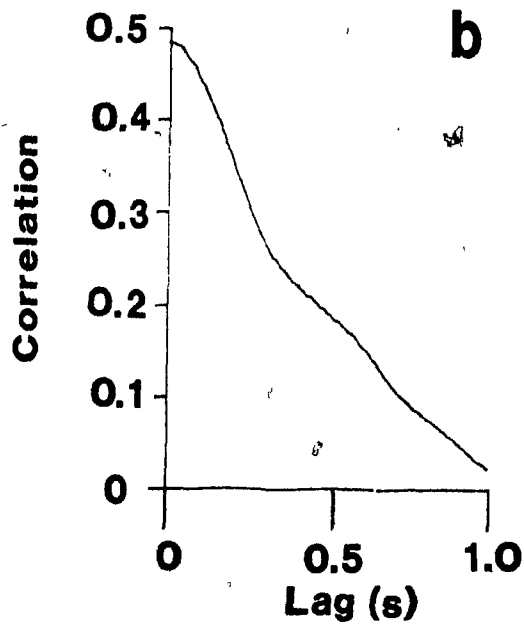
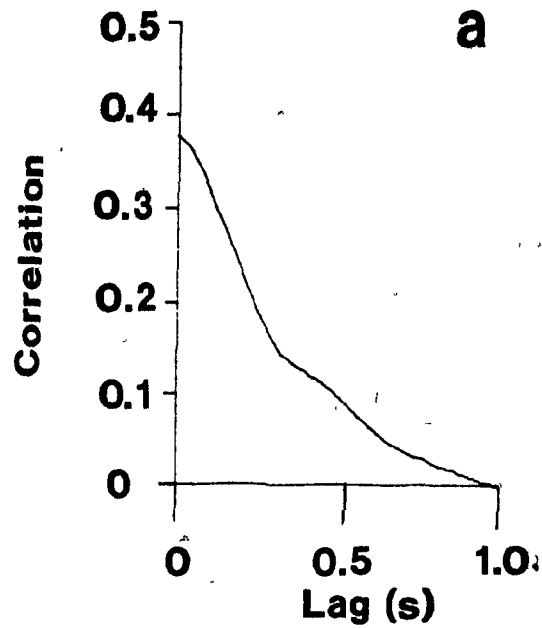


Fig: 6.13. Cross correlations between the sound envelopes from the two microphones. a) The dependent microphone signal allowed to lag. b) The non-dependent microphone signal allowed to lag. The maximum correlation occurs at zero lag in both cases, indicating that the microphones are in phase.

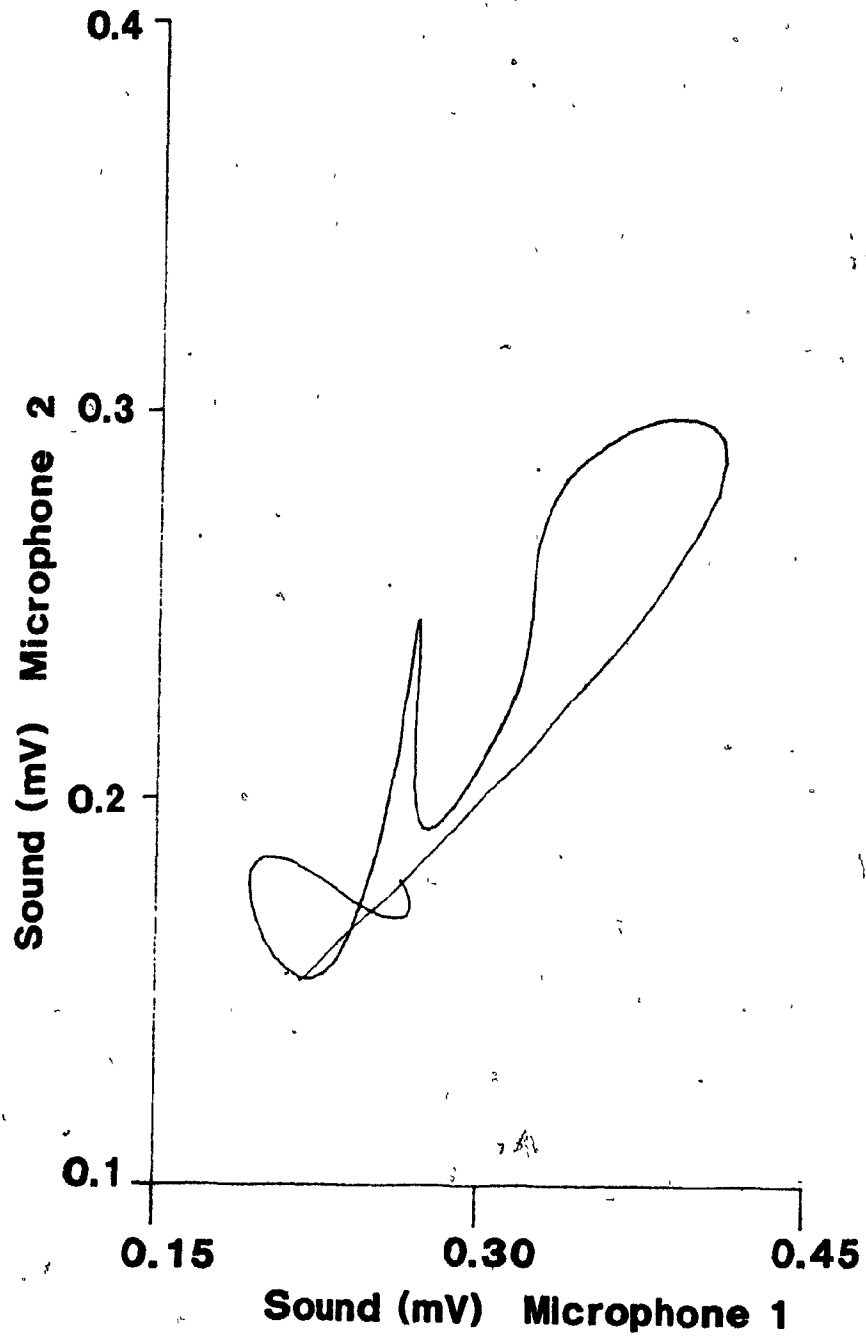


Fig. 6.14. Looping seen if one microphone signal is plotted against the other. Although the cross-correlations show zero phase shift, the hysteresis effects cause loops to form when the sound amplitude from one microphone is plotted against the other. One breath, subject 3, case 1.

moderate angles by Ploysongsang et al. (1979) and Ploysongsang (1983) in normal subjects and smokers. Their measurement techniques may be the cause. Druzgalski et al (1980) published only the oscilloscope tracings in which the signals from the microphones showed bursts at different times. There was no mention of high-pass filtering to reduce muscle noise, and some of the bursts may have been exactly that. Ploysongsang et al. (1979) and Ploysongsang (1983) measured differences in phase between the microphone signals by displaying one sound as a function of the other on the oscilloscope and measuring the resultant loop. This technique may have given them erroneous results because of the hysteresis in the sound signals (Fig. 6.9); the data which are shown in this way in Fig. 6.14 are in phase although the plot of the sound envelopes against each other forms a loop. A calculation of the lag made by assuming the signals to be sinusoidal functions of time and measuring the Lissajous figure could yield a spurious phase difference.

6.3.4 SPECTRAL ANALYSIS

The power spectrum of a signal is its power as a function of frequency, the average magnitude squared of the Fourier transform. It is the frequency domain representation of a stochastic process.

6.3.4.1 Bandwidth

Power spectra of the raw sound signals were analysed for changes in power and bandwidth with flow. During both inspiration and expiration, significant power was present from 0 to about 350 Hz, although the magnitudes were higher during inspiration. The maximum power occurred between 120 and 240 Hz, in good agreement with the range of 116 to 225 Hz reported by Shreiber et al. (1981). Despite the

moderate angles by Ploysongsang et al. (1979) and Ploysongsang (1983) in normal subjects and smokers. Their measurement techniques may be the cause. Druzgalski et al (1980) published only the oscilloscope tracings in which the signals from the microphones showed bursts at different times. There was no mention of high-pass filtering to reduce muscle noise, and some of the bursts may have been exactly that. Ploysongsang et al. (1979) and Ploysongsang (1983) measured differences in phase between the microphone signals by displaying one sound as a function of the other on the oscilloscope and measuring the resultant loop. This technique may have given them erroneous results because of the hysteresis in the sound signals (Fig. 6.9); the data which are shown in this way in Fig. 6.14 are in phase although the plot of the sound envelopes against each other forms a loop. A calculation of the lag made by assuming the signals to be sinusoidal functions of time and measuring the Lissajous figure could yield a spurious phase difference.

6.3.4 SPECTRAL ANALYSIS

The power spectrum of a signal is its power as a function of frequency, the average magnitude squared of the Fourier transform. It is the frequency domain representation of a stochastic process.

6.3.4.1 Bandwidth

Power spectra of the raw sound signals were analysed for changes in power and bandwidth with flow. During both inspiration and expiration, significant power was present from 0 to about 350 Hz, although the magnitudes were higher during inspiration. The maximum power occurred between 120 and 240 Hz, in good agreement with the range of 116 to 225 Hz reported by Shreiber et al. (1981). Despite the

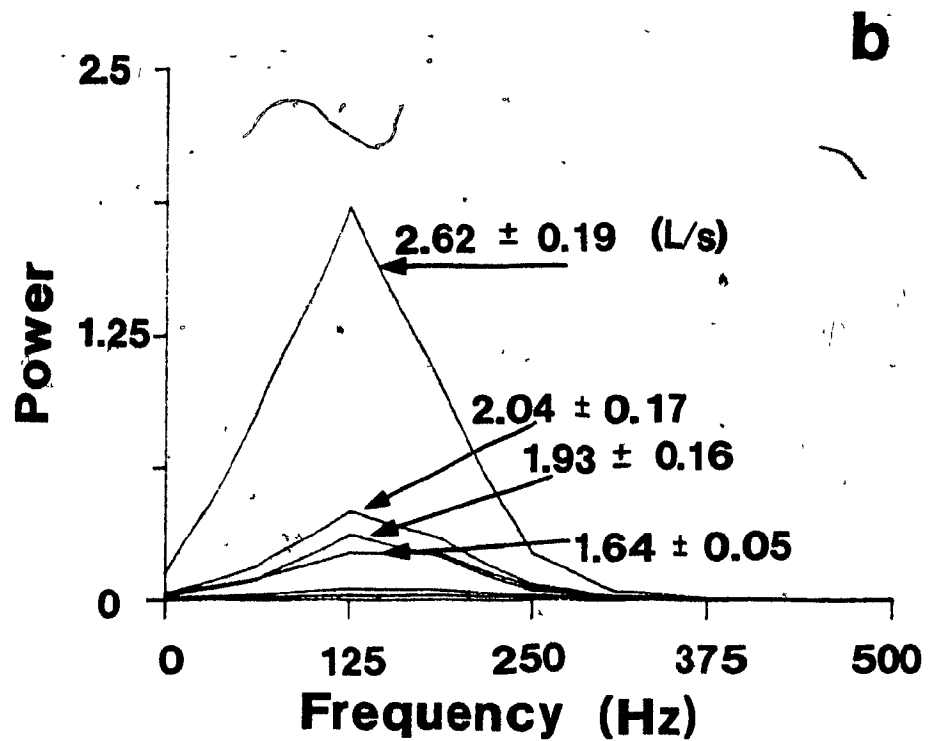
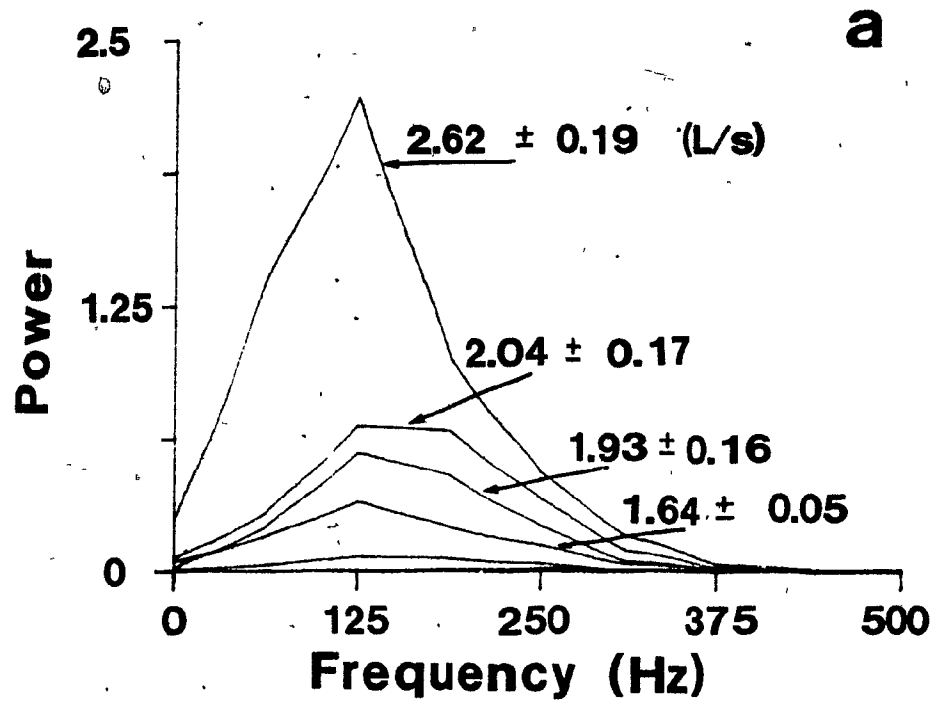


Fig. 6.15. Power spectra at constant flow. Power in arbitrary units. Flows marked as mean \pm standard deviation. a) Inspiration, non-dependent microphone. b) Inspiration, dependent microphone. Subject 3, case 2.

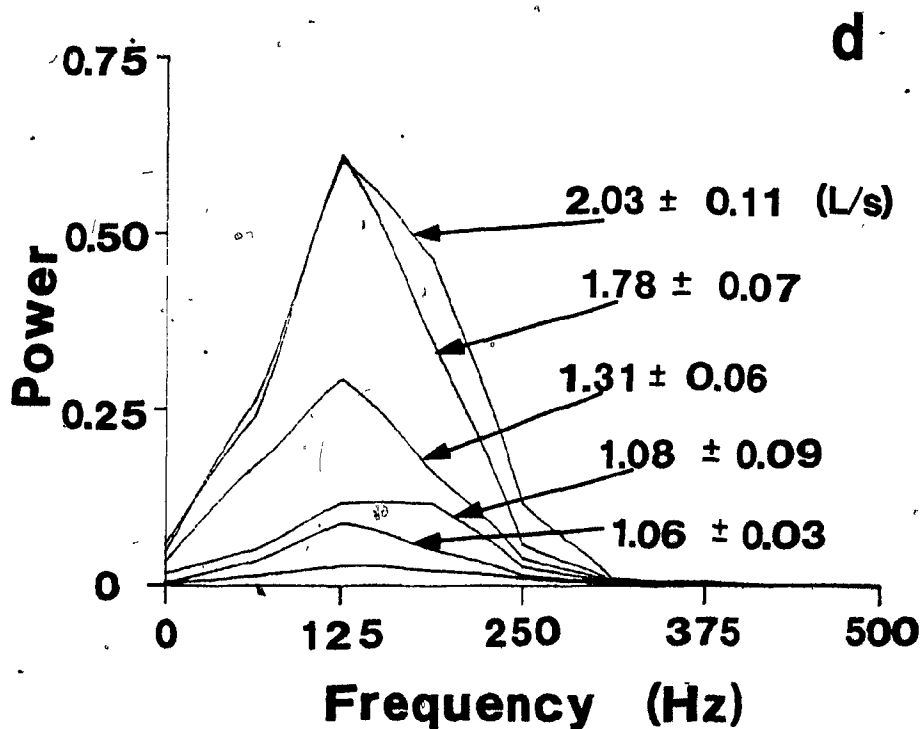
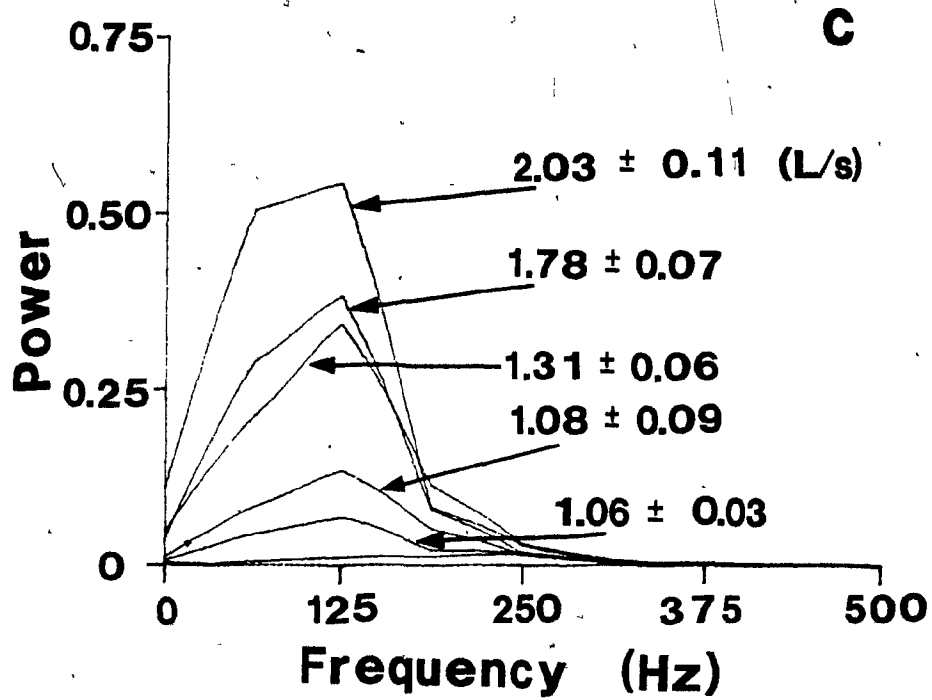


Fig. 6.15 -- continued. c) Expiration, non-dependent microphone.
d) Expiration, dependent microphone. Subject 3, case 2.

analog high-pass filtering at the time of the data acquisition, a non-negligible amount of power was present at frequencies below 100 Hz, meaning that the total power in the low frequency bands, whether signal or noise, was much higher than the signal power above 100 Hz.

Some examples of power spectra at different constant flows are shown in Fig. 6.15. The total power increased with flow. For similar magnitudes of flow, the total sound power during expiration was considerably less than that during inspiration.

6.3.4.2 Total Power as a Function of Flow

The static relationship between the smoothed rectified sound and flow squared is equivalent to one between sound power and flow raised to the fourth exponent. To check the value of the exponent over regions of constant flow, the equation was linearized using a logarithmic transformation. The sound power, obtained for the same regions of constant flow of the tracking experiments (cases 2, 3, 5, and 6) that were used to calculate the frequency spectra, was computed as the variance of the raw sound signals. The slopes of the log-log relationship between sound power and mean flow, corresponding to the exponents of the flow, were obtained by linear regression (Table 6.8). The standard deviation of the slopes were calculated as if the distribution of the errors in measurement were normal. Although after the logarithmic transformation, the distribution would have been skewed, the normal approximation remains a fair indication. With only 5 to 7 constant flows, more involved analysis was not expected to yield more precise results.

TABLE 6.8
LOG-LOG PLOTS OF POWER VS INSPIRATORY FLOW:
SLOPES

		MICROPHONE 1							
		Case: 2		3		5		6	
Subject		slope	SD	slope	SD	slope	SD	Slope	SD
1		3.31	0.49	----	----	4.53	0.97	6.74**	0.52
2		3.98	1.79	6.01**	0.53	3.75	1.13	5.08	0.91
3		4.25	0.15	2.12**	0.42	3.47	0.64	5.99	0.57
4		3.43	0.65	3.92	1.50	3.97	0.50	3.75	0.68
5		----	----	----	----	4.19*	0.61	----	----
6		4.14	0.72	7.62**	0.51	4.93*	0.29	6.35**	0.22
7		3.77	1.81	----	----	4.63	0.38	3.57	0.71
8		4.60	0.58	2.15	1.73	3.37	0.63	6.38**	0.66

		MICROPHONE 2							
		Case: 2		3		5		6	
Subject		slope	SD	slope	SD	slope	SD	Slope	SD
1		3.88	0.25	----	----	5.75	0.72	5.27**	0.30
2		2.15	0.75	3.22	0.44	4.17	0.53	3.74	1.11
3		4.65	0.51	4.64	2.31	3.16	0.46	4.25*	0.45
4		2.94	0.52	----	----	3.30	0.34	3.36*	0.22
5		4.50	2.33	4.29	0.84	4.54	0.39	4.98	1.21
6		3.12**	0.19	3.47	0.36	4.18	0.44	6.06	1.72
7		3.08	1.28	5.03	1.21	----	----	----	----
8		4.08	0.53	----	----	4.37	0.87	3.98	0.37

* = different from 4 at the 95% confidence level.

** = different from 4 at the 99.75% confidence level.

The exponents of the constant inspiratory flows (slopes of the logarithmic-logarithmic relationship) did not differ significantly from 4 in most experiments. Of those that deviated, the majority were larger than 4, and more occurred when the added resistance was in place.

Most relations between the logarithm of the measured power and the logarithm of the constant flow were linear for inspiratory flow. In some cases where very low constant flows were present, a threshold effect was seen, with the relationship holding only above some low flow, the value of which could not be determined with so few points of constant flow. The tracking experiments were designed to avoid low flow rates where little sound would be generated, but the threshold flow appears to be higher for some subjects than for others. Generally, however, a single power of the flow rate could be used to model the sound generation during inspiration. A higher order polynomial was not required.

During expiration, the relation between flow and sound power was more complicated. Although the logarithmic relationship appeared to be linear in most cases, many showed great scatter. However, the exponents were not significantly different from four in the majority of the measurements.

6.3.4.3 Power at a Frequency as a Function of Flow

As some degree of shifting of the spectral peaks was suspected, the changes of the power of the 60 Hz bands was studied as the flow rate increased. Frequencies from 0 Hz to 360 Hz were considered for inspiratory sounds and from 0 to 300 Hz for expiratory

sound, to cover the bands containing significant power. For inspiratory flows the exponents did not differ significantly with frequency, indicating that the fourth power of flow could be used to model each frequency band also, but statistical uncertainty of the values precluded any firm conclusions about shifts in frequency. The intercepts in the logarithmic relations, the gains of power with flow, had their maxima in the 120 to 240 Hz bands.

6.4 DISCUSSION

6.4.1 STATICS: THE ALGEBRAIC RELATION

6.4.1.1 *Goodness of Fit*

Inspiration

The static relationship during inspiration showed a high correlation between flow squared and the amplitude of the sound pressure. That this was the best power law relationship was confirmed by the exponent of 4 found in the constant flow-power relationship. The quadratic relationship of sound amplitude to flow has not been reported previously. In fact, other functions have been assumed. Leblanc et al. (1970) plotted their data as a linear function of the flow. The points were picked off a chart recorder tracing and the fit appears to have been done by eye; no regression coefficient was reported. A quadratic curve also could be fit by eye to the published plots without changing the apparent goodness of fit. Banaszak et al. (1973) reported that the sound amplitude increased with the flow. They measured at only three flow rates and therefore could not show the relationship. Wooten et al. (1978) published a schematic plot of sound amplitude as a curvilinear function of flow without including actual points. They called the relationship exponential but did not show it

to be. Dosani and Kraman (1983) and Kraman and Austrheim (1983) assumed that the sound was a linear function of the flow above 1.3 L s^{-1} when they divided the sound intensity by the flow to generate a flow-independent index, although Dosani and Kraman (1983) stated that below 1.3 L s^{-1} , the relationship was not always linear.

Very recently, Kraman (1984) presented data in an attempt to establish that there was a linear relation. Sounds recorded from four subjects breathing near FRC were treated. The peak airflow of each breath, maintained for a brief period only, was compared with either the average or the peak sound amplitude for that breath. Sound amplitudes also were divided by the simultaneous flow before being averaged over a breath. Regression lines between flows greater than 1.4 L s^{-1} and the treated sound amplitudes accounted for 62% to 77% of the variance of the maximum sound amplitudes and slightly more for the mean values. However, a slope significantly different from zero was seen in three of the four cases between the sound amplitude divided by flow and flow.

The linear relation found by Kraman (1984) may be related to his technique. The use of the mean amplitude of the sound in conjunction with the instantaneous maximum of the flow during the cycle was not justified by the author. The connection between the mathematical fit of one on the other and the physical generation of the sounds is not clear. In the measurement of the peak sound amplitude from the oscilloscope tracing with calipers, a significant error would be inevitable, and the single point estimate also would have a high statistical uncertainty. Although the linear regressions may have provided as good a fit as did a higher order polynomial, the scatter in the data shown on the published plots would make conclusive statements

difficult to make. Furthermore, the author mentioned that sounds generated for flows below 1.4 L s^{-1} were close to the noise level, suggesting that the microphone coupling was problematic, since even in a noisy environment the lung sounds were distinct for flows below 1 L s^{-1} in the experiments reported here. The curvilinearity may have been obscured by restricting the measurement to the higher flow range.

In the experiments reported here, the inspiratory flow squared was very highly correlated with the simultaneously occurring sound amplitude for most cases (Table 6.3). In all cases, over 1000 points of simultaneous flow and sound were compared. The best-fit exponent for the relation between flow and sound amplitude, the square root of sound power, was two. Because the sound amplitude is a measure of energy, the relationship may be presumed to be between kinetic energy and sound.

Expiration

A kinetic energy relationship, if this is what it is, should hold for all flows in both directions. A few of the inspiratory and most of the expiratory sound envelopes were not linear functions of the flow squared. However, kinetic energy is a function of velocity squared, not of flow rate squared. If the total cross-sectional area at the level of sound generation remained constant throughout a breath, the two would differ by only a scaling factor, but if the sound was generated in lung generations where substantial area changes occurred, if airways opened or closed, or if the sites of sound production moved up- or downstream, mouth flow and local velocity might not be proportional. Furthermore, if the distribution of the total flow among regions changed during a breath, the relationship between

the total flow and the local flow would itself vary with time. As in the lateral decubitus position the expiratory flow from the individual lungs has been shown to occur sequentially, the dependent lung emptying first (Chapter 5; Frazier et al., 1976), the absence of a linear relationship between expiratory flow squared and sound in the decubitus subjects (Cases 4, 5, and 6) might have been related to flow redistribution.

6.4.1.2 Static Parameters

Gains

The static gains, the increase in sound amplitude with flow squared, could not be compared among subjects (Table 3). Differences in body type (Table 1) must influence the transmission properties of the chest wall. Even consecutive trials of the same manoeuvre on the same subject showed some differences in gain, probably the result of differences in microphone coupling (Table 3, Subject 7r). Dosani and Kraman (1983) reported reproducible differences from points only a few centimeters apart on the same subject. Kraman and Austrheim (1983) showed that even the transmission of sound applied at the mouth varied from point to point and among subjects. The gain represents the strengths of the sound generators weighted according to their location relative to the measurement site, the transmission properties of the intermediate tissue, the number of generation sites, and the attachment and sensitivity of the microphone. Although the amplitudes of the sounds from the individual sites should be functions of the local cross sections and of the regional flow, the sites may be in the central airways and thus be the same for both microphones. The number of unknowns destroys the value of the gain as an absolute measure.

Offsets

The offsets in the linear relationship predicted the values of the sound amplitude at zero flow. As such they were a measure of the background noise. Large offsets suggest poor coupling with its resultant pickup of the room noise, particularly when they occurred where low percentages of the variance were accounted for by the linear fit.

6.4.1.3 Ratios of the Gains

The ratios of two simultaneous gains from the same subject involved fewer variables than do the gains themselves. The gains were flow rate independent and their ratios partially subject independent. Differences in microphone coupling and in local chest wall thickness remained, but common transmission effects were likely to be removed in the ratios. The resultant values were similar to the breath sound index of Ploysongsang et al. (1977, 1978), with one important difference. By performing the regression on flow squared before making the comparison, information on the validity of the linear model for each set of data was obtained. Furthermore, inspiration and expiration were treated separately because the functional relationship with sound is different in each case.

6.4.1.4 Effects of Subject Position

In the lateral decubitus position, the hydrostatic gradient in the abdomen has a strong effect on the volume of the dependent lung and on its ventilation. The gradient in static pleural pressure greater than that between apex and base in the upright posture (Kaneko et al., 1966; Milic-Emili et al., 1966), causes the non-dependent lung

to be more fully inflated than the dependent lung. Furthermore, during the diaphragmatic contraction of inspiration, the dependent lung is partially isolated from the pressure gradient and expands, but during expiration when the diaphragm relaxes, the abdominal contents press in the cephalad direction and the mediastinum presses down, causing considerable deflation of the dependent lung (Roussos et al., 1976). The emptying that results is asynchronous, with the dependent lung leading (Frazier et al, 1976).

Moving to the lateral decubitus position also caused a decrease in the ratio of the sound amplitude of the non-dependent to the dependent lung (Table 6.5), in most cases because of opposite changes in the two regions. Thus, qualitatively, the lung sounds appeared to indicate the distribution of ventilation (LeBlanc et al., 1970; Ploysongsang et al., 1977, 1978). However, the present data do not support the hypothesis fully. The decrease in the ratios of the gains for those cases where the linear fit was good for both microphones in both positions ranged from 12% to 85%. As an increase of 85% in the tidal volume distribution would be predicted (Chapter 3) to require an increase of slightly more than that in the ratio of pleural pressure swings, such a change seems unlikely. More probably, both the ratios of the sounds and the ratios of regional ventilation depended on related factors of flow rate but not on each other. Changes in the acoustic transmission properties caused by the regional inflation were possible, for example.

6.4.1.5 Effects of Added Resistance

Dynamic pressure-flow curves for a normal lung (Hyatt et al., 1970) show that the pressures generated during breathing at a given flow rate increase considerably in the presence of an external resistive load. The activity of the respiratory muscles that is necessary to generate the flow increases considerably. However, these changes caused no consistent alteration of the lung sounds. As the resistance forced at least some subjects to maximal respiratory efforts, evident from their subjective impressions, from the lift of their shoulders and upper chests during inspiration, and from their inability to sustain the maximum flow rates, all the inspiratory muscles were in use. If the sounds had been caused by muscle activity or by microphone movement, they would have increased dramatically during these manoeuvres.

With the resistance in place, greater pleural pressure swings were needed to generate the flows. If the changes in the amplitude of the pleural pressure swings were uniform over the lung, the distribution of ventilation may have remained unchanged. If, however, the greater use of intercostal and accessory muscles that was evident increased the relative pressure swing over the non-dependent lung zones, the distribution would have become more uniform, particularly in the lateral decubitus position (Chevrolet et al., 1979). If this was the case, the sound distribution did not reflect it.

6.4.1.6 Hysteresis

Sound generation in the lungs entails the dissipation of energy. Recruitment and expansion of small airways during inspiration also will absorb energy to overcome the surface tension of the fluid sealing them and in the elastic distention of the tissue. The hysteresis may have shown the absorption of a fraction of the available energy by the expanding the lung tissues during the some portions of inspiration. Once more airways were open less work would be done on the tissues, and the sound amplitude could be greater for the same flow.

The elastic distention of the lung tissues has itself been suggested as a possible source of the sound. However, the direction of some of the hysteresis loops does not support the hypothesis. The distention is greater and there is more tissue rubbing at the start of inspiration than there is later when the lung is more fully inflated, yet many of the loops demonstrated lower sound during early inspiration.

Local changes in lung volume with their resultant alterations in the sound transmission properties might occur in a non-consistent pattern. Regional effects of air and blood volume could explain the pattern seen, but this cannot be determined from the data.

6.4.2 DYNAMICS

Because naturally driven respiratory flow changes relatively slowly, it is not surprising that the dynamic relationship between the flow squared and smoothed rectified sound could not be characterized. The maximum frequency at which the human respiratory system can be

driven is about 7 Hz, and at that frequency the tidal volume approaches zero, before the respiratory muscles reach the limits of their contraction and relaxation times (Agostoni, 1970). Methods to generate higher frequencies would change the pattern of airflow and probably of sound generation. One could drive the system with a high frequency positive pressure ventilator or with high frequency chest wall compression, but by definition one would not be investigating normal breath sounds. One also could measure the response to a step change in flow by asking a subject to generate high pressures against an occluded mouthpiece and opening it suddenly. The airflow transient would be difficult to analyse and might not move enough air to generate sounds. Also, the elastic recoil of the chest might damp out the desired high frequencies.

The non-linear behaviour of the lung sound generating system further complicates the measurement of system dynamics. Even with sufficient high frequencies in the input, the hysteresis loops and other nonlinearities would cause difficulties. Although it is possible to calculate higher order dynamic terms when doing systems identification, it requires careful construction of the input signal (Marmarelis and Marmarelis, 1978), an impossibility for voluntary breathing. As even the first order term of a non-linear system can be distorted unless the input is properly constrained (Marmarelis and Marmarelis, 1978), and since the true input to the many possible subsystems generating the sound is unmeasurable and almost certainly not simply a constant fraction of the flow at the mouth, the systems identification problem seems insurmountable with noninvasive techniques.

6.4.3 THE GENERATION OF BREATH SOUNDS

Sounds over the normal lung may be thought to result from phenomena related to airflow, from vibrations caused by the expanding tissue, or from nonpulmonary sources like muscle sound and skin movement. Muscle is an unlikely source of the sounds reported here, because the increased muscle activity caused by breathing against a resistance did not affect the sounds. The flow squared dependence and the hysteresis also would be difficult to explain if microphone movement and muscular activity were the sound generators. Tissue expansion and rub was discounted as the source of breath sounds by the experiments of Bullar (1884) who showed that an excised lung in a sealed box produced breath sounds when expansion was caused by decreasing the surrounding pressure with the trachea open to the atmosphere but that it was silent when the trachea was occluded and the lung expanded without airflow. Furthermore, the flow squared relationship would be difficult to explain by tissue distension. Airflow phenomena are the most probable source of breath sounds.

A possible mechanism for the generation of sounds in a branching network like the lungs is that which causes sound at low speed in an air duct with a splitter in the flow (Nelson and Morfey, 1981). The theory, which was developed for rigid spoilers in straight ducts and shown by the authors to extend to splitters in exit flows, may be expected to be a first approximation to the situation of elastic structures with curved walls. The fluctuations in pressure caused by the separation of flow on the sides of the spoiler generate the sound. This fluctuating pressure is proportional to the steady force on the obstacle. For sound of wavelength greater than the cross-sectional dimensions of the duct, the sound power is proportional to the fourth

power of the average velocity in the constriction:

$$\text{Sound Power} = K^2 (St) [\sigma^2 (1-\sigma^2)]^2 C_D^2 U_c^4$$

where $K^2 (St)$ decreases with the Strouhal number, fd/U_c , U_c is the average velocity in the constricted duct, σ is the ratio A/A_c , where A is the cross-sectional area of the duct before the constriction, A_c is the cross-sectional area of the constricted region, and C_D is the drag coefficient of the splitter. In the lung, this would imply that the sounds during inspiration were produced at the bifurcations in the tracheobronchial tree and had power proportional to the drag coefficient, squared, the velocity downstream of the bifurcation to the fourth power, and a function of the areas in the parent and daughter tubes. Most sound would be generated at the locations of the larger pressure drops. The lung sound measurements reported here are in agreement with the fourth power dependence on the flow; the other quantities were not determined.

The site of production of breath sounds may lie in the peripheral airways or in the first few generations of the tracheo-bronchial tree. While efforts to find correlations between lung sounds and regional ventilation (Leblanc et al., 1970; Ploysongsang et al., 1977, 1978, 1982) assumed the former and subtraction pneumonography (Kraman, 1980) was used to try to prove it, many authors have maintained the latter. Hannon and Lyman (1929) and Gavriely et al. (1981) suggested that tracheal noise was transmitted throughout the chest. Banaszak et al (1973) postulated that the sounds came from the vicinity of the carinas of the larger bronchi. This is consistent with the theory of sound generation presented above.

6.4.4 PHASE RELATIONSHIP

Model predictions indicated that a phase difference in flow might occur when the pleural pressure swings on two compartments were out of phase with each other or were very different in magnitude (Chapter 3). Measurements made with krypton-81m for regular breathing in the lateral decubitus position showed a considerable phase lag in most cases (Chapter 5). Frazier et al (1976) demonstrated sequential emptying of the lungs in the lateral decubitus positions. Nonetheless, the lung sounds over the dependent and non-dependent zones were in phase in all but two cases where they were only 10° different, even in the lateral decubitus measurements.

Lung sound pressure is probably a function of the velocity at the sites of generation, as is discussed above. The velocity is a function of both the flow rate and the cross-section of the airways. The sounds, which are in phase, are thus functions of the flow, a variable which may have a definite lag between the lungs when subjects are in the lateral decubitus position, and the area. Either the sound is generated centrally and transmitted with differential attenuation to the measurement locations, or the local cross-sectional areas must compensate for the lag in the volumetric flows. In the latter case, two possible mechanisms suggest themselves. Either the number of open airways of the caliber for sound generation varies with flow to stabilize the local velocities or the size of the airways in which the sounds are generated changes to keep the velocities constant at the sites of generation. In the first case, increases in local flow would be matched by increases in the number of areas producing sound and therefore in the total sound amplitude. The total cross-sectional area would increase as the $2/3$ power of the total flow, adding a dependence

on flow to the $4/3$ power to the gain term in the relationship between flow at the mouth and sound. This might be part of the reason for the failure of the linear relationship between flow squared and sound amplitude during expiration. In the second instance, the gain would not change with increasing local flow rate but the ratio of velocity to diameter would decrease. The first possibility requires that the critical pressure to open the airways that generate the sound be just in excess of the product of their resistance multiplied by the flow rate of sound generation. The second requires that the sound be generated only when the kinetic energy reaches a critical level and that the mechanism of its production dissipate enough energy that the critical value not be attained downstream. The data available cannot be used to prove or disprove either hypothesis.

The simplest, and therefore most likely explanation for the sounds to be in phase is that they are generated in the central airways where most of the pressure drop occurs. The differences between the microphones would then be the result of differences in the transmission properties of the lungs. The changes with subject position could be explained by the increased density of the dependent lung in the left lateral decubitus position relative to the seated posture. The addition of the resistance would not change the transmission of sound. Intersubject differences could be very large, depending on body composition. The hysteresis could be caused by the time-varying regional distribution of the air causing regional differences in the acoustical properties.

6.4.5 SPECTRA

The frequencies of the measured lung sounds were the same throughout a breath, but there were considerable differences in power during inspiration and expiration and at different flows. When the different frequency bands were considered separately for the variation of sound power with the flow, even those below 100 Hz showed an increase with flow rate. Because Rice (1983) stated that the lung parenchyma did not pass frequencies below 100 Hz, and because the analog filter severely attenuated sounds at the low frequencies, the result was initially surprising. However, the literature contains considerable disagreement about the transmission properties of lung tissue. Forgacs (1978) claimed that the upper cut-off frequency was 200 Hz. Kraman (1983b) called the lung a sharp band-pass filter but showed transmission spectra at least as wide as his band-limited source, from 125 Hz to 500 Hz. In agreement with the present data, Kraman (1983a) showed that there were sounds at frequencies as low as 50 Hz that could be related to respiration but that the noise power at low frequencies was as large. Banaszak et al. (1973) found that sound power from 75 Hz to 275 Hz increased as a function of flow rate and that the lowest frequencies were the loudest, and McKusick et al. (1955) measured breath sounds at frequencies from 60 Hz to 350 Hz. Clearly, all statements about the frequency transmission properties of the lung must be questioned.

The acoustic properties of lung tissue are not documented. Since it may be considered to be a foam composed of air bubbles embedded in a viscoelastic matrix and containing strands of stiffer material, its behaviour can be expected to be complex. For example, a rubber matrix containing air particles has a strong resonant frequency

in the kilohertz range that is a function of the bubble size, bubble concentration, and properties of the rubber (Gaunaud and Barlow, 1984). No evidence was seen that resonance in the lung affected the measurements. However, because of the complexity of the relationships involved, an experimental study of the sound transmission properties of lung tissue is needed.

Attempts to measure the transmission properties of the entire chest have been made by Ploysongsang et al. (1977, 1978), Kraman and Austrheim (1982), and Kraman (1983b) by putting a speaker at the mouth and recording the sounds over the chest at different locations. Unfortunately, as Kraman and Austrheim (1982) point out, the transmission paths from the mouth to the measuring sites are different from those from within the parenchyma. To determine more useful transmission details, a wide-band input signal would have to come from within the lung.

6.4.6 SUGGESTIONS FOR FURTHER WORK

6.4.6.1 *Problems of Methodology*

The problems of microphone attachment during the experiments were considerable. Smaller, lighter microphones would be easier to fix to the skin and should be used. The microphones should be calibrated and identical.

Although good signals were obtained in a noisy environment if the microphones were well coupled to the skin, the experiments would have been better in a quiet room. The amplifier hum and ventilation fan noise would be relatively easy to eliminate by soundproofing, but the noise sometimes generated in the pneumotachometer at high flow rates would be more difficult to control. It might be better to

measure volume changes with a spirometer to remove a source of noise that, like the signal, is related to the flow.

6.4.6.2 Suggested Studies

Until more is known about the site at which sound is generated in the lung and the manner in which it propagates through the tissue, any hypotheses about the overall sound signal will remain vague. To test the applicability of the theory of Nelson and Morfey (1981) to a branching structure like the airways, acoustic experiments should be performed in a bifurcating model. From that model of sound generation, if it should prove to be true, the locations of the sound generators could be estimated based on pressure drop measurements. The transmission of sound should be studied from a known sound source placed within the lungs to measure the frequency dependent attenuation as a function of lung inflation. With the data from those experiments the study of lung sounds could yield more concrete results.

6.5 CONCLUSIONS

Lung sound measurements are problematic. The zone measured is unknown, the transmission properties of the tissues are unclear, and whether or not either is constant throughout a breath is indeterminate. Nevertheless, interesting properties can and have been measured.

Lung sound amplitude varied with the second power of flow during inspiration. During expiration the expression was not significantly different although the data were not well represented by a power law function. This linear relationship between flow squared and sound was independent of the pressures needed to generate the flows and of the pattern of breathing within the ranges considered. The

gains in the relationship were variable among subjects. They did not seem to be a direct reflection of the ventilation distribution.

The lung sounds measured with both microphones were in phase, even in situations where the regional volume is known to change sequentially. The most likely explanation for this phenomenon is that the sounds were generated centrally. The regional differences then were caused by variations in transmission properties of the lung and chest wall.

Identification of the dynamic system between total flow and sound pressure is probably impossible. The frequency limitations of the respiratory system prevent investigations much beyond 3 Hz where the linear system is still one of static gain. Non-linearities such as hysteresis or the volume effects reported by others (Leblanc et al., 1970) complicate the problem. Other nonlinear effects such as changes in the cross-sectional area of the regions producing the sound either because of shifts in the location of sound generation or because of physical alterations with lung inflation may complicate the situation further. Because inspiratory and expiratory sounds must be treated as separate input signals, the production of a zero mean input with a normal distribution of amplitudes is impossible, and any detailed system analysis would be very difficult.

Normal lung sounds in adults showed no spectral shifting with flow rate or flow direction. Only the magnitude of the power changed. The gains in power at different frequencies were not uniform, the largest lying in the range between 120 and 240 Hz.

Lung sounds may give qualitative information about the distribution of regional ventilation. However, on a quantitative level, they do not appear to measure it. The sounds themselves are directly related to the second power of the airflow, not to regional volume changes.

CHAPTER 7

CONCLUDING SUMMARY

7.1 SYNOPSIS

A three-part study of tidal breathing in normal human subjects has been presented in this thesis. A mathematical model of pleural pressure-driven ventilation was used to study the effects of the magnitude and frequency of pressure variations on tidal volume distribution. A relationship between the quantity of inhaled krypton-81m, a radioisotope, in the lungs and the regional flow per unit volume was derived, and krypton-81m was used to measure the dynamics of breathing. Breath sounds were studied in relation to the airflow at the mouth. The findings of each section will be summarized briefly.

7.1.1 THE PLEURAL PRESSURE-DRIVEN MODEL

The model consisted of two parallel compartments with identical pressure-volume and pressure-flow characteristics. The mechanical properties at any time therefore were determined by the pressures, volumes and flows in the individual compartments. Regional inhomogeneity at the start of inspiration was caused by a static pleural pressure difference between the compartments. As the breathing cycle progressed, the effects of the pressure changes, volume changes and flows altered the mechanical properties.

The ratio of the tidal volumes delivered to the two compartments was almost independent of the amplitude and frequency during breathing from functional residual capacity (FRC) if the ratio of pleural pressure swings on the compartments was held constant. When

the pressure swings were identical, the volume delivered to the dependent (lower) compartment was greater than that to the upper by an amount that depended on the static pleural pressure. The difference between the compartments was slightly greater with larger tidal volumes. Also, if the driving pressure on one compartment led that on the other, a greater proportion of the air entered the compartment that filled later. Nevertheless, these changes in the distribution of the inspired volume were minimal. They were attributable to the different pressure-volume operating points of the compartments.

Because of the shape of the pressure-volume curve, the effects of small static pressure differences was a function also of the starting volume. At extremely low volume, the non-dependent region was more compliant than the dependent zone and received more tidal volume. As the initial lung volume was increased, the situation became that described above. At high volume, the tidal volume again favoured the dependent compartment.

Changes in the ratio of the pleural pressure swings on the compartments caused almost proportional alteration in the tidal volume distribution. This effect, although modified by the tidal volumes and frequencies of breathing, dominated the control of the distribution of air. Moreover, the ratio of the pleural pressure swings affected the sequence of ventilation; phase differences in filling and emptying of the compartments were generated when the pressure swings were in phase but of very different magnitudes over the compartments.

Different waveforms of pleural pressure variation generated flows of different forms to the compartments, but the overall tidal volume effect was very similar. For step changes in pressure (square

wave), the non-dependent compartment received slightly more air than it did with sinusoidal or triangular pressure swings. Nonetheless, the tidal volume distribution between the compartments remained primarily a function of the pleural pressure ratio with the resistance and compliance in each compartment causing secondary effects.

7.1.2 A MODEL OF KRYPTON-81m DYNAMICS

The lung was divided into two arbitrary regions. In one, the convection zone, convection in the expansile airways was the only method of tracer transport. In the other, the respiratory zone, there was no bulk flow, the dimensions were constant, and gas moved by molecular diffusion only. The airway cross-section increased exponentially with distance in both zones but with different coefficients of the exponent in each region. The equations for the regions were solved analytically to obtain the time-varying concentration profiles of krypton-81m. The concentrations, integrated over the region, yielded the activity-time curves. Because of the times and distances involved, the concentrations in the conducting region were more important than those in the respiratory zone. The ratio of the time derivative of the krypton-81m activity to the activity itself modelled the ventilation per unit volume. This derivation allowed the interpretation of the krypton-81m activity during an average breath.

7.1.3 KRYPTON-81m MEASUREMENTS

Experiments were performed using krypton-81m and a gamma camera. Healthy human subjects breathed a mixture of krypton-81m and air while they lay on their left sides, their backs against the camera. Four different patterns of regular breathing were studied, 12 breaths min^{-1} at the comfortable tidal volume, 12 breaths min^{-1} at twice the tidal volume established in the earlier measurement, 24 breaths min^{-1} with its comfortable tidal volume, and 24 breaths min^{-1} at twice that volume. The activity was analysed using the classic steady state method (Fazio and Jones, 1975) and the dynamic method of Chapter 4.

During the experiments, the krypton-81m was diluted with air in a gas bag before being delivered to the subject. Both the flow of air and that of krypton-81m were constant; the bag inflated and deflated during breathing. The reservoir with its steady feed maintained the concentration of the isotope at the trachea almost constant during inspiration. Since both the dynamic model in Chapter 4 and the steady state analysis assume a constant inlet concentration, such a delivery system is essential if lung scans are to be interpreted quantitatively. Even qualitatively, the activity profiles in the lungs of a seated subject were altered by the absence of the mixing chamber. However, stronger krypton-81m generators are required because of the increased residence time of the gas in the circuit.

The distribution of the average volumetric flow and thus of the tidal volume was obtained from the steady state scans. Neither the ratios of the counts nor those of the average flows in the non-dependent and dependent lungs varied significantly with frequency

or tidal volume. This result was consistent with the model of Chapter 3 if the distribution of the pleural pressures over the lungs was unchanged. Because the pleural pressures were not measured, it can only be postulated that this was the case.

In order to study the changes of krypton-81m activity in the lung during a breath, a representative breath was constructed. Sixteen images were framed, each consisting of the sum over all the breaths of the activity from one-sixteenth of a cycle. In the measurements where a pneumotachograph signal was available, the flow per unit volume calculated using the method of Chapter 4 for the entire lung field compared well with that calculated from the pneumotachograph. The method was applied to the analysis of the right and left lungs individually.

The flow per unit volume in subjects in the left lateral decubitus position was greater in the dependent than in the non-dependent lung. It increased with both tidal volume and frequency, but particularly with frequency. The increases as well as the magnitudes were larger in the dependent lung. The ratio of the flows in the lungs, computed using the flow per unit volume curves and values of the relative volume of the lungs from the literature, indicated that the dependent lung received more flow than the non-dependent lung for most of the cycle of a normal breath. The flow to the non-dependent region dominated only for a brief time when the direction of airflow changed. Sequential ventilation was evident also, with one compartment filling while the other was emptying at end inspiration and end expiration. This implies the direct exchange of gas between the lungs in normal subjects in the lateral decubitus position.

7.1.4 BREATH SOUND MEASUREMENTS

Breath sounds were recorded at the surface of the chest. Two microphones were used simultaneously, one more dependent than the other, in each of the seated and left lateral decubitus positions. Sounds were recorded for regular breathing, for tracking of step changes in flow, and for similar tracking through a flow resistor.

The amplitude of the breath sounds was found to be proportional to the square of the flow rate, but with different gains on inspiration and expiration. The fit of relation was excellent on inspiration but poor on expiration. As other investigators have found, the gains showed very large intersubject variability, related perhaps to the differences in body type. The ratios of the gains from non-dependent to dependent microphones also showed a considerable range, again in accord with the literature values. When the subjects moved from the seated to the lateral decubitus position, the ratios decreased but by different amounts for different subjects. As neither the pattern of breathing nor the presence of the resistor had any consistent effect on the ratios, it is unlikely that the sound was of muscular origin.

A linear dynamic systems analysis between inspiratory or expiratory flow squared and the sound amplitude showed no relationship beyond that of the static gain. The sounds were in phase with each other and with the flow at the mouth, but there was hysteresis evident between the flow squared and the sound amplitude. The most plausible explanation for the phase relationship and hysteresis is that the sound is generated in the larger airways and is transmitted to the measurement locations, the attenuation depending on the local air and

blood volume.

The power spectrum of the sounds calculated for periods of constant flow showed increases of power with flow and lower power on expiration than on inspiration but no shifting of frequency as a function of flow or of flow direction. The power at all frequencies increased with the fourth power of the flow.

7.2 SIGNIFICANCE OF THE PRESENT WORK

The following, taken from the principal results given above, represent the major significance of the present work:

1. The model study showed that phase differences between flows can be generated by pressures that are in phase and that pressure swings slightly out of phase may generate more uniform distributions than those in phase. Furthermore, the waveforms of the pressure swings, while influencing the shape of the flow curves, have minimal effect on the distribution of a tidal volume within the lung.

2. The dynamic krypton-81m model represents the first interpretation of the activity-time curve over a representative breath. The information obtained non-invasively agrees with that from intubated subjects.

3. The regional ventilation per unit volume was found as a function of time, rather than as a single average value over a breath.

4. The relationship of lung sound amplitude to the square of the flow is substantiated here for the first time.

When working with krypton-81m, activity-time curves constructed from lung scans acquired in list mode may be used, through the application of the dynamic model, to obtain information about the ventilation per unit volume and the sequence of flows in different lung regions. The technique could be useful for physiological investigation of normal subjects or as a further diagnostic procedure when a lung scan is being performed. In the latter case, the patient would have no more radiation exposure; the test would be performed on the data already acquired. The physiological measurements could be performed under a variety of conditions including during exercise. The regional ventilation per unit volume as a function of time could provide useful information about poorly ventilated regions. A distinction would be possible between areas that received air slowly and those that were ventilated late.

Concerning lung sounds, previous authors have assumed the relation between air flow and lung sound to be either linear or curvilinear. The few tests that have been made have been based on a small number of points over a limited range of flows. The functional relation, $(\text{sound amplitude}) = (\text{flow})^2$, provides a first step in the understanding of the source of the sound. If the sounds are related to the kinetic energy as seems reasonable from the flow squared fit, then the probable source of the sound is in the larger airways where the velocities are high. Experiments should be designed to investigate this possibility.

BIBLIOGRAPHY

- Acevedo, J. C., Susskind, H., Goldman, A. G., Atkins, H. L. and Pate, H. P. (1980). Index for the detection of localized V and Q abnormalities. Fed. Proc. 39:575.
- Agostoni, E. (1970). Dynamics. In: The Respiratory Muscles: Mechanics and Neural Control. E. J. Campbell, E. Agostoni and J. N. Davis (Eds.) Saunders, Philadelphia.
- Alderson, P. O. and Line, B. R. (1980). Scintigraphic evaluation of regional pulmonary ventilation. Semin. Nucl. Med. 10:218-242.
- Alderson, P. O., Vieras, F., Housholder, D. F., Mendenhall, K. G. and Wagner, H. N. Jr. (1979). Gated and cinematic perfusion lung imaging in dogs with experimental pulmonary embolism. J. Nucl. Med. 20:407-412.
- Amis, T. C., Ciofetta, G., Clark, J. C., Hughes, J. M. B., Jones, H. A. and Pratt, T. A. (1977). Effect of posture on distribution of pulmonary ventilation and perfusion studied with ^{81m}Kr and ^{85m}Kr . J. Physiol. 272:76p-77p.
- Amis, T. C., Ciofetta, G., Clark, J. C., Hughes, J. M. B., Jones, H. A. and Pratt, T. A. (1978). Use of krypton 81m and 85m for measurement of ventilation and perfusion distribution within the lungs. Br. J. Radiol. Special Rpt. 15:52-59.
- Amis, T. C. and Jones, T. (1980). Krypton-81m as a flow tracer in the lung: theory and quantitation. Bull. europ. Physiopath. resp. 16:245-259.
- Arnot, R. N., Clark, J. C., Herring, A. N., Chakrabarti, M. K., and Sykes, M. K. (1981). Measurements of regional ventilation using nitrogen-13 and krypton-81m in mechanically ventilated dogs. Clin. Phys. Physiol. Meas. 2:183-196.
- Bajzer, Z. and Nosil, J. (1977). A simple mathematical lung model for quantitative regional ventilation measurement using ^{81m}Kr . Phys. Med. Biol. 22:975-980.
- Bajzer, Z. and Nosil, J. (1980). Lung ventilation model for radioactive tracer tidal breathing. Phys. Med. Biol. 25:293-307.
- Bake, B., Wood, L., Murphy, B., Macklem, P. T. and Milic-Emili, J. (1974). Effect of inspiratory flow rates on regional distribution of inspired gas. J. Appl. Physiol. 37:8-17.
- Banaszak, E. F., Kory, R. C. and Snider, G. L. (1973) Phonopneumography, Am. Rev. Resp. Dis. 107:449-455.

- Bartsch, P. and Linsmaux, D. (1980). Scintigraphie de ventilation au krypton-81m. Bull. europ. Physiopath. respir. 16:261-270.
- Bindslev, L., Santesson, J. and Hedenstierna, G. (1981). Distribution of inspired gas to each lung in anesthetized human subjects. Acta Anaesth. Scand. 25:297-302.
- Blide, R. W., Kerr, H. D. and Spicer, W. S. Jr. (1964). Measurement of upper and lower airway resistance and conductance in man. J. Appl. Physiol. 19:1039-1042.
- Bohadana, A. B., Peslin, R. and Uffholtz, H. (1978) Breath sounds in the clinical assessment of airflow obstruction. Thorax 33:345-351.
- Bouhuys, A., Lichtneckert, S., Lundgren, C. and Lundin, G. (1961). Voluntary changes in breathing pattern and nitrogen clearance from lungs. J. Appl. Physiol. 16:1039-1042.
- Briscoe, W. A. and DuBois, A. B. (1958). The relationship between airway resistance, airway conductance and lung volume in subjects of different age and body size. J. Clin. Invest. 37:1279-1285.
- Bullar, J. F. (1884). Experiments to determine the origin of the respiratory sounds. Proc. Royal Soc. London 37:411-423.
- Chang, H. K. and van Grondelle, A. (1981). Role of applied pleural pressure in ventilation distribution during cyclic breathing. Progress in Resp. Res. 16:1638-1644.
- Charbonneau, G., Racineux, J. L., Sudraud, M. and Tuchais, E. (1983) An accurate recording system and its use in breath sounds analysis. J. Appl. Physiol. 55:1120-1127.
- Chevrolet, J. C., Emrich, J., Martin, R. R. and Engel, L. A. (1979). Voluntary changes in ventilation distribution in the lateral posture. Respir. Physiol. 38:313-323.
- Chevrolet, J. C., Martin, J. G., Flood, R., Martin, R. R. and Engel, L. A. (1978). Topographical ventilation and perfusion distribution during IPPB in the lateral posture. Amer. Rev. Resp. Dis. 118:847-854.
- Chowdhury, S. K. and Majumder, A. K. (1981). Digital spectrum analysis of respiratory sounds. IEEE Trans. Biomed. Eng. BME 28:784-788.
- Ciofetta, G., Silverman, M. and Hughes, J. M. B. (1980). Quantitative approach to the study of regional lung function in children using krypton-81m. Br. J. Radiol. 53:950-959.
- Clark, J. C., Jones, T. and Macintosh, A. (1970). ^{81m}Kr : An ultra short lived inert gas tracer for lung ventilation and perfusion studies with the scintillation camera. Radioactive Isotope in Klinik und Forschung 9:444-451.

- Cutillo, A., Omboni, E. and Delgrossi, S. (1972). Effects of respiratory frequency on distribution of inspired gas in normal subjects and in patients with chronic obstructive lung disease. *Am. Rev. Resp. Dis.* 105:756-767.
- Dalquist, G. and Bjork, A. (1972). *Numerical Methods*, N. Anderson (Trans.). Englewood Cliffs, New Jersey, Prentice Hall.
- Daly, W. J. and Bondurant, S. (1963). Direct measurement of respiratory pleural pressure changes in normal man. *J. Appl. Physiol.* 18:513-518.
- Deconinck, F., Vincken, W. and Bossuyt, A. (1981) Dynamic lung imaging with Kr-81m. *Eur. J. Nucl. Med.* 6:A10.
- DeLand, F. H. and Mauderli, W. (1972). Gating mechanism for motion-free liver and lung scintigraphy. *NM J. Nucl. Med.* 13:939-941.
- Dollfus, R. E., Milic-Emili, J. and Bates, D. V. (1967). Regional ventilation of the lung studied with boluses of ^{133}Xe . *Respir. Physiol.* 2:234-246.
- Dosani, R. and Kraman, S. S. (1983). Lung sound intensity in normal man: a contour phonopneumographic study. *Chest* 4:628-631.
- Druzgalski, C. K., Donnerberg, R. L. and Campbell, R. M. (1980). Techniques of recording respiratory sounds. *J. Clin Eng.* 5:321-330.
- Elliott, I. B. (1972) Flap, a simplified simulation system for time-share users. *Simulation* 19:19-21.
- Engel, L. A. and Prefaut, C. (1981). Cranio-caudal distributions of inspired gas and perfusion in supine man. *Respir. Physiol.* 45:43-53.
- Fazio, F. and Jones, T. (1975). Assessment of regional ventilation by continuous inhalation of radioactive krypton-81m. *Br. Med. J.* 3:673-676.
- Fazio, F., Palla, A., Santolicandro, A., Solfanelli, S., Fornai, E. and Giuntini, C. (1979). Studies of regional ventilation in asthma using ^{81}mKr . *Lung* 156:185-194.
- Fixley, M. S., Roussos, C. S., Murphy, B., Martins, R. R. and Engels, L. A. (1978). Flow dependence of gas distribution and the pattern of inspiratory muscle contraction. *J. Appl. Physiol.* 45:733-741.
- Forgacs, P., Nathoo, A. R. and Richardson, H. D. (1971). Breath sounds. *Thorax* 26:288-295.
- Forkert, L., Anthonisen, N. R. and Wood, L. D. H. (1978). Frequency dependence of regional lung washout. *J. Appl. Physiol.* 45:161-170.

- Frazier, A. R., Rehder, K., Sessler, A. D., Rodarte, J. R. and Hyatt, R. E. (1976). Single breath oxygen test for individual lungs in awake man. *J. Appl. Physiol.* 40:305-311.
- Gaunaud, G. C. and Barlow, J. (1984). Matrix viscosity and cavity size distribution and the dynamic effective properties of perforated elastomers. *J. Acoust. Soc. Amer.* 75:23-34.
- Gavriely, N., Palti, Y. and Alroy, G. (1981). Spectral characteristics of normal breath sounds. *J. Appl. Physiol.* 50:307-314.
- Georgi, P., Vogt-Moykopf, I., Helus, F. and Ostertag, H. (1979). Ventilation studies with krypton-81m. *Thor. Cardiovasc. Surg.* 27:359-361.
- Gibson, A. J., Pride, N. B., O' Cain, C. and Quagliato, R. (1976). Sex and age differences in pulmonary mechanics in normal non-smoking subjects. *J. Appl. Physiol.* 41:20-25.
- Gill, J. and Veibel, E. R. (1972). Morphological study of pressure-volume hysteresis in rat lungs fixed by vascular perfusion. *Respir. Physiol.* 15:190-213.
- Goris, M. L., Daspit, S. G., Walter, J. P., McRae, J. and Lamb, J. (1977). Applications of ventilation lung imaging with 81m krypton. *Radiol.* 122:399-403.
- Grant, B. J. B., Jones, H. A. and Hughes, J. M. B. (1974). Sequence of regional filling during a tidal breath in man. *J. Appl. Physiol.* 37:158-165.
- Guttman, I., Wilks, S. S. and Hunter, J. S. (1971). *Introductory Engineering Statistics*, 2nd edition. John Wiley and Sons, New York.
- Hardin, J. C. and Patterson, J. L. (1979). Monitoring the state of the human airways by analysis of respiratory sound. *Acta Astronautica* 6:1137-1151.
- Harf, A. and Hughes, J. M. B. (1978). Topographical distribution of \dot{V}_A/\dot{Q} in elderly subjects using krypton-81m. *Respir. Physiol.* 34:319-327.
- Harf, A. and Meignan, M. (1980). Calculs de \dot{V}_A/\dot{Q} régionaux. *Bull. europ. Physiopath. resp.* 16:299-308.
- Harf, A., Pratt, T. and Hughes, J. M. B. (1976). Regional ventilation perfusion ratios at rest and on exercise using krypton-81m. *Bull. eur. Physiopath. resp.* 12:P195.
- Harf, A., Pratt, T. and Hughes, J. M. B. (1978). Regional distribution of \dot{V}_A/\dot{Q} in man at rest and with exercise measured with krypton-81m. *J. Appl. Physiol.* 44:115-123.

- Heaf, D. P., Helms, M. B., Gordon, I. and Turner, H. M. (1983). Postural effects on gas exchange in infants. *N. Engl. J. Med.* 308:1505-1508.
- Hedenstierna, G., Bindslev, L., Santesson, J. and Norlander, O. P. (1981). Airway closure in each lung of anesthetized human subjects. *J. Appl. Physiol.* 50:55-64.
- Hida, W., Suzuki, S., Sasaki, H., Fujii, Y., Sasaki, T. and Takishima, T. (1981). Effect of ventilatory frequency on regional transpulmonary pressure in normal adults. *J. Appl. Physiol.* 51:678-685.
- Hughes, J. M. B. (1979). Short-life radionuclides and regional lung function. *Br. J. Radiol.* 52:353-370.
- Hunter, I. W. and Kearney, R. E. (1984). Nexus: a computer language for physiological systems and signal analysis. *Comp. Biol. Med.* 14:385-401.
- Hyatt, R. E., Sittipong, R., Olafsson, S. and Potter, W. A. (1970). Some factors determining pulmonary pressure-flow behavior at high rates of airflow. In: *Airway Dynamics: Physiology and Pharmacology.* A. S. Bouhuys (Ed.). C. C. Thomas, Springfield, Illinois.
- Isabey, D. and Chang, H. K. (1981). Steady and unsteady pressure-flow relationships in central airways. *J. Appl. Physiol.* 51:1338-1348.
- Jaeger, M. and Matthys, H. (1970). The pressure flow characteristics of the human airways. In: *Airway Dynamics: Physiology and Pharmacology.* A. S. Bouhuys (Ed.). C. C. Thomas, Springfield, Illinois.
- Jansson, L. and Jonson, B. (1972). A theoretical study of flow patterns of ventilation. *Scand. J. Resp. Dis.* 53:237-246.
- Jones, R. L., Overton, T. R. and Sproule, B. (1977). Frequency dependence of ventilation distribution in normal and obstructed lungs. *J. Appl. Physiol.* 42:548-553.
- Kaneko, K., Milic-Emili, J., Dolovich, M. B., Dawson, A. and Bates, D. V. (1966). Regional distribution of ventilation and perfusion as a function of body position. *J. Appl. Physiol.* 21:767-777.
- Kaplan, E., Gergans, G. A., Milo, T., Friedman, A. M. and Sharp, J. T. (1982). Dynamic imaging of the respiratory cycle with ^{81m}Kr . *Chest* 81:312-317.
- Kawakami, K., Katsuyama, N., Fukuda, Y., Mori, Y., Shimada, T. and Iikura, Y. (1981). *Clin. Nucl. Med* 6:463-467.
- Kinsler, L. E., Frey, A. R., Coppens, A. B. and Saunders, J. V. (1982). *Fundamentals of Acoustics.* John Wiley and Sons, New York.

- Knipping, von H. W., Bolt, W., Valentin, H., Venrath, H. and Endler, P. (1957). Regionale Funktionsanalyse in der Kreislauf- und Lungen-Klinik mit Hilfe der Isentopenthorakographie und der selektiven Angiographie der Lungengefasse. Munchen. med. Wochschr. 99:1-3.
- Knipping, von H. W., Bolt, W., Venrath, H., Valentin, H., Lundes, H. and Endler, P. (1955). Eine neue Methode zur Prufung der Herz- und Lungenfunktion. Dtsch. med. Wschr. 80:1146-1147.
- Knoll, G. F. (1979). Radiation Detection and Measurement. John Wiley and Sons, New York.
- Kraman, S. S. (1980). Determination of the site of production of respiratory sounds by subtraction phonopneumography. Am. Rev. Resp. Dis. 122:303-309.
- Kraman, S. S. (1983a). Does the vesicular lung sound come only from the lungs? Am. Rev. Resp. Dis. 128:622-626.
- Kraman, S. S. (1983b). Lung sounds: relative sites of origin and comparative amplitudes in normal subjects. Lung 161:57-64.
- Kraman, S. S. (1983c). Speed of low-frequency sound through lungs of normal men. J. Appl. Physiol 54:304-308.
- Kraman, S. S. (1984). The relationship between air-flow and lung sound amplitude in normal subjects. Chest 86:225-229.
- Kraman, S. S. and Austrheim, O. (1983). Comparison of lung sound and transmitted sound amplitude in normal man. Am. Rev. Resp. Dis. 128:451-454.
- Kronenberg, R. S., Wangensteen, O. and Ponto, R. A. (1976). Frequency dependence of regional lung clearance of ^{133}Xe in normal men. Respir. Physiol. 27:293-303.
- Lavender, J. P., Irving, H. and Armstrong, J. D. II (1981). Krypton-81m ventilation scanning: Acute respiratory disease. AJR 136:309-316.
- Leblanc, P., Macklem, P. T. and Ross, W. R. D. (1970). Breath sounds and distribution off pulmonary ventilation. Am. Rev. Resp. Dis. 102:10-16.
- Li, D. K., Treves, S., Heyman, S., Kirkpatrick, J. A. Jr., Lambrecht, M., Ruth, T. J. and Wolf, A. P. (1979). Krypton-81m: A better radiopharmaceutical for assessment of regional lung function in children. Radiol 130: 741-747.
- Lillington, G. A., Fowler, W. S., Miller, R. D. and Helmholtz, H. F. (1959). Nitrogen clearance rates of right and left lung in different positions. J. Clin. Invest. 38:2026-2034.

- Line, B. R., Cooper, J. A., Spicer, K. M., Jones, A. E., Crystal, R. G. and Johnston, G. S. (1980). Radionuclide cinepneumography: flow-volume imaging of the respiratory cycle. *J. Nucl. Med.* 21:219-224.
- Lutchen, K. R., Primiano, F. P. and Saidel, G. M. (1982). A nonlinear model combining pulmonary mechanics and gas concentration dynamics. *IEEE Trans. Biomed. Engg.* BME-29:629-641.
- Majumder, A. K. and Chowdhury, S. K. (1981). Recording and preliminary analysis of respiratory sounds from tuberculosis patients. *Med. Biol. Eng. Comp.* 19:561-564.
- Marmarelis, P. Z. and Marmarelis, V. Z. (1978). *Analysis of Physiological Systems: the White Noise Approach.* Plenum Press, New York.
- Meignan, M., Harf, A., Oliviera, L., Simonneau, G., Cavellier, J. F., Lejonc, J. L. and Cinotti, L. (1981). Functional images of computed ventilation perfusion ratios (V/Q) with $^{81m}\text{Krypton}$ in acute pulmonary embolism (P.E.). *Eur. J. Nucl. Med.* 6:A21.
- Milic-Emili, J. (1977). Ventilation. In: *Regional Differences in the Lung.* J. B. West (Ed.). Academic Press, New York. pp. 167-199.
- Milic-Emili, J., Henderson, J. A. M., Dolovich, M. B., Trop, D. and Kaneko, K. (1966). Regional distribution of inspired gas in the lung. *J. Appl. Physiol.* 21:749-759.
- Murphy, B. G. and Engel, L. A. (1978). Models of the pressure-volume relationship of the human lung. *Respir. Physiol.* 32:183-194.
- Murphy, R. L. (1981). Auscultation of the lung: past lessons, future possibilities. *Thorax* 36:99-107.
- Murphy, R. L. H., Holford, S. K. and Knowler, W. C. (1977). Visual lung sound characterization by the time-expanded wave-form analysis. *N. Eng. J. Med.* 296:968-971.
- Nairn, J. R. and Turner-Varwick, M. (1969). Breath sounds in emphysema. *Br. J. Dis. Chest* 63:29-37.
- Nelson, P. A. and Morfey, C. L. (1981). Aerodynamic sound production in low speed air ducts. *J. Sound Vibr.* 79:263-289.
- O'Donnell, D. M. and Kraman, S. S. (1982). Vesicular lung sound amplitude mapping by automated flow-gated phonopneumography. *J. Appl. Physiol.* 53:603-609.
- Otis, A. B., McKerrow, C. B., Bartlett, R. A., Mead, J., McIlroy, M. B., Selverston, N. J. and Radford, E. P. Jr. (1956). Mechanical factors in distribution of pulmonary ventilation. *J. Appl. Physiol.* 8:427-443.

- Papanicolaou, N. and Treves, S. (1980). Pulmonary scintigraphy in pediatrics. *Semin Nucl Med* 10:259-285.
- Parker, R. P., Smith, P. H. S. and Taylor, D. M. (1978). *The Basic Science of Nuclear Medicine*. Churchill Livingstone, Edinburgh.
- Pasterkamp, H., Fenton, R., Leahy, F. and Chernick, V. (1983). Spectral analysis of breath sounds in normal newborn infants. *Med. Instrum.* 14:355-357.
- Pedley, T. J., Sudlow, M. F. and Milic-Emili, J. (1972). A non-linear theory of the distribution of pulmonary ventilation. *Respir. Physiol.* 15:1-38.
- Ploysongsang, Y. (1983). The lung sounds phase angle test for detection of small airway disease. *Respir. Physiol.* 53:203-214.
- Ploysongsang, Y., Dosman, J. and Macklem, P. T. (1979). Demonstration of regional phase differences in ventilation by breath sounds. *J. Appl. Physiol.* 46:361-368.
- Ploysongsang, Y., Macklem, P. T. and Ross, W. R. D. (1978). Distribution of regional ventilation measured by breath sounds. *Am. Rev. Resp. Dis* 117:657-664.
- Ploysongsang, Y., Martin, R. R., Ross, W. R. D., Loudon, R. G. and Macklem, P. T. (1977). Breath sounds and regional ventilation. *Am. Rev. Resp. Dis.* 116:187-199.
- Ploysongsang, Y., Pare, J. A. P. and Macklem, P. T. (1982). Correlation of regional breath sounds with regional ventilation in emphysema. *Am. Rev. Resp. Dis.* 126:526-529.
- Rehder, K., Hatch, D. J., Sessler, A. D. and Fowler, W. S. (1972). The function of each lung of anesthetized and paralyzed man during mechanical ventilation. *Anesth.* 37:16-26.
- Rehder, K., Knopp, T. J., Brusasco, V. and Didier, E. P. (1981). Inspiratory flow and interpulmonary gas distribution. *Am. Rev. Resp. Dis.* 124:392-396.
- Rehder, K., Sessler, A. D. and Rodarte, J. R. (1977). Regional intrapulmonary gas distribution in awake and anesthetized-paralyzed man. *J. Appl. Physiol.* 42:391-402.
- Rice, D. A. (1983). Sound speed in pulmonary parenchyma. *J. Appl. Physiol* 54:304-308.
- Robertson, P. C., Anthonisen, N. R. and Ross, D. (1969). Effect of inspiratory flow rate on regional distribution of inspired gas. *J. Appl. Physiol.* 26:438-443.
- Roussos, C. S., Fixley, M., Genest, J., Cosio, M., Kelly, S., Martin, R. R. and Engel, L. A. (1977). Voluntary factors influencing the distribution of inspired gas. *Am. Rev. Resp. Dis.* 116:457-467.

- Roussos, C. S., Fubuchi, Y., Macklem, P. T. and Engel, L. A. (1976). Influence of diaphragmatic contraction on ventilation distribution in horizontal man. *J. Appl. Physiol.* 40:417-424.
- Roussos, C. S., Martin, R. R. and Engel, L. A. (1977). Diaphragmatic contraction and the gradient of alveolar expansion in the lateral posture. *J. Appl. Physiol.* 43:32-38.
- Sampson, M. G. and Smaldone, G. C. (1984). Voluntary induced alterations in regional ventilation in normal man. *J. Appl. Physiol.* 56:196-201.
- Scheid, P. and Piiper, J. (1980). Intrapulmonary gas mixing and stratification. In: *Pulmonary Gas Exchange Vol. I.*, J. B. West (Ed.) Academic Press. pp. 87-130.
- Schor, R. A., Shames, D. M., Weber, P. M. and Dos Remedios, L. V. (1978). Regional ventilation studies with Kr-81m and Xe-133; a comparative analysis. *J. Nucl. Med.* 19:348-353.
- Schreiber, J. R., Anderson, W. F., Wegmann, M. J. and Waring, W. W. (1981). Frequency analysis of breath sounds by phonopneumography. *Med. Instrum.* 15:331-334.
- Secker-Walker, R. H., Alderson, P. O., Wilhelm, J., Hill, R. L., Markham, J., Baker, J. and Potchen, E. J. (1975). The measurement of regional ventilation during tidal breathing: a comparison of two methods in healthy subjects, and patients with chronic obstructive lung disease. *Br. J. Radiol.* 48:181-189.
- Secker-Walker, R. H., Hill, R. I., Markham, J., Baker, J., Wilhelm, J., Alderson, P. O. and Potchen, E. J. (1973). The measurement of regional ventilation in man: a new method of quantitation. *J. Nucl. Med.* 14:725-732.
- Shykoff, B. E., van Grondelle, A. and Chang, H. K. (1982). Effects of unequal pressure swings and different waveforms on distribution of ventilation: a nonlinear model simulation. *Respir. Physiol.* 48:157-168.
- Smaldone, G. C., Mitzner, W. and Itoh, H. (1983). Role of alveolar recruitment in lung inflation: influence on pressure-volume hysteresis. *J. Appl. Physiol.* 55:1321-1332.
- Spaventi, S., Nosal, J., Bajzer, Z. and Pardon, R. (1978). Clinical and experimental applications of a new mathematical lung model for krypton 81m inhalation. *Br. J. Radiol. Special Rpt.* 15:60-68.
- Susskind, H., Acevedo, J. C., Pate, H. R. and Brill, A. B. (1981). Nonuniformity of regional ventilation as a sensitive indicator of gas exchange. *Fed. Proc.* 40:538.
- Susskind, H., Acevedo, J. C., Pate, H. R., Harold, W. H. and Brill, A. B. (1982). Nonuniform distribution of regional ventilation in pulmonary disease. *Fed. Proc.* 41:1126.

- Susskind, H., Atkins, H. L., Goldman, A. G., Acevedo, J. C., Pate, H. R., Richards, P. and Brill, A. B. (1981). Sensitivity of Kr-81m and Xe-127 in evaluating nonembolic pulmonary disease. J. Nucl. Med. 22:781-786.
- Susskind, H., Goldman, A. G., Acevedo, J. C., Atkins, H. L. and Pate, H. R. (1980). Topographical distribution of V and Q in impaired lungs. Fed. Proc. 39:576.
- Susskind, H., Iwai, J., Acevedo, J. C., Rasmussen, D. L., Heydinger, D. K., Pate, H. R., Yonekura, T., Harold, W., and Brill, A. B. (1982). Lung impairment in nonsmoking and smoking coal miners. Am. Rev. Resp. Dis. 125:159.
- Sybrecht, G., Landau, L., Murphy, B. G., Engel, L. A., Martins, R. R. and Macklem, P. T. (1976). Influence of posture on flow dependence of distribution of inhaled ¹³³Xe boli. J. Appl. Physiol. 41:489-496.
- Touya, J. J., Price, R. R., Patton, J. A., Erickson, J., Jones, J. P. and Rollo, F. D. (1979). Gated regional spirometry. J. Nucl. Med. 20:620.
- Urquhart, R. B. McGhee, J., Macleod, J. E. S., Banham, S. V. and Moran, F. (1981). The diagnostic value of pulmonary sounds: a preliminary study by computer-aided analysis. Comp. Biol. Med. 11:129-139.
- Weibel, E. R. (1963). Morphometry of the Human Lung. Academic Press, New York.
- Weiss, E. B. and Carlson, C. J. (1972). Recording of breath sounds. Am. Rev. Resp. Dis. 105:835-839.
- Wooten, F. T., Waring, W. W., Wegmann, M. J., Anderson, W. F. and Conley, J. D. (1978). Method for respiratory sound analysis. Med. Instrum. 12:254-257.
- Yano, Y., McRae, J. and Anger, H. O. (1970). Lung function studies using short lived ^{81m}Kr and the scintillation camera. J. Nucl. Med. 11:674-679.